2011

Biochemical Evaluation of Lignin-like Molecules

Jay Thakkar
Virginia Commonwealth University

BIOCHEMICAL EVALUATION OF LIGNIN-LIKE MOLECULES

A Dissertation submitted in partial fulfillment of the requirements for the degree of Doctor of Philosophy at Virginia Commonwealth University.

by

JAY N THAKKAR

M.S. in Pharmaceutical Sciences, Virginia Commonwealth University, 2006

Director: Dr. Umesh R. Desai

Professor, Department of Medicinal Chemistry

Virginia Commonwealth University

Richmond, Virginia

May 2011

ACKNOWLEDGMENTS

I am extremely grateful to my advisor Dr. Umesh Desai for his continuous encouragement, critical comments and timely advices during my prolonged stay at the Virginia Commonwealth University. I am highly appreciative of him for the precious time he has devoted for getting me prepared for my defense seminar. He gave me a lot of freedom to work and was always open to new ideas. He has advocated both scientific and essential non-scientific knowledge that will not only help me grow as a scientist but also a better individual in life.

I would like to express my gratitude to my graduate committee members, Dr. Donald Brophy, Dr. Darrell Peterson, Dr. Martin Safo and Dr. Shijun Zhang who were really supportive of my research work and for their valuable comments and suggestions on my dissertation. I would like to thank Dr. Scarsdale for training me in advanced NMR techniques and was always willing to answer any questions that I had. I would like to thank Dr. Michael Hindle and Dr. Mathew Hartman for training me on MS and allowing me use the instrument for my studies. I would also like to thank Dr. Erika Martin for training me on TEG and HAS used in my studies. I have been lucky to be associated with these pleasant people who have imparted a great deal of knowledge to me.

I would like thank Dr. Gunnar Gunnarson, Dr. Phil Mosier and Dr. Aiye Liang for their direct or indirect help in my research. Gunnar was the first person to have worked with when I started. He was my mentor and I enjoyed working with him. Phil is one of the most helpful people I have met during these years, research or non-research he has always helped everyone. Aiye, a good

friend, colleague and my Chinese language teacher enlightened me with the “real” Chinese food and culture. I had wonderful time working with her on several projects.

I would like to thank the department secretaries Mrs. Michelle Craighead and Sharon Lee for taking care of a lot of trivial to complex issues I encountered and for their willingness to help when needed.

I am grateful to all the members from Dr. Desai’s group both past and present for creating an excellent working environment, for useful and stimulating scientific discussions. The diverse group of people in the lab helped me learn a lot about other cultures, countries and politics. I would like to thank Brian who trained me on fibrometer used in my studies. Brian and Tim, two very contrasting Americans educated us about the US and its culture. I am thankful to Shrenik for his help in taking care of my paper work during my absence.

I would specially like to thank Joseph Timothy King for taking care of all things inside and outside the lab or department on my behalf during my 1 year absence from the lab. He was always ready to help, just a phone call away. His help has saved me a lot of time and more importantly eased my life. During this 1 year things would have been extremely difficult for me without him. He is also a good friend of mine “the chipotle buddy”.

I would like to thank the department of medicinal chemistry for the excellent education and providing me an opportunity to pursue MS and PhD. I would also like to appreciate the facilities that were provided to me by the Institute for Structural Biology and Drug Discovery and all the members at the Institute who have been very friendly.

I am thankful to NIH and AHA who have supported my research funding for most part, over all these years.

I had a small home away from home with Arjun, Chandravel and Ruban being the members of the family. I would also like to thank my friend Rahul who was always excited to welcome me during my short stays in Richmond over the past one year.

Finally, I would like to thank my parents and my wife who have waited patiently for a very long time. They have been highly supportive and understanding without which things would have been difficult.

Table of Contents

List of Tables

List of Figures

Abbreviations

ACS: Acute Coronary Syndrome

APC: Activated Protein C

APTT: Activated Partial Thromboplastin Time

AT: Anti-Thrombin

CA: Caffeic Acid

CD: Dehydropolymer of caffeic acid

CEM: Clot Elastic Modulus

CV: Cardio Vascular

CVD: Cardio Vascular Disease

DHP: Dehydroploymer

DIC: Disseminated Intravascular Coagulation

DMF: dimethyl formamide

DTI: Direct Thrombin Inhibitor

DVT: Deep Vein Thrombosis

FA: Ferulic Acid

FD: Dehydropolymer of ferulic acid

GAG: Glycosaminoglycan

GlcA*p*: glucuronic acid

GlcN*p*: glucosamine

GPC: Gel Permeation Chromatography

HAS: Hemostasis Analysis System

HIT: Heparin-Induce Thrombocytopenia

HMWK: High Molecular Weight Kininogen

HPLC: High Performance Liquid Chromatography

HRP: Horse Radish Peroxidase

HS: Heparan Sulfate

HSPG: Heparan Sulfate Proteoglycans

HSV: Herpes Simplex Virus

LMWH: Low Molecular Weight Heparin

MWCO: Molecular Weight Cut-Off

NMWC: Nominal Molecular Weight Cut-Off

NSAIDs: Non-Steroidal Anti-Inflammatory Drugs

PAA: Poly Acrylic Acids

PCF: Platelet Contractile Force

PE: Pulmonary Embolism

PEG: Polyethylene glycol

PF: Platelet Factor

Pg: Plasminogen

PS: Polystyrene Standards

PSS: Polystyrene Sulfonate Standards

PT: Prothrombin Time

SEC: Size Exclusion Chromatography

SERPIN: Serine Protease Inhibitor

TAFI: Thrombin-Activable Fibrinolysis Inhibitor

TEAST: Triethylamine sulfur trioxide-complex

TEG: Thromboelastograph

TF: Tissue Factor

TFPI: Tissue Factor Pathway Inhibitor

TGT: Thrombin Generation Time

TMS: Tetramethylsilane

tPA: Tissue-type Plasminogen Activator

UFH: Unfractionated Heparin

USFDA: United States Food & Drug Administration

VTE: Venous Thromboembolism

WBC: White Blood Cells

WHO: World Health Organization

Abstract

BIOCHEMICAL EVALUATION OF LIGNIN-LIKE MOLECULES

By Jay N Thakkar, PhD

A Dissertation submitted in partial fulfillment of the requirements for the degree of Doctor of Philosophy at Virginia Commonwealth University.

Virginia Commonwealth University, 2011

Director: Dr. Umesh R. Desai

Professor, Department of Medicinal Chemistry

Current anticoagulants carry a serious risk of bleeding complications. In addition, narrow therapeutic index, drug interactions, immunological reactions, toxicity and high cost to benefit ratio limits the effective use of these drugs in patients with thrombotic conditions.

Heparin is the most widely used anticoagulant. We hypothesized that one of the major drawback of heparins, its non-specific interaction with the plasma proteins arises as a result of negative charges. To reduce these non-specific interactions, our laboratory designed sulfated low molecular weight lignin (LMWL) like biomacromolecules, which were found to be direct inhibitors of thrombin and factor Xa, acting through a unique exosite-2 mediated process.

To elucidate the structural basis of this mechanism, we studied unsulfated and size fractionated LMWLs. Detailed enzyme inhibition studies with sulfated and unsulfated LMWLs of ferulic and caffeic acid oligomers revealed that sulfation was not absolutely critical for dual inhibition property and smaller oligomers can yield a potent anticoagulant. Mechanistically, unsulfated LMWLs retained exosite-2 mediated inhibition mechanism. A major advantage expected of the unsulfated LMWLs is the possibility that orally bioavailable anticoagulants may become possible.

To identify target specific structures within the heterogeneous population of sulfated LMWLs, we prepared sulfated *β-O-4*-linked oligomer using chemical synthesis. Enzyme inhibition studies revealed that the sulfated *β-O-4* LMWL were highly selective direct inhibitors of thrombin. These results show for the first time that specific structural features on LMWL scaffold dictate inhibition specificity. Studies in plasma and blood display highly promising anticoagulant profile for further studies in animals.

To further study the LMWL scaffold as macromolecular mimetic of heparin; we investigated their effect in preventing cellular infection by herpes simplex virus-1 (HSV-1). Based on previous findings on sulfated lignins a size-dependent study on unsulfated LMWLs was done. The unsulfated lignins were found to not only inhibit HSV-1 entry into mammalian cells, but were more potent than sulfated lignins. Interestingly, shorter chains were found to be as

active as the longer ones, suggesting that structural features, in addition to carboxylate groups, may be important. It can be expected that unsulfated lignins also antagonize the entry of other enveloped viruses, like HIV-1 and HCV that utilize heparan sulfate to gain entry into cells. The results further present major opportunities for developing lignin-based antiviral formulations for topical use.

CHAPTER 01

Introduction

1.1 Background

Cardiovascular disease (CVD) is estimated to be responsible for 17.1 million deaths per year, making it number one cause of death worldwide.[1-4] WHO estimates that by 2030, the number people dying from CVD, mainly heart disease and stroke is expected to reach 23.6 million. The advancement of safe and adequate treatment options for thrombotic disorders has proven elusive for over half a century. The problem probably lies in the complexity of the hemostatic system, which maintains the balance between thrombus formation and blood flow primarily through the action of a serine protease known as thrombin.[5] Inhibition of this enzyme would be beneficial for the treatment and prevention of a multitude of CVDs.[6-7] Current therapies reduce the risk of recurrent CVDs but are plagued with side effects, dosage maintenance difficulties, and undesirable delivery methods.[8] Consequently, there is significant medicinal potential for the design and synthesis of novel anticoagulant agents that are both potent and selective with minimal side effects.

1.2 Hemostasis

The role of hemostasis is to maintain an unimpeded flow of blood and return its fluidity following vascular injury.[5,9] A systematic understanding of the hemostatic system is necessary in order to design and develop newer anticoagulant agents. The hemostatic system refers to the complex interaction of plasma coagulation and fibrinolytic proteins, platelets, and the blood vasculature.[10-11] Hemostasis is further sub-categorized into; 1)

Primary hemostasis – in this a clot is formed at the site of injury through aggregation of platelets. 2) Secondary hemostasis – the platelet plug formed strengthens through tandem fibrin meshwork forming via the complex coagulation cascade. 3) Tertiary hemostasis – the clot retracts and is slowly lysed by plasmin.[12] The hemostatic system is stimulated through the activation of the fVII-tissue factor complex and the aggregation of circulating platelets.[5,10] The two responses combined produce the hemostatic plug. The controlled occurrence of these discrete responses require coordination between the platelet and coagulation cascade, which is attained through the employment of the plasma protease, thrombin.[13] Thus, thrombin is the vital link between these two systems.

1.3 Pathology of Improperly Regulated Hemostasis

Hemostasis is a complex balance of events which, if improperly regulated can lead to various complications during an injury. Inadequacies in hemostasis can lead to hemorrhage, while inappropriate or excessive hemostasis can lead to thrombosis.[14-19] Both of these are complex in nature that occur in the coagulation and fibrinolytic systems. In view of the fact that the coagulation and fibrinolytic system are inter-linked, any distortion of the coagulation system is amplified by the fibrinolytic system.

Technically hemorrhage signify bleeding. Apart from trauma, hemorrhage can occur due to several factors; 1) intravascular changes or decrease in the clotting factors, 2) intramural changes caused due to aneurysms or arteriovenous malformation, and 3) extravascular changes caused due to H. *pylori* infection, brain tumor or abscess.[14-15]

Other factors that can cause bleeding are drugs such as NSAIDs, which inhibit production of thromboxane and activation of platelets.[16-17]

Thrombosis implies formation of a blood clot, which eventually blocks the circulation of blood flow. Thrombosis can occur due to several factors; 1) genetic deficiencies or autoimmune disorders leading to hypercoagulability, 2) exposure of tissue factor (TF) to the blood coagulation system caused during trauma, surgery or infection and 3) disturbed blood flow, which can occur due to long periods of sedentary behavior (eg: traveler's thrombosis), atrial fibrillation, venous stasis, obstruction of blood flow, certain type of cancers and cancer therapies. [18-19]

A large percentage of population is at risk of developing a pathological thrombus whether in the form of a stroke, venous thromboembolism, or arterial thrombosis.[20] Generally speaking, undesirable clots are a result of unregulated or unwarranted generation of thrombin, leading to an increase in thrombin-activable fibrinolysis inhibitor (TAFI) activation. Excessive TAFI activation would extenuate fibrinolysis and consequently hinder the restoration of blood flow in a timely manner.[21-22]

1.4 The Coagulation Cascade

The coagulation cascade is a complex ordered set of proteolytic events that occurs in the body when a blood vessel is injured **(figure 01)**.[23] Each enzyme of the coagulation pathway is present as a protease zymogen in plasma, which on activation undergoes proteolytic cleavage to discharge the active factor from the antecedent molecule.[24] The

activation is functional through a series of positive and negative feedback loops. Eventually, the pathway leads to production of thrombin, which promotes fibrin formation to form a clot, thereby down regulating the procoagulant activity.[25] Thrombin generation occurs via two pathways, the *intrinsic* and the *extrinsic pathway*, which converge at fX to a single common pathway resulting in the production of thrombin (fIIa). [26]

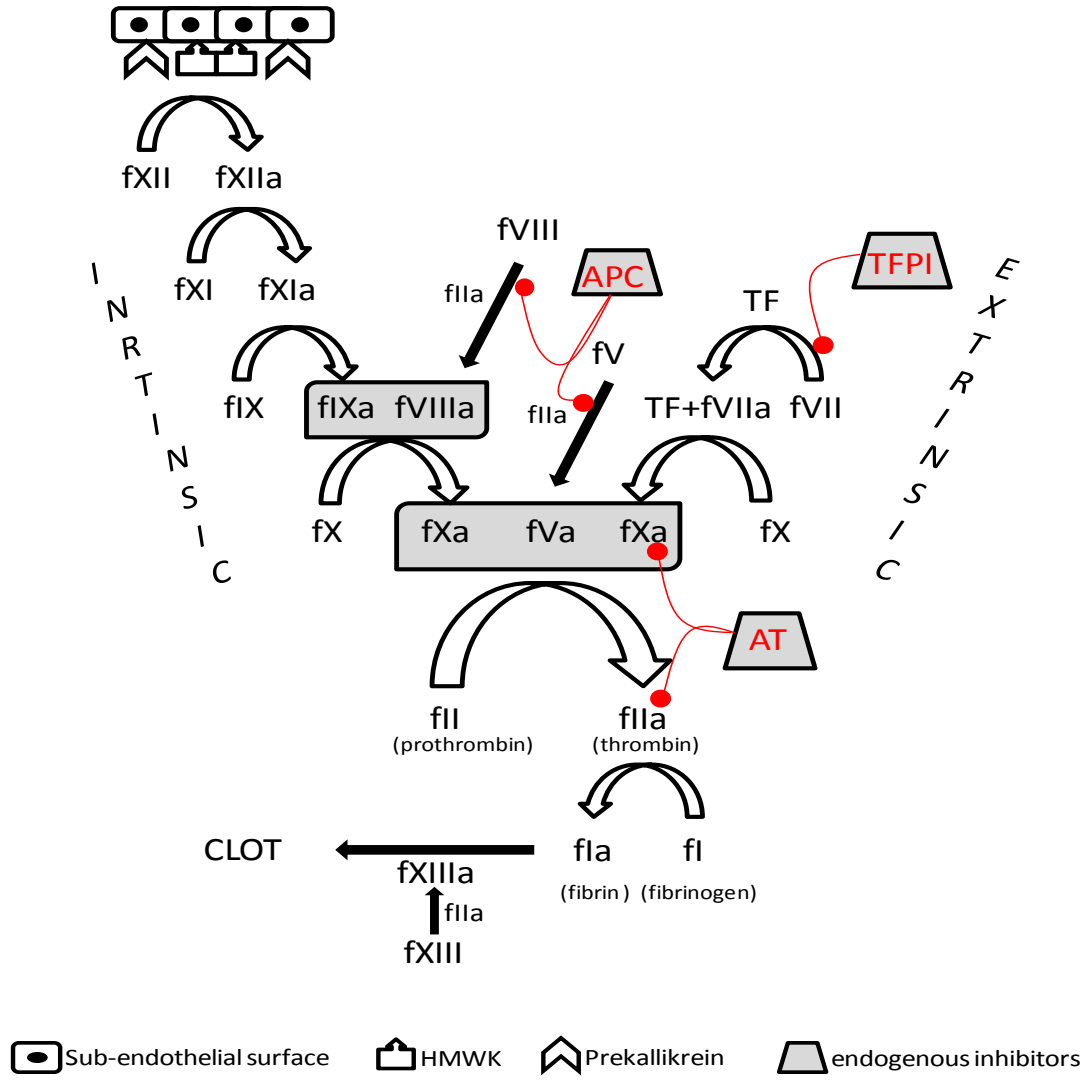

Figure 01. Simplified coagulation cascade
HMWK - high molecular weight kininogen; AT – antithrombin; APC – activate protein C and TFPI – tissue factor pathway inhibitor

1.4.1 *Intrinsic Pathway*

It is also called as the contact pathway, and is less significant and not very well understood in terms of its role in hemostasis under normal physiological conditions.[23,27] The contact pathway gets its name from the fact that the coagulation system is activated to form a clot when blood comes into contact with negatively charged surfaces or with sub-endothelial connective tissues.[28] The first step is binding of fXII (Hageman factor) to the sub-endothelial surface followed by an injury. Prekallikrein, and high molecular weight kininogen (HMWK) also bind at the surface activating fXII to fXIIa. During this activation fXII is cleaved into two chains, which stay connected through a disulfide bond.[29] The lighter of the two chains contain the active site and is termed as the activated fXII (fXIIa).[29] fXII can auto-activate or activate through a feedback mechanism by activating prekallikrein thus amplifying the pathway. fXIIa then activates fXI to fXIa in presence of HMWK and Ca^{+2} ions secreted from platelets. fXIa in turn catalyzes the conversion of fIX to fIXa in presence of Ca^{+2} ions. Eventually, fX is activated to fXa, a process that can also occur through the extrinsic pathway. fX activation is brought about by a molecular complex containing fIXa, fVIII, Ca^{+2} ions and phospholipids provided by the platelet surface, where this reaction usually takes place.[25] The precise role of fVIII in this reaction is not clearly understood. Its presence in the complex is obviously indispensable, as seen by the serious consequences of fVIII deficiency experienced by haemophiliacs.[30] fVIII is altered by thrombin, to its activated form, promoting the activation of fX. Although the physiological contribution of the contact pathway to coagulation remains elusive, recent data suggest that it plays some role in physiological

blood coagulation, since mice deficient in fXII have been shown to be protected against both stroke and arterial thrombosis.[31]

1.4.2 *Extrinsic Pathway*

It is also called as the TF pathway and is the major physiological pathway for fibrin formation.[23,27] It provides a swift response to tissue injury, generating fXa almost instantaneously, as opposed to the seconds or even minutes required for the intrinsic pathway to activate fX.[32] The main function of the extrinsic pathway is to enhance the activity of the intrinsic pathway.[32] The pathway sets in at the site of injury in response to the release of the procoagulant, TF, which is present in most human cells bound to the cell membrane.[23,27,32] The activation process for TF is not clearly understood. On activation, TF binds rapidly to fVII activating it to form a TF + fVIIa complex, which in presence of Ca^{+2} ions and phospholipids instantaneously activates fIX and fX. fXa can further activate fVII, which forms the link between the two pathways along with fIX activation.[25]

1.4.3 *The Common Pathway*

This is the most crucial step in the coagulation cascade, which harbors fX (fXa) and is responsible for thrombin generation.[23,26] Through the sequential activation of several zymogens in the extrinsic and the intrinsic pathway, prothrombin (fII) is ultimately activated via fXa and the prothrombinase complex (fVa, prothrombin, phospholipids and Ca^{+2} ions). The prothrombinase complex activates prothrombin to thrombin (fIIa) 300,000-fold more efficiently that fXa alone.[33] The fundamental role of thrombin is

conversion of fibrinogen (fI) to fibrin (fIa) to form a fibrin mesh-work, which are eventually cross-linked by fXIIIa to form a stable fibrin clot.[25-26] In addition, thrombin also activates fVIII, fV and their inhibitor, protein C (1000-fold higher in presence of thrombomodulin) and FXIII.[34] Following activation of the either pathways the coagulation cascade is maintained in a prothrombotic state by the persistent activation of fVIII and fIX to form the tenase complex, until its down-regulation by the anticoagulant pathways. The three major endogenous anticoagulants in our body are antithrombin III (AT), activated protein C (APC) and tissue factor pathway inhibitor (TFPI).[35]

1.5 Fibrinolysis

The clot formed as a result of an injury does not stay for ever. Gradually, the blood clot is reorganized and reabsorbed by a process termed fibrinolysis **(figure 02)**.[23] This is accomplished by a non-specific proteolytic enzyme, plasmin. Tissue-type plasminogen activator (tPA) secreted from endothelial cells and urokinase activates the zymogen plasminogen (Pg) to form the serine protease plasmin, which is responsible for degrading the fibrin clot and restoring the blood fluidity.[36-37] Analogous to the coagulation cascade a series of stepwise events occur during fibrinolysis, which involves a fine balance between plasmin/antiplasmin and thrombin/thrombomodulin activities.[38] In essence, coagulation and fibrinolysis systems work in cooperation to maintain hemostasis at the site of injury while ensuring fluidity of the blood elsewhere.

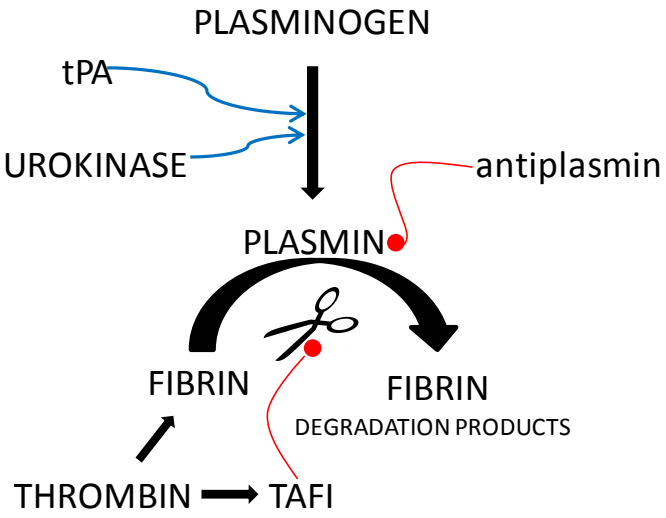

Figure 02. Fibrinolysis mechanism
tPA – tissue-type plasminogen activator; TAFI – thrombin-activatable fibrinolysis inhibitor
Blue arrows denote stimulation and red lines inhibition.

1.6 Thrombin and the Coagulation System

Thrombin has been termed as the master regulator enzyme in blood coagulation.[39] It is the last enzyme in the coagulation cascade and its ultimate product is a formation of a stable clot.[26] Thrombin, a trypsin-like serine protease ensues from the circulating zymogen precursor protein, prothrombin.[40-41] Prothrombin cleaves to form an enzyme with an overall ellipsoid-like structure comprising of a small A-chain and a catalytic B-chain.[42-43] The catalytic activity of thrombin is not only dictated by its active site but also by recognition sites (exosite-1 and exosite-2), which modulate the specificity of the enzyme.[40,44] Understanding of the interactions between thrombin and its substrate is crucial in the identification and design of novel medicinal agents that would interact and regulate the activity of the enzyme **(figure 03)**. An interesting aspect of thrombin in the

hemostatic system is its contrasting dual nature where it acts as both an anticoagulant and a pro-coagulant.[5] Activity of thrombin is primarily controlled by two systems; 1) AT and 2) protein C and protein S.

The major regulator of thrombin activity is the plasma serine protease inhibitor (SERPIN) AT. AT directly interacts with the active site of thrombin as well as the other major coagulation enzymes (factors Xa, VIIa, IXa, XIa, XIIa, and plasma kallikrein) hampering the formation of both the tenase and prothrombase complexes.[5,26] Heparin cofactor accelerates the inhibition of thrombin by AT with a 1,000-fold greater potency.[5,45]

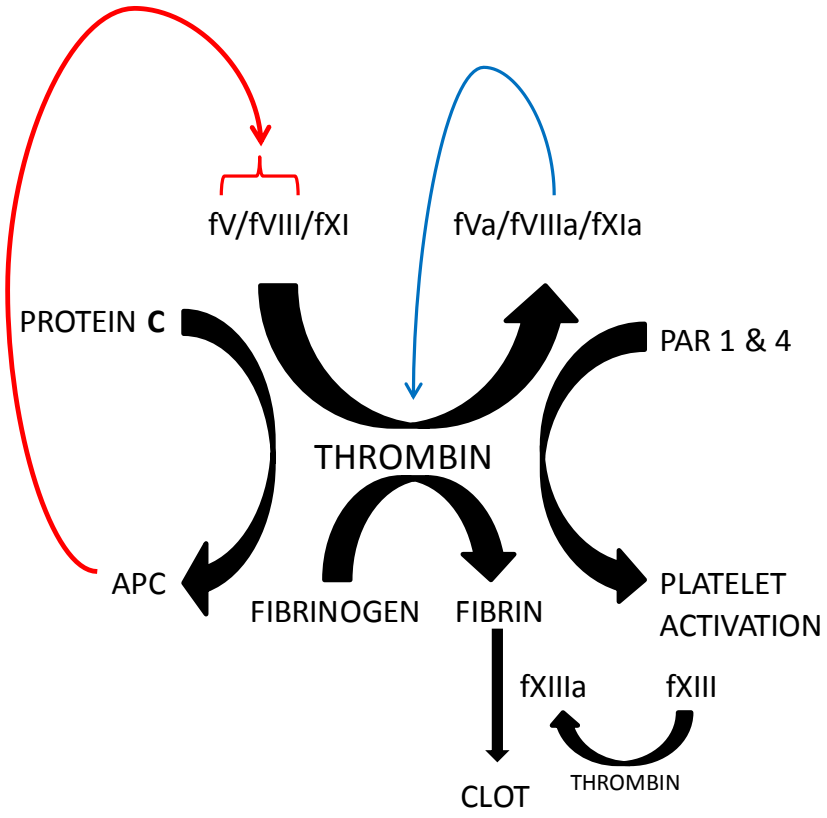

Figure 03. Critical role of thrombin
APC – activate protein C; PAR – protease activate receptor.
Blue arrows denote stimulation and red inhibition.

Protein C is activated by thrombin to activated protein C (APC), which is further enhanced in presence of endothelial protein C receptors and thrombomodulin. APC inactivates fVa and fVIIIa, two cofactors of thrombin, thus reducing the rate of thrombin formation.[5,45] Protein S acts as a cofactor for APC, and serves as APC's receptor to localize its inhibitory role. The anticoagulant role of thrombin is dependent on a finite number of thrombomodulin binding sites.[45-46] When these sites are exceeded, it converts thrombin into a physiologic pro-coagulant enzyme. Heparin cofactor II, a SERPIN is a specific thrombin inhibitor whose activity is potentiated by the glycosaminoglycan (GAG), dermatan sulfate.[47]

Although the enzymatic role of thrombin in the hemostatic process is significant and impressive, it also has many other biological roles that are far more intricate.[48-49] Some of these include the role of thrombin in platelet activation and aggregation.[50-51] Two substrates on human platelets, protease-activated receptors 1 and 4 lead to platelet activation when stimulated.[52-53] Platelets have the ability to aggregate at the site of injury which leads to the development of acute myocardial syndrome and coronary artery occlusion. The non-hemostatic role involves the stimulation of chemotaxis of white blood cells (WBC), generation and discharge of cytokines, fibroblast proliferation and mitogenesis.[54-56] Effects of thrombin on endothelial cells leads to the release of a variety of biological mediators.[49,57-58] Although not well defined, evidence of a role in cancer cell adhesion has been speculated.[59]

1.7 Anticoagulant Treatment

Thrombin plays a crucial role in coagulation of blood, hence prophylaxis or treatment of thromboembolic disorders aim to block thrombin generation or inhibit thrombin's activity. There are two primary approaches employed by drug researchers in designing anticoagulants; 1) to directly inhibit thrombin with active site inhibitors or allosteric modulators such as hirudin and 2) to impede formation of thrombin by inhibiting the precursors in the coagulation cascade or by disrupting the metabolic pathway (indirect inhibition) such as heparin.[60-61]

Indirect inhibitors such as coumarin, dicoumarol, and warfarin are vitamin-K antagonists and have been some of the most commonly administered anticoagulants **(figure 04)**. These agents work by inhibiting synthesis of biologically active forms vitamin-K dependent clotting factors (fII, fVII, fIX, fX, protein C and protein S) of the coagulation system.[62-63] Carboxylation of these coagulation factors enhances their binding to

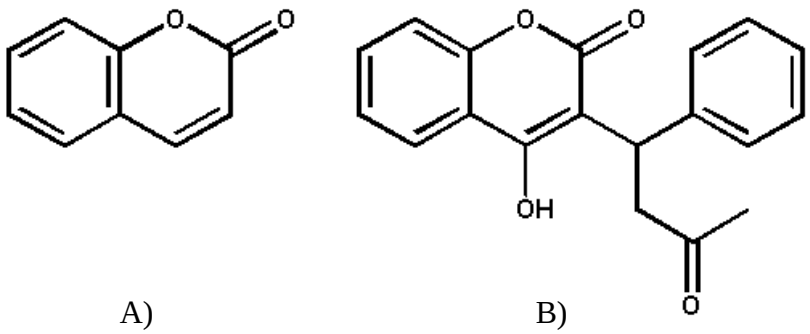

A) B)

Figure 04. Vitamin-K antagonist indirect inhibitors of thrombin
A) coumarin and B) warfarin

phospholipid surfaces, thereby accelerating blood coagulation.[64] For example, warfarin inhibits the vitamin-K epoxide reductase, which hampers the formation of reduced

vitamin-K required for γ-carboxylation of these clotting factors.[64-65] Heparin and low molecular weight derivatives of heparin (LMWH) are other indirect inhibitors frequently used in clinical settings **(figure 05)**.[66] Heparin is a sulfated GAG produced by mast cells, which activates the endogenous anticoagulant, AT.[67] Specific sequences in heparin and LMWH bind AT and bring about a conformational change in the endogenous inhibitor that leads to 1,000-fold acceleration in the rate of AT activity.[67-68] This is a two step process, which includes accelerated inhibition of fXa followed by a bridging mechanism of heparin, which brings thrombin and AT into close proximity.[62,69] The mechanism of inhibition varies slightly for each protease.

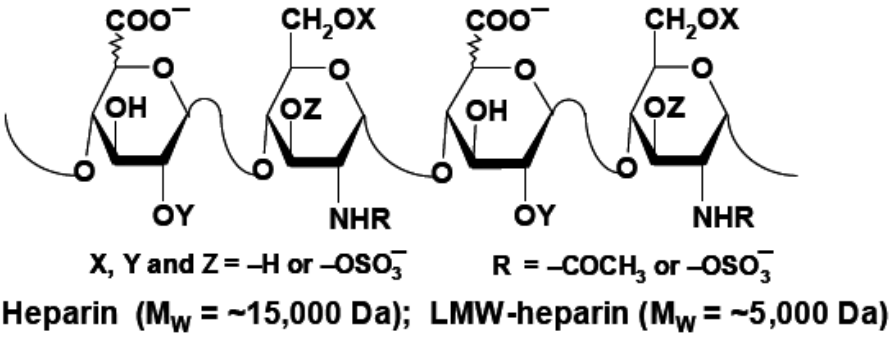

Figure 05. AT activator indirect inhibitors of thrombin
Heparin and low molecular weight heparins (LMWH)

Direct thrombin inhibitors such as hirudin, recombinant hirudin (lepirudin and desirudin) and bivalirudin bind at the active site and exosite I; whereas, argatroban and ximelagatran bind exclusively at the active site of thrombin bringing about disruption of the catalytic arsenal leading to cessation of thrombin activity **(figure 06)**.[70-73]

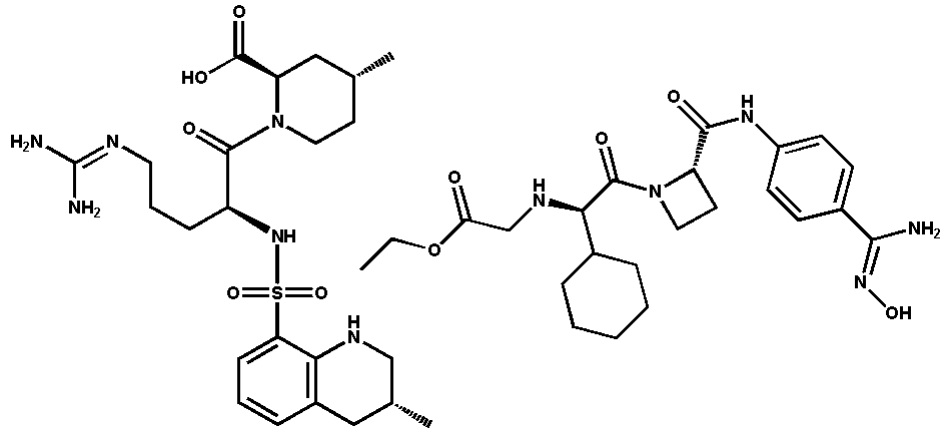

A) **B)**

Figure 06. Direct inhibitors of thrombin
A) Argatroban and B) Ximelagatran

1.8 Medical Role of Anticoagulant Therapy

The most promising application of a novel anticoagulant agent would be prevention of acute coronary syndrome (ACS), stroke and venous thromboembolism (VTE). ACS is an umbrella term covering a spectrum of clinical conditions ranging from unstable angina to acute myocardial infarction.[74-75] About every 26 seconds, an American encounters a coronary event, and about every minute one will die as a result of an acute thrombus obstructing the coronary artery.[76] A stroke, sometimes called a brain attack, occurs when a clot blocks the blood supply to the brain or when a blood vessel in the brain bursts.[77] Approximately 25% of all strokes are associated with aberrations in the cardiovascular system.[78] These abnormalities lead to the development of a secondary embolus that blocks the cerebral circulation resulting in ischemia and neuronal damage.[79-80] Cardioembolic strokes can be treated with anticoagulants following atrial fibrillation, intracardial thrombus or endocarditis.[81] About every 40 seconds someone in the US has a

stroke and every 4 minute someone dies of stroke.[76] VTE, 3rd most common cardio vascular (CV) illness refers to a number of medical conditions that result from abnormal thrombosis including deep vein thrombosis (DVT) and pulmonary embolism (PE).[62] About 1 million people are affected by VTE in the US alone.[77] VTE is caused by three major factors: blood hypercoagulability (excessive clotting), blood-flow stasis (immobility), and vessel wall damage (atherosclerosis).[62] Therefore, by modulating the activity of the hemostatic system, we can attempt to treat and prevent these serious and often fatal medical conditions. Novel anticoagulants that are safer and effective can potentially treat these conditions by inhibiting the circulating detached thrombi in patients with high risk factors such as race, hypertension, diabetes, and hypercholesterolemia.[78] Anticoagulant treatment is absolutely requisite in patients with predisposition for these conditions. Current available anti-thrombotic treatments require constant clinical monitoring due to the variation in individual response to the drugs.[79] These remedies minimize the risk of recurrent cardiovascular episodes, but accompany the risk of bleeding in part because they act systemically.[79] A new generation of anticoagulants with better efficacy and fewer side effects could potentially revolutionize the treatment options for thrombotic disorders.

1.9 Limitations of Current Anticoagulant Therapy

The current anticoagulant therapies are plagued with several limitations; heparin has poor subcutaneous absorption, variable effect due to binding to multiple plasma proteins, and the development of thrombocytopenia (decrease in normal levels of platelets).[62-63,80] LMWH, synthesized in an effort to improve the bioavailability and overcome the non-

specific plasma proteins interaction must be administered subcutaneously limiting their use for outpatient therapy, in addition the patient needs to be monitored on regular basis.[63,80] Smaller molecules and peptide derivatives suffer a set back due to one or several of the following factors; drug-drug, drug-food interactions, narrow therapeutic window, significant bleeding risk and inability to inhibit clot bound thrombin.[81] The need to develop highly desirable anticoagulants and an extensive knowledge of the coagulation cascade has guided the researchers to focus their attention on the common pathway of the coagulation system. In theory, any single enzyme in the coagulation cascade could be targeted to bring about the anticoagulation effect. However, fXa and thrombin, that are common to both the intrinsic and the extrinsic pathway, can be targeted resulting in a more effective anticoagulant.[82] Designing direct inhibitors of fXa appears to be an improved strategy to eliminate most of the side effects of current anticoagulants and make it viable to inhibit both the circulating as well as platelet bound fXa without affecting the platelet function.[83] Further, selective direct inhibitors of thrombin called as direct thrombin inhibitors (DTIs) can be designed to inhibit the free circulating as well as the clot bound thrombin.[63,84] Inhibitors of thrombin and fXa are fertile areas of exploration and are further advanced in development than most other candidates.[85-86]

1.10 Direct fXa Inhibitors

The amount of an activated coagulation factor produced from its inactive precursor amplifies at each stage of the coagulation cascade. Consequently, targeting fXa in the common pathway could be an effective approach for developing newer anticoagulants **(figure 07)**.[87] In addition, fXa is known to be the primary site of amplification; one

molecule of fXa catalyzes the formation of ~1000 thrombin molecules.[88] Currently available fXa inhibitor work through AT mediation, hence called indirect inhibitors (Fondaparinux and Idraparinux).[89-90] Direct fXa inhibitors (eg: rivaroxaban and apixaban) are AT independent and are 10,000 fold more selective for fXa over other related proteinases **(figure 08)**.[91-93] fXa inhibition results in down regulation of thrombin formation (not thrombin activity) via both the pathways by blocking the interaction with prothrombin.[94] This allows the circulating thrombin to perform its vital functions, thus potentially maintaining hemostasis at sites of hemostatic challenge. Another advantage of direct fXa inhibitors is that it inhibits free fXa as well as platelet bound fXa, which is part of the prothrombinase complex and clots.[94] Outside the coagulation system fXa has shown to exhibit proinflammatory activity.[95]

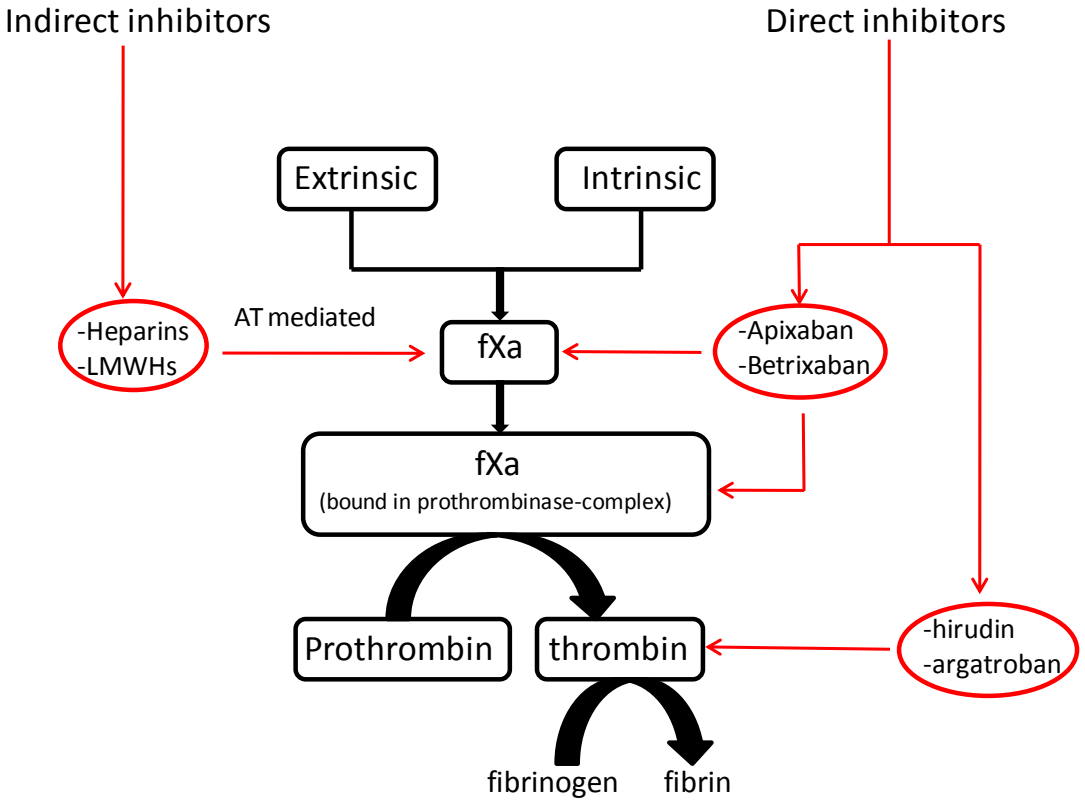

Figure 07. Pivotal position of fXa and thrombin in the coagulation cascade and mode of action of a few fXa and thrombin inhibitors.

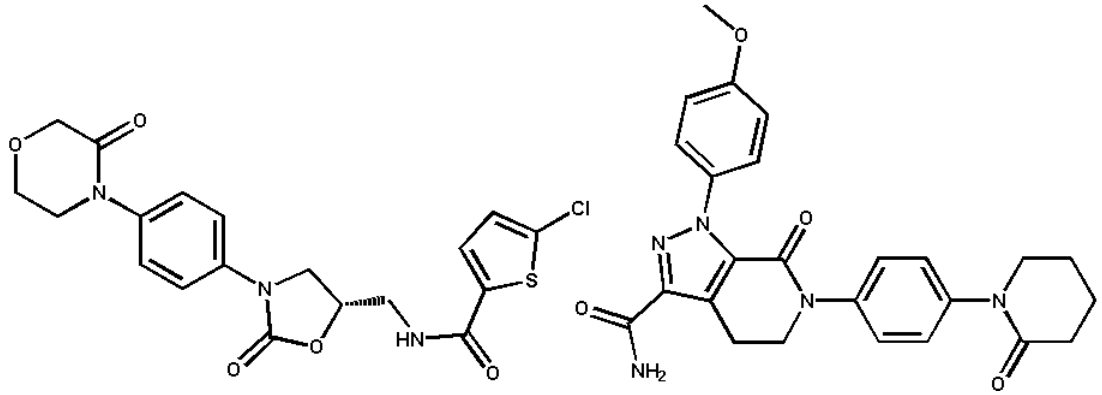

A) **B)**

Figure 08. Chemical structures of direct fXa inhibitors
A) Rivaroxaban and B) Apixaban

1.11 Direct Thrombin Inhibitors (DTIs)

Given the fundamental role thrombin plays in vasculature and platelet signaling, it can be rationalized that DTIs would have a positive outcome on vascular physiology. The most critical aspect related to thrombus formation is the evasion of clot bound active thrombin from its inhibitors such as heparin.[96] Thrombus thus serves as a reservoir of active thrombin, which amplifies its own generation by activation of fV, fVIII and fXI.[97] It can further stimulate thrombus growth by locally activating platelets and converting fibrinogen to clottable fibrin.[25-26] It activates fXIII to form stable clots and enhance resistance to fibrinolysis.[25-26] In addition, after discontinuation of heparin therapy, there can be a reactivation of the coagulation system as the fibrin-bound thrombin reactivates fX within the thrombus, prompting further thrombin generation.[98] Thrombin inhibition could thus lead to multiple effects for anticoagulation. DTIs (hirudin, lepirudin, argatroban, dabigatran) require no preceding interaction prior to their action on thrombin

unlike the indirect acting, which require AT mediation **(refer figure 07)**.[70-73] DTIs put a check on thrombin from interacting effectively with its substrates thus prevent fibrin formation, obstruct thrombin-mediated feedback activation, delimit thrombus growth, inhibit activation of platelet factor 4 (PF4), protein C and many other functions of thrombin.[99]

Thrombin also plays an important role in inflammation and cellular proliferation where DTIs may represent an adjuvant therapy **(figure 09)**.[100] DTIs can be univalent (interact with one site) or bivalent (interact with 2 sites).[101] Unlike direct fXa inhibitors DTIs fail to block thrombin generation. Both the DTIs and direct fXa inhibitors will provide more predictable anticoagulant responses because they are not bound to plasma proteins.

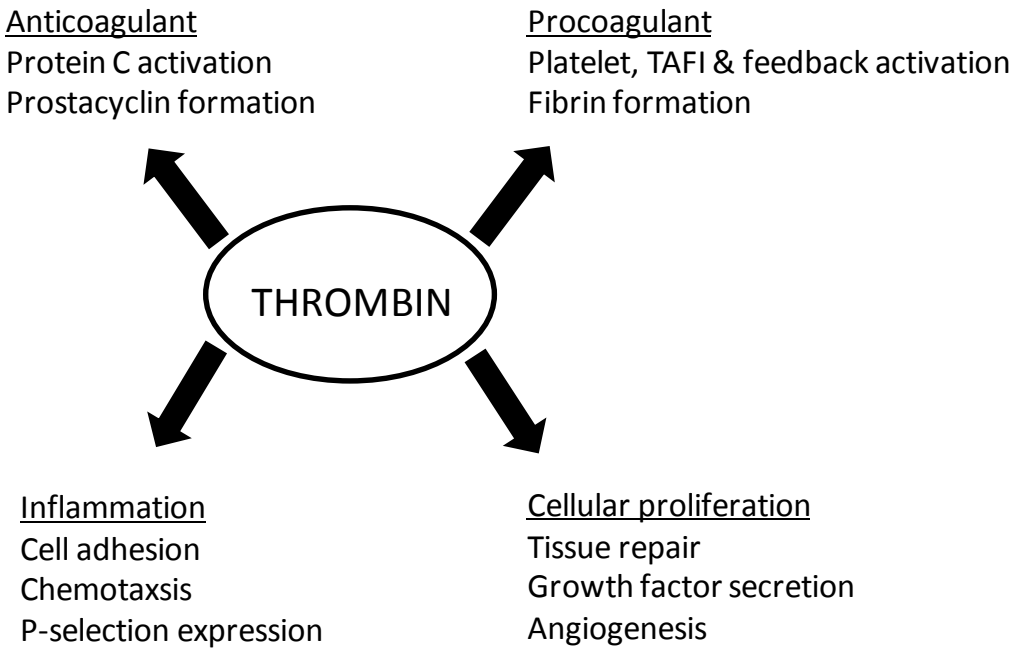

Figure 09. Various functions of thrombin within and outside the coagulation cascade[82]

1.12 Limitations of Current Direct fXa and Thrombin Inhibitors

DTIs, like hirudin, form a nearly irreversible bond with the enzyme.[71] An improvement in form of bivalirudin acts as a selective and reversible inhibitor of thrombin however; problems with parenteral delivery and rapid clearance have limited its use for a wider range of conditions.[102] These issues were addressed by new class of DTIs like melagatran, but were unsuitable for oral administration.[103] A prodrug of melagatran in form of ximelagatran had hepatotoxic and adverse cardiac effects.[104] In late 2010, USFDA had approved dabigatran but not without an added caution "life-threatening and fatal bleeding".[105] The oral fXa inhibitors have variable and transient effects on the prothrombin time.[106] A potential drawback of the newer anticoagulants is the lack of specific antidotes, shorter half life and lack of lab markers to monitor the drug activity.[107] Additionally, since there are no routine monitoring tests it will be difficult to determine whether suboptimal results are due to failure of therapy or poor patient compliance. It is evident that newer agents may change the future of anticoagulation therapy and provide improved patient care. With new opportunities will come new challenges, but the benefits of new oral anticoagulant offsets any drawbacks. The results of clinical trials with DTIs and direct fXa inhibitors validate both thrombin and factor Xa as potential targets, and there is no convincing evidence that one target is better than another.[108] Head-to-head comparisons will reveal any meaningful differences in efficacy or safety among the newer agents. Such assessment seems unlikely because of potential commercial risks. Even if one exhibits the superiority in targeting over the other, the variation will be more reflective of the dose and the pharmacological properties of the drugs rather than the drug target.

1.13 Bifunctional Inhibitors

From the preceding discussions it is clear that neither the DTIs nor direct fXa inhibitors can inhibit both generation and circulating (free and bound) thrombin, the mainstay in the formation of a clot. Hence, the theory of bifunctional inhibitors has been conceived, which will inhibit both the serine proteases simultaneously in the common pathway. Both the proteases can be inhibited by co-administering inhibitors specific for the enzymes. This proposition is not cost effective and will require preclinical and clinical trials to study drug interactions and side effects.[109] The other viable way for simultaneous inhibition of both the proteases is to design an inhibitor that would directly inhibit both thrombin and fXa. Such inhibitors with dual functionality are termed as bifunctional inhibitors. Bifunctional inhibitor is not a new concept in the field of anticoagulation, UFH inhibits both thrombin and fXa via the AT mediation. The disadvantage UFH carries along is its non-specific binding interactions with other proteins in the system leading to numerous side effects.[110] There are no bifunctional anticoagulant drugs on the market, though a few are in the drug discovery phase.

1.14 Structure of Thrombin

Thrombin has distinctive structural features that control specificity. A closer look at the surface reveals uneven charge distribution with localized positively and negatively charged pockets in (**figure 10)**.[111-112] There are four distinct binding sites on thrombin as depicted in **figure 11.** These sites recognize a variety of different molecules and present the diverse functions of thrombin.[40,44] All of the physiologic effects of thrombin are a

direct result of its catalytic activity.[114] Substrate specificity, however, is determined by several accessory binding domains that exist in clusters.[114]

1.14.1 *Active site*

This is the substrate binding site, which also mediates interactions with fibrinogen, protein C and AT-III. [112] The active site of thrombin is very similar to that of trypsin and chymotrypsin.[40-41] There are deeply situated specificity pocket (S1) that consists of the catalytic triad Ser195-His57-Asp102 surrounded by hydrophobic residues at the rim. Asp189 lining the S1 pocket electrostatically interacts with cationic substrates. S2 and S3 pockets are more hydrophobic and acidic respectively while the S4 pocket has a preference for aliphatic groups.[112]

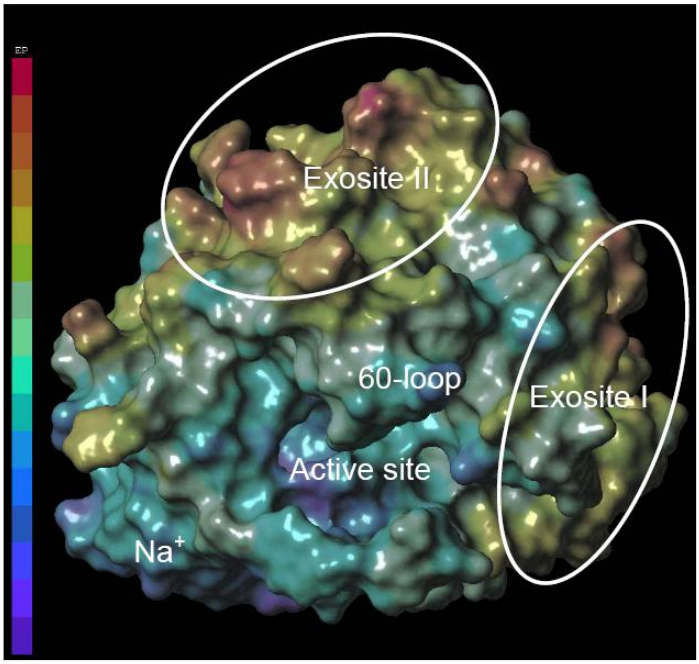

Figure 10. Thrombin surface electron density map with electrostatic potentials.[113]
The more basic the protein surface, the more red that area appears.

1.14.2 *Exosite I*

Also called as fibrinogen binding site, it is an anionic binding electropositive site.[112] Exosite I recognizes carboxyl terminal domain of hirudin, hirudin-like region of PAR-1 and fifth and sixth EGF-like domains of thrombomodulin.[115] It is located to the right of the thrombin active site cleft, mainly placed on the 70 to 80 loop and bordered by the 37-loop and segment Lys109-Lys110. In its center, the exposed side chains of Tyr76 and Ile82 form a hydrophobic cap, which is surrounded by side chains of several lysines and arginines interspersed by a few hydrophobic side chains. The strong positive charge is only partially compensated by the acidic residues Glu77 and Glu80 involved in an ionic cluster beneath the surface.[112]

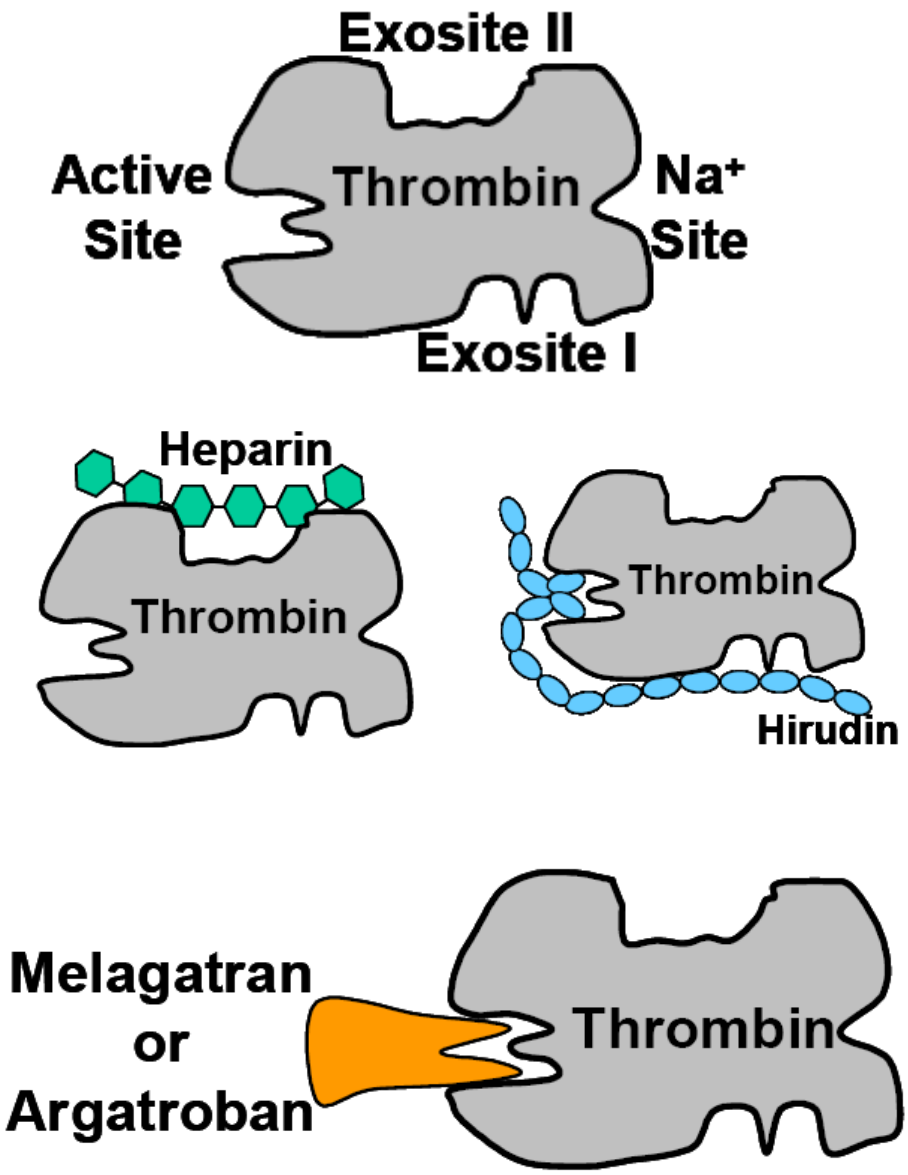

Figure 11. Cartoon representation of thrombin showing the four binding sites and different molecules recognizing them.[113]

Heparin binds at the exosite-II, hirudin binds to both the active site and fibrinogen recognition site (exosite-I) melagatran and argatroban binds at the active site.

1.14.3 *Exosite II*

Also called as the heparin binding site, it is the second electropositive, anionic binding site located opposite to exosite I.[112] Exosite II recognizes carboxyl terminal region of B-chain of thrombin and highly sulfated polysaccharide like heparin and chondroitin sulfate of thrombomodulin.[116] At this surface, a small hydrophobic Leu234-based channel is surrounded by basic residues Arg93, Arg101, Arg165, Arg233, Arg126, Lys236, Lys235, Lys240, and His91, with most of their side chain charges not compensated by adjacent negative charges. This uncompensated strong electropositive charge attracts polyanionic molecules like heparin to recognize exosite II.[112]

Both exosites differentially influence the active site and this allosteric effect plays a major role in the specificity and reactivity of thrombin towards its macromolecular substrates.[117] Exosites are located at approximately opposite ends of the thrombin molecule and approximately 10–20 Å away from the active site.[117]

1.14.4 *Sodium ion binding site*

Na^+ ion binding site has been confined to a site in the center of the 222 loop situated in a solvent-filled cavity behind the S1 specificity pocket located near Asp189.[112] The bound Na^+ ion, located more than 15 Å away from the catalytic triad, is coordinated in an octahedral manner by the carbonyl oxygens of Arg221 and Lys224 and by four internal water molecules, and is further stabilized by the negative charges of Asp221 and Asp222.[112] Thrombin has greater catalytic efficiency in the presence of Na^+ ions than in the absence of Na^+ ions.

1.15 Structure of fXa

The active site of fXa is smaller and less hydrophobic than the active site of thrombin.[118] Refer **figure 12** for active site of fXa. The active site is divided into four sub-pockets, S1 to S4. The major component of selectivity and binding is attributed to S1 sub-pocket. The S2 sub-pocket is small, shallow, not well defined and it merges with the S4 sub-pocket. The S3 sub-pocket is solvent exposed located on the rim of the S1 pocket. The S4 sub-pocket has three ligand binding domains, namely the hydrophobic enclave, the cationic hole and the water site. fXa inhibitors commonly bind in an L-shaped conformation, where one group of the ligand occupies the anionic S1 pocket lined by residues Asp189, Ser195, and Tyr228, and another group of the ligand occupies the aromatic S4 pocket lined by residues Tyr99, Phe174, and Trp228. Typically, a fairly rigid linker group bridges these two interaction sites.[118]

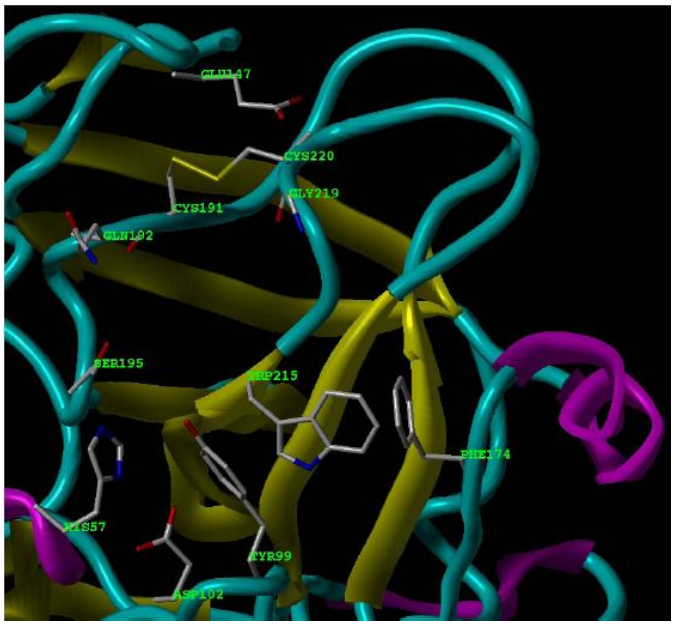

Figure 12. Active site of fXa with key residues displayed[113]

1.16 Conclusion

Normal hemostasis is essential for regulation of blood flow. An improperly regulated hemostasis can cause hemorrhage or thrombosis leading to life threatening conditions. Thrombosis occurs due to excessive hemostasis and a thrombus thus formed can lead to stroke, venous thromboembolism or arterial thrombosis, which are leading causes of death worldwide. Thrombus formation is a product of excessive generation of thrombin in the coagulation cascade, which in turn is regulated by numerous other coagulation enzymes. In the coagulation cascade, activating the AT or inhibiting the up-regulated coagulation enzymes in intrinsic and extrinsic pathways can be targeted to indirectly impede the formation of thrombin. Current antithrombotic agents that work through indirect inhibition prevent the formation of thrombus, thus reducing the risk of recurrent cardiovascular events but not without serious side effects. The major set back is the non-selectivity of these drugs for the target and their inability to inhibit clot bound thrombin. Targeting fXa and thrombin, which are common to both the intrinsic and extrinsic pathways could result in a better anticoagulant as they would inhibit both free and clot bound thrombin. Direct fXa and thrombin inhibitors are fertile areas of research where a mono- or bifunctional inhibitors concept has been envisioned but has been largely remained unsuccessful in delivering an ideal anticoagulant. Hence, there still exists the need to design a potent anticoagulant with minimal side effects.

CHAPTER 02

Identification of an Optimum Size of DHP as a Lead for Structure-based Drug Design

2.1 Background

Hypercoagulability increases the risk of inappropriate or excessive thrombus (blood clot) formation resulting in serious disseminated intravascular coagulation (DIC), venous thrombosis, thromboembolism, cardiovascular complications, or in some cases multiple organ failure.[62,74-75,81] Current anti-thrombotic therapies are able to reduce the risk of recurrent cardiovascular events, but not without serious side effects, the most widespread of all being bleeding.[62-63,80] One of the major reasons for this has been attributed to the non-specific binding of these drugs to plasma proteins. [62-63,80] The quest to discover more cost effective and safer drug has led researchers to explore deeper into understanding the specific mechanism and role of each step in the entire coagulation system. Years of research and experience has resulted in numerous drugs targeting different and multiple coagulation factors, yielding an enhanced perception of the need for development of better and efficient drugs. Specifically targeting the common pathway in the coagulation cascade is one such fruit of our conception. There are few drugs that specifically act on the proteinases, thrombin and fXa in the common pathway but most are in pre-clinical or clinical evaluation stage.[70-73,89-93] These and the ones that are approved continue to inherit the complications from their early ancestors. Hence, the need still exists to develop new and improved anticoagulant agents that would eliminate the poor traits of their early ancestors.

Advancement in this direction has been challenging as there are numerous hurdles that have been dragging back the entire drug development process. It is important that the new drugs reduce excessive bleeding, liver toxicity, inhibit both free and clot-bound thrombin. It also necessitates investigating, which inhibition strategy will yield more efficient results in inhibition of thrombin, the ultimate and pivotal proteinase in the coagulation cascade. Will inhibiting either of the one proteinase, thrombin and fXa or simultaneous inhibition of both would be more efficacious? We don't know but regardless, numerous unanswered questions make the field anticoagulation drug design extremely exciting, compelling and challenging.

2.2 Rationale

All the anticoagulants used today have severe side effects, which may even lead to death. The most common anticoagulants used for treatment of thrombotic disorders are heparin in its unfractionated form or LMWH and coumarins (warfarin).[63,80] The heparins have risks of bleeding and heparin-induced thrombocytopenia (HIT).[80,118] Fondaparinux and idraparinux, a heparin pentasaccharide; peptidomimetics like agratroban, ximelgatran and razaxaban; and hirudins like desirudin and bivalirudin showed to lower these risk factors but still possessed the negative traits of their precursors.[70-73,89-93] In addition, patient variability, narrow therapeutic index, drug-interactions, immunological reactions, liver toxicity and high cost to benefit ratio limits the effective use of these drugs in patients with thrombotic conditions.[81]

For more than three decades the anticoagulant drug discovery has revolved around heparin and its derivatives, possessing a polysaccharide backbone. Our lab has take a step forward in this field by designing molecules, which are not heparin-based (non-polysaccharide) and they act through either through activation of AT or direct inhibition of thrombin and fXa.[119-121] As a proof of concept our lab has shown that linear polyacrylic acids (PAA), which have only the carboxyl functionality, were able to bind AT with poor affinities resulting in acceleration of the inhibition of thrombin and fXa.[122-123] PAA do not have a polysaccharide backbone and they are devoid of sulfates too! Later, to improve the affinity a more rigid skeleton like a phenyl ring with functional group that can be derivatized to a sulfated was chosen. The carboxylic functionality was retained for it to be amenable for structural modification to be transformed into an orally available drug. Based on these features three types of synthetic lignins called as dehydropolymers (DHPs) were synthesized enzymatically and later sulfated.[124-125] The three precursors chosen for enzymatic reactions were caffeic acid, ferulic acid and sinapic acid and the sulfated polymers were termed as CDS, FDS and SDS. DHPs are structurally dissimilar from all the current anticoagulants. The oligomeric, polyanionic, polydisperse and micro-heterogeneity of DHPs are similar to that of heparin while the aromatic backbone is a distinct feature. All three DHPs showed direct dual inhibition of thrombin and fXa through exosite-2 mediation on thrombin.[123-124] CDS was the most potent of the 3 DHPs and SDS the least. It has also been shown that the unsulfated DHPs were a weaker anticoagulant as compared to its sulfated counterpart.[123]

DHPs as a dual inhibitor were completely a new class of anticoagulant and it was imperative to determine what in this mixture could have dictated the activity. This inspiration comes from heparin where a specific sequence such as the pentasaccharide dictates its activity as an anticoagulant **(figure 13)**. To elucidate this aspect we conducted chain length dependence studies on our sulfated and unsulfated DHPs. This chapter talks about the importance of the sulfates groups in context of our DHPs and the effective size of a working lead molecule, which would be a more potent anticoagulant possibly carrying fewer side effects.

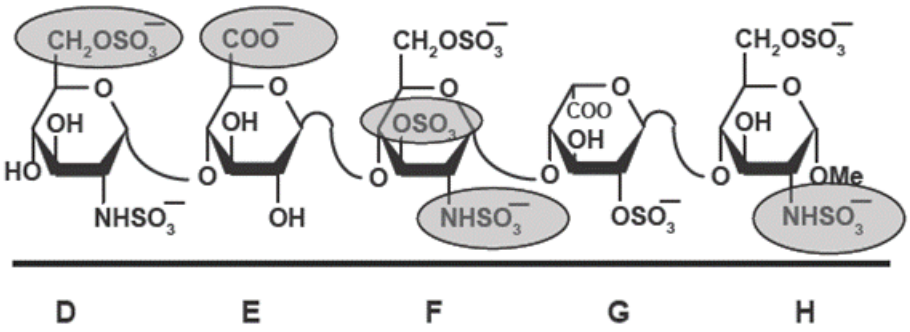

Figure 13. Structure of pentasaccharide binding sequence.

2.3 Experimental Methods

2.3.1 Proteins, biologicals and chemicals

Horseradish peroxidase (HRP) with activity of 250–600 330 U/mg (Sigma, St. Louis, MO). Human plasma proteinases, fXa, and α-thrombin (Haematologic Technologies, Essex Junction, VT). Chromogenic substrates purchased from American Diagnostica (Greenwich, CT): Spectrozyme fXa (Methoxycarbonyl-*D*cyclohexylglycyl-Gyl-Arg-*p*-nitroanilide) Spectrozyme TH (H-*D*hexahydrotyrosol-Ala-Arg-*p*-nitroanilide). Stock

solutions of proteins were prepared as follows: For fXa 20 mM Sodium phosphate buffer, pH 7.4, 0.1mM EDTA, 0.1% PEG 8000 For thrombin 20 mM Tris-HCl buffer, pH 7.4, containing 100 mM NaCl and 2.5 mM $CaCl_2$, 0.1% PEG 8000. Pooled citrated human plasma for coagulation time assays (Valley Biomedical Winchester, VA). Activated partial thromboplastin time reagent containing ellagic acid (APTT-LS), thromboplastin-D and 25 mM $CaCl_2$ (Fisher Diagnostics Middletown, VA). Competitive ligands used - Exosite 1 ligand Tyr63-sulfated hirudin-(54-65) labeled with 5-(carboxy)fluorescein ([5F]-Hir[54-65](SO3-)). Exosite 2 ligand unfractionated porcine heparin (Sigma-Aldrich St. Louis, MO). 30% hydrogen peroxide, TEAST complex, ferulic acid (FA) and caffeic acid (CA) were from Sigma (St. Louis, MO). Enoxaparin (MR 4,500) (Aventis Pharmaceuticals). All other chemicals were of analytical reagent grade from either Aldrich Chemicals (Milwaukee, WI) or Fisher (Pittsburgh, PA) and used without further purification.

2.3.2 Oxidative coupling and sulfation of 4-hydroxycinnamic acid derivatives

The DHPs of CA and FA were prepared by the so-called 'zutropfverfahren' procedure. Briefly, in a three-neck flask slow addition of 200mL CA or FA (25mM in 10mM sodium phosphate buffer pH 8.0) and 100mL H_2O_2 (75mM in the same buffer) to a 50mL solution of HRP (10mg in the same buffer) was carried out at room temperature (RT) and in dark over a period of 5 hours. Three additional aliquots of H_2O_2 (75 mM) were added over the next 72 h. At the end of polymerization the solution was freeze-dried, redissolved and desalted to obtain the CD and FD polymers.

DHPs were sulfated with TEAST complex. Briefly, the lyophilized DHP sample (50 mg) was dissolved in dry DMF (15 mL) containing TEAST (200 mg) and stirred for 24 h at 60 °C. After the removal of most of the DMF in vacuo, the remaining product was taken up in 30% aqueous sodium acetate, the sodium salt precipitated using ~10 volume of cold ethanol. The precipitated product was further purified with dialysis using Amicon dialysis membrane (MWCO 3-30K).

2.3.3 Fractionation of CD and FD using centrifugal filtration

The polymerization reaction mixture was dissolved in deionized water and filtered through Millipore filter (NMWC 30 kDa) at 4000 *g*. Filtration was continued until the retentate volume was approximately 200 μL. This process was repeated five more times and the final retentate was labeled as **F30** fraction. The filtrates from the above process were pooled, lyophilized, redissolved in deionized water and then further fractionated in the manner described above using a 10 kDa filter. The retentate so obtained was labeled as **F10** fraction. This process was repeated to obtain **F5** and **F3** fractions using 5 and 3 kDa membranes. The retentates were collected and lyophilized to obtain four fractions in yields of 15-20, 5-8, 3-5, and 1-2%, respectively.

2.3.4 Sulfation of the DHP fractions

All the DHP fractions were sulfated using triethylamine–sulfur trioxide complex. Briefly, each fraction of DHP sample (50 mg) was dissolved in dry DMF (15 mL) containing triethylamine–sulfur trioxide complex (200 mg) and stirred for 24 h at 60 °C. After the removal of most of the DMF under high vacuum, the remaining product was taken up in

30% aqueous sodium acetate. This was followed by precipitation of the sodium salt using ~10 volumes of cold ethanol. The precipitated product was further purified using Millipore filter (NMWC 3-30 kDa) at 4000 *g*.

2.3.5 Structural characterization

2.3.5.1 Determination of molecular weight of sulfated and unsulfated DHP fractions

The number and weight average molecular weight of unsulfated DHP fractions was measured using gel permeation chromatography (GPC). Size exclusion chromatography (SEC) was employed in case of sulfated DHP fractions for determination of peak average molecular weight. In both cases the system was composed of LC10Ai pumps and a SPD-10A VP UV-vis detector controlled by a SCL-10A VP system controller connected to a computer. For SEC each fraction was analyzed using Asahipak GS320 HQ column with an isocratic flow rate of 0.7 mL/min of 0.1 N NaOH at pH 11.0. Polystyrene sulfonate standards (PSS) were used for calibration purposes. For GPC each fraction was analyzed using Phenogel 5 μ (Phenomenex, Torrance, CA, 7.6 mm i.d. x 300 mm). The mobile phase consisted of 100% tetrahydrofuran at a constant flow rate of 0.7 mL/min. Polystyrene standards (PS) were used for calibration purposes. The relationship between logarithm of the molecular weight and the elution volume (V) of the standards was found to be linear with a correlation coefficient of 0.98 and 0.99. The wavelength of detection for CD and FD fractions was set at 280 nm. Each chromatogram was sliced into 1000 time periods providing 1000 M_R with the corresponding absorbance (A) values. These values were used to calculate number average molecular weight (M_N), weight average

molecular weight (M_W) and polydispersity (P) parameters from equations 1, 2, and 3, respectively, for each fraction.

$$M_N = \frac{\sum A_i \times M_i}{\sum A_i} \quad \ldots\ldots (1) \qquad M_W = \frac{\sum A_i \times M_i^2}{\sum A_i \times M_i} \quad \ldots\ldots (2)$$

$$P = \frac{M_W}{M_N} \quad \ldots\ldots (3)$$

2.3.5.2 Elemental analysis

Elemental Analysis of DHP samples was obtained from Atlantic Microlabs (Norcross, GA).

2.3.5.3 NMR

^{1}H- and ^{13}C- NMR spectra were recorded with a Bruker AVANCE II 400 FT-NMR (400 MHz) spectrometer in water-*d* and DMSO-*d* for sulfated and unsulfated fractions with tetramethylsilane (TMS) as an internal standard. Chemical shifts (δ) are reported in δ-values (ppm).

2.3.6 Prothrombin time and activated partial thromboplastin time

Clotting time was determined in a standard 1-stage recalcification assay with a BBL Fibrosystem fibrometer (Becton-Dickinson, Sparles, MD). For PT and APTT assays, the reagents were pre-warmed to 37 °C. For PT assays, 10 µL of the anticoagulant (or the

reference molecule) was mixed with 90 µL of citrated human plasma, incubated for 30 s at 37 °C quickly followed by addition of 200 µL pre-warmed thromboplastin. For APTT assays, 10 µL of the anticoagulant was mixed with 90 µL citrated human plasma and 100 µL 0.2% ellagic acid. After incubation for 240 s, clotting was initiated by quickly adding 100 µL of 25 mM $CaCl_2$. Each experiment was performed in duplicate. The averaged data was fitted using a quadratic equation to calculate the concentration of the anticoagulant necessary to double the clotting time (2 × PT or 2 × APTT).

2.3.7 Proteinase inhibition

Direct inhibition of thrombin and fXa by sulfated and unsulfated DHP fractions was determined through a chromogenic substrate hydrolysis assay. For these assays, a 10 µL DHP fraction at several different concentrations was diluted with appropriate buffer system in a PEG 20,000 coated polystyrene cuvettes. This was followed by addition of the 5µL of proteinase, thrombin (960nM) or fXa (1µM) and incubated at 37°C for 10 minutes. Following incubation, 10µL of spectrozyme TH (2mM) or spectrozyme fXa (5mM) was rapidly added and the residual thrombin activity was quantified by measuring the initial rate of hydrolysis from the linear increase in absorbance at 405 nm as a function of time under conditions wherein less than 10% substrate is consumed. Relative residual proteinase activity at each activity measured under otherwise identical conditions, except for the absence of the inhibitor. Logistic equation 4 was used to fit the dose dependence of residual proteinase activity to obtain IC_{50}.

$$Y = Y_O + \frac{Y_M - Y_O}{1 + 10^{(\log[L]_O - \log IC_{50}) \times HC}} \quad \ldots\ldots (4)$$

In this equation Y is the ratio of residual thrombin activity in the presence of the inhibitor to that in its absence; Y_M and Y_0 are the maximum and minimum possible values of the fractional residual thrombin activity, respectively; IC_{50} is the concentration of the inhibitor that results in 50% inhibition of enzyme activity, and HS is the Hill slope. HS does not represent co-operativity because the sulfated and unsulfated DHP fractions are a highly complex species that may possess multiple binding modes and geometries. Sigmaplot 9.0 (SPSS, Inc. Chicago, IL) was used to perform non-linear curve fitting in which Y_M, Y_O, IC_{50} and HS were allowed to float.

2.3.8 Mechanistic studies

2.3.8.1 *Michaelis-Menten kinetics*

Several concentrations of Spectrozyme TH (0.25 to 25 μM) were treated with 4 nM thrombin in presence of fixed concentration of inhibitor (0 - 5 μg/mL). The initial rate of substrate hydrolysis was monitored from the linear increase in A_{405} in 20 mM Tris-HCl buffer, pH 7.4, containing 100 mM NaCl, 2.5 mM $CaCl_2$ and 0.1 % PEG 8000 at 25 °C. The data obtained was fitted by the standard Michaelis-Menten equation to calculate that apparent K_M and V_{MAX}.

2.3.8.2 *Competitive binding studies with exosite ligands [5F]-Hir[54-65](SO_3-) or porcine heparin*

Inhibitor-dependent thrombin inhibition studies in the presence of [5F]-Hir[54-65](SO_3-) or porcine heparin were performed in a manner similar to that described above using the chromogenic substrate hydrolysis assay. Briefly, a solution of inhibitor over several

different concentrations and thrombin (4nM) was incubated for 10 minutes at 37°C with either [5F]-Hir[54-65](SO_3-) (0 and 86 nM) or porcine heparin (0, 20 and 100 μM) in 20 mM Tris-HCl buffer, pH 7.4, containing 100 mM NaCl, 2.5 mM $CaCl_2$ and 0.1 % PEG 8000. Following incubation, Spectrozyme TH was added to yield a final concentration of 20μM and its hydrolysis was measured as the initial change in absorbance at 405. The molecular weight of bovine heparin was assumed to be 15000, as reported in the literature. The dose-dependence of the fractional residual proteinase activity at each concentration of the competitor was fitted by equation 04 to obtain the apparent concentration of inhibitor required to reduce thrombin activity to 50% of its initial value ($IC_{50,app}$).

2.3.9 *Cellular toxicity studies*

The alamar blue assay was performed with a fluorimetric method using HepG cells in a 96-well plate. The wells contained 100 μL of medium containing cells to which 10 μL of alamar blue was added and incubated for 4 hours at 37°C. The plates were exposed to an excitation wavelength of 531 nm and the emission at 590 nm was recorded on a Perkin Elmer fluorimeter. The percent viability was expressed as fluorescence emitted by treated cells compared to control (medium or vehicle only).

2.4 Results

2.4.1 Synthesis of unsulfated and sulfated DHPs and its fractions

Based on our earlier reports from our work we know that sulfated DHPs of CA (CDS) and FA (FDS) were potent dual inhibitors of thrombin and fXa. Both are a heterogeneous and complex mixture of molecules containing variety of chain lengths and linkages posing a hindrance in identification of the effector molecule. To identify the optimum chain length, which can be further optimized we decided to synthesize them on large scale. Both CD and FD were synthesized from their respective starting monomers using oxidative coupling reaction using an enzyme, HRP **(figure 14)**. This reaction generates free radical intermediates, which reacts with monomers to form a coupled product. This reaction persists until stopped to form longer oligomers and possibly variable linkages at the point of attachment. β-O-4 and β-5 type of linkages are easily feasible with this type of reaction as also seen in natural lignins which contain high amount of these linkage-types in addition to others.

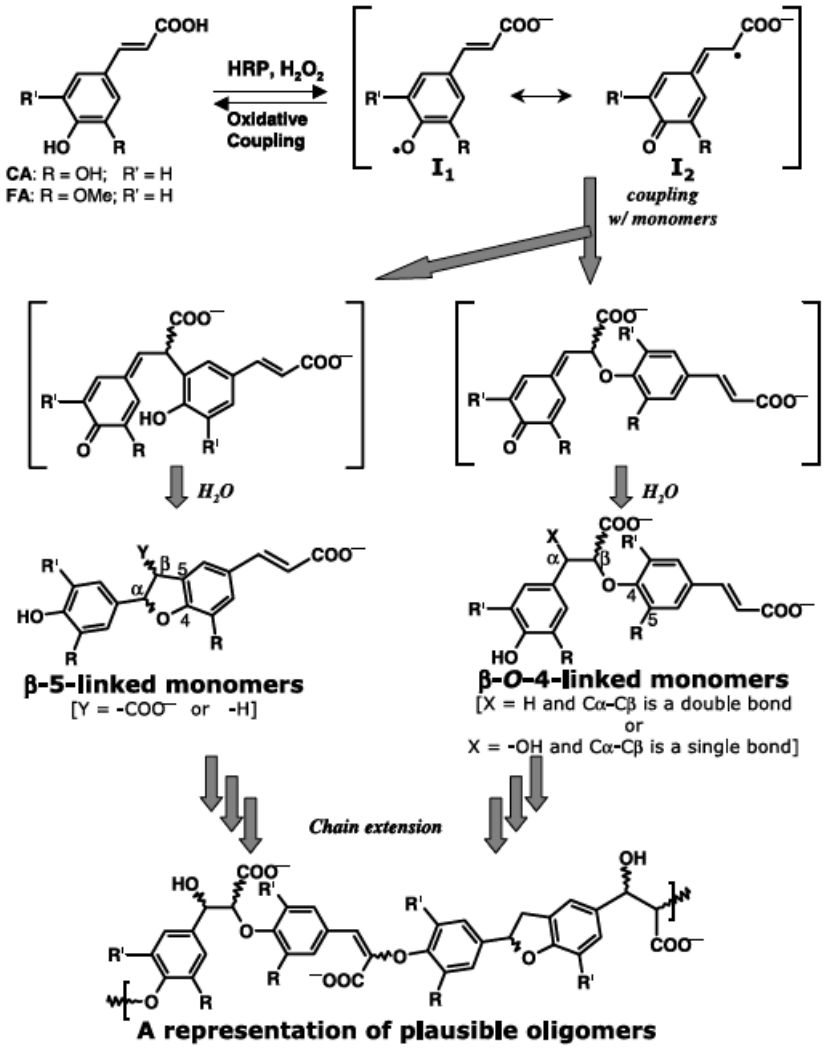

Figure 14. Chemo-enzymatic synthesis of 4-hydroxycinnamic acid-based dehydropolymers (DHPs), CD and FD.
Horseradish peroxidase (HRP)-catalyzed oxidative coupling of caffeic acid (CA) or ferulic acid (FA) in the presence of H_2O_2 generates oligomers of size 3–34 U. Phenolic oxidation generating radical intermediates I1 and I2 couple with starting material to give oligomers with different types of inter-monomeric linkages. The most common linkages formed include *β-O-4* and *β-5*.[124]

MWCO filters (30kDa to 3kDa) where they were fractionated based on their molecular size **(figure 15)**. In all, five samples of each DHP were obtained from this exercise. The samples that passed through the MWCO filter 3kDa were discarded as it would contain high amount of salt and unreacted starting material, if any.

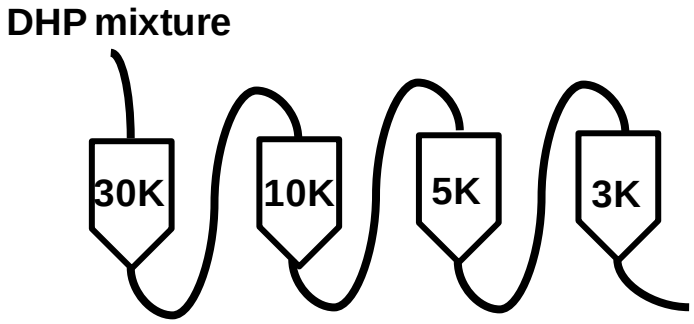

Figure 15. Fractionation of CD and FD using MWCO filters ranging from 30 – 3 kDa

Further 50mg of all 10 samples were subjected to sulfation to yield the sulfated counter part of each DHP. DHPs were sulfated using TEAST complex under conditions established earlier in our lab and a brief description can be found in the methods section. In this reaction the free hydroxyl and the free phenolic groups are sulfated **(figure 16)**. Introduction of sulfate groups impart a greater anionic character to the DHPs.

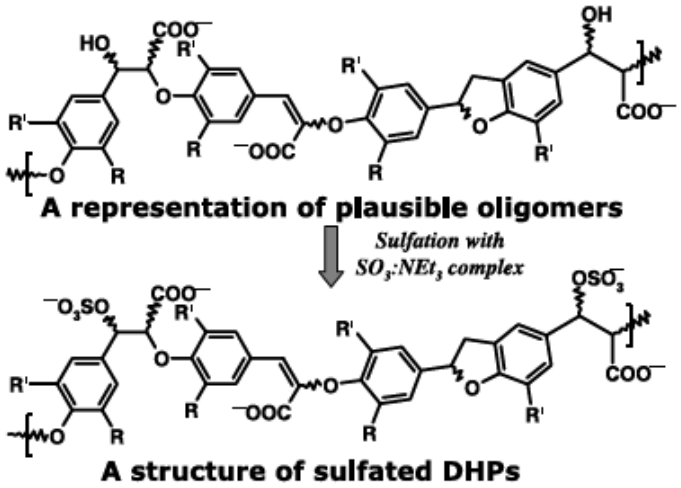

Figure 16. Sulfation of CD and FD using triethylamine sulfur-trioxide complex

2.4.2 Molecular weight and size determination

To determine molecular weight of the sulfated and unsulfated DHPs and its fraction SEC and GPC respectively were employed. PS and PSS standards were used for GPC and SEC methods respectively **(figure 17)**. In both cases DHPs of FA were found to be larger in size, generating longer chains. The peak average molecular weight (M_P) of unsulfated CD fractions ranged from 900 to 2210 while for FD fractions it was found to be 750 to 7700. The M_P of sulfated CD fractions ranged form 950 to 2890 while for sulfated FD fractions it was less than 1550 to 9780. Chain lengths were calculated by dividing the M_P by the molecular weight of the starting monomer, which was in turn back calculated from the standard curve, obtained using PS. The molecular weight of the CA and FA were determined to be 262 and 226 respectively. The average peak chain length for CD fractions using PS standards ranged from 3.4 to 8.4 whereas, for FD oligomers it was found to range from 3.3 to 24.0 **(Table 01)**. This implies the wider chain distribution pattern for FD fractions (7.3-fold) and CA (2.5-fold). The apparent molecular weight calculated for sulfated fractions using SEC were found to be the lowest for 3CDS (950) and highest for 30FDS (9780). Further, the difference in the molecular weights of the sulfated and the unsulfated DHPs obtained by SEC and GPC gives an apparent molecular weight of the total number of sulfates that might be present. Using the difference and dividing it by the chain length we can calculate the apparent number sulfates groups on DHPs **(Table 02)**. The apparent average number of sulfates for all CD fractions was determined to be 3 sulfates per dimer with the exception of 3CD having 0.2 sulfate per monomer. A similar calculation for FD fractions revealed an average of 1 sulfate per dimer for all fractions. The average number of sulfates for the parent mixture of DHPs of

both CA and FA were 1 and 0.5 sulfate per monomer. Overall, this indicates that CD fractions are smaller in size (~3-fold) and more sulfated (2-3-fold) than the FD fractions, overall imparting a more anionic character to them. The M_N values for the unsulfated CD and FD fractions ranged from 1052 to 7558, while M_W was found to be in the range of 2084 and 16464. This when compared with M_P values indicate the presence of greater number of smaller chains in the mixture. Refer **Table 01** below for all the molecular weight characteristics for each fraction of the unsulfated DHPs and their chain lengths.

Table 01: Molecualr weight characterization of CD and FD fractions

	M_N[a] (Da)	M_W[a] (Da)	M_P[a] (Da)	P[b]	L_R[c]
FD_3	1270	5299	750	4.2	3.3 (1-25)[c]
FD_5	2750	9690	1300	3.5	5.7 (1-44)
FD_{10}	4997	13209	2650	2.6	11.7 (1-58)
FD_{30}	7558	16464	7700	2.2	34.0 (1-72)
FD_{MIX}	5322	11525	5440	2.2	24.0 (1-49)
CD_3	1052	2084	900	2.0	3.4 (1-9)
CD_5	1629	6927	1100	4.3	4.2 (1-28)
CD_{10}	2484	8588	1470	3.5	5.6 (1-46)
CD_{30}	3937	12788	1980	3.2	7.6 (1-50)
CD_{MIX}	4264	13272	2210	3.1	8.4 (1-51)

[a]Number, weight, and peak average molecular weights were obtained by GPC analysis. [b]Polydispersity. [c]The peak average chain length was calculated from the ratio of M_P and molecular weight of the two monomers calculated using PS standard curve. Numbers in brackets refer to the range of chain lengths (see Experimental Methods).

Table 02: [a]Peak average molecular weights obtained by GPC analysis (see Experimental Methods).

	M_P S (Da)	M_P US (Da)	M_P (S-US) (Da)	S_T	L_R	S/unit
FA		226.4[a]				
CA		262.1[a]				
03FD		750			3.3	
05FD	1550	1300	250	3.1	5.7	0.54
10FD	3170	2650	520	6.5	11.7	0.56
30FD	9780	7700	2080	26.0	34.0	0.76
FD	6350	5440	910	11.4	24.0	0.47
03CD	950	900	50	0.6	3.4	0.18
05CD	1690	1100	590	7.4	4.2	1.76
10CD	2200	1470	730	9.1	5.6	1.63
30CD	2880	1980	900	11.3	7.6	1.49
CD	2890	2210	680	8.5	8.4	1.01

M_P S refers to peak average molecular weight of sulfated fractions obtained by SEC analysis.
M_P US refers to peak average molecular weight of unsulfated fractions obtained by GPC analysis.
M_P (S-US) refers to peak average molecular weight of sulfate(s) obtained by subtracting unsulfated fractions from the sulfated ones.
S_T refers to total number of sulfates present obtained by dividing peak average molecular weight of sulfate(s) by calculated molecular weight of sulfate.
L_R refers to peak average chain length calculated from the ratio of M_P and molecular weight of the two monomers calculated using PS standard curve.
S/unit refers to apparent number of sulfates calculated from the ratio of total number of sulfates *(S_T)* and peak average chain length *(L_R)*.

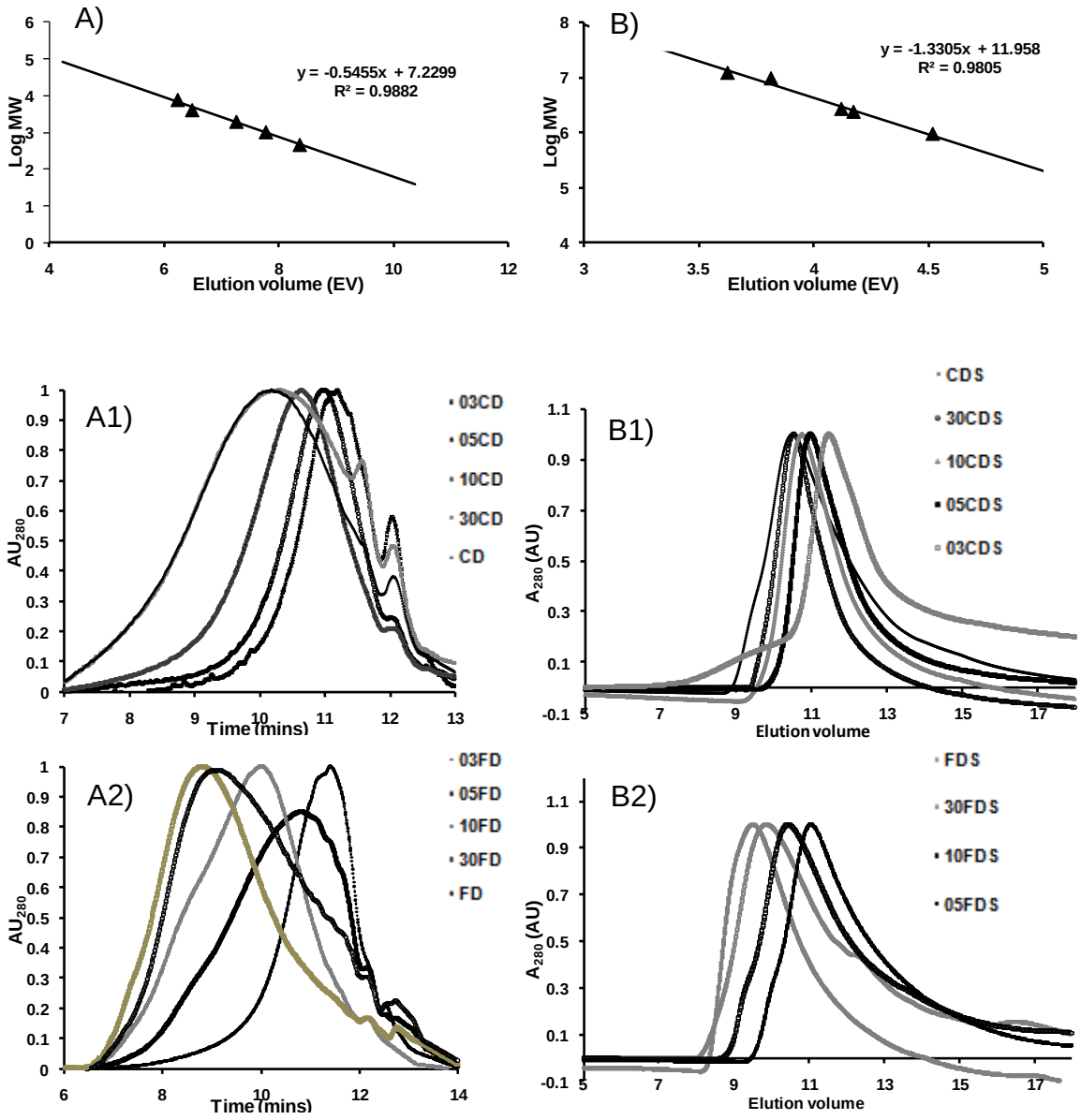

Figure 17. GPC and SEC of CD and FD fractions using PS and PSS as standards, respectively.

A) & B) represent the linear curve obtained using PS (using GPC) and PSS (using SEC), respectively. A1) & A2) are the chromatograms acquired using GPC for CD and FD fractions, respectively. A2) and B2) are the chromatograms acquired using SEC for CDS and FDS fractions, respectively.

2.4.3 Elemental analysis

To assess the level of sulfation elemental analysis was carried out to determine the composition of each element. Average chain length determined by GPC was used to calculate the theoretical number of sulfates for all samples. The number of sulfates for CDS30, CDS10, FDS30 and FDS10 using elemental analysis were found to be 0.38, 0.33, 0.2 and 0.16 per monomer which were fairly similar compared to the theoretical numbers **(Table 03)**. The difference arises due to the heterogeneous nature of the samples making it extremely difficult to assign an exact size or composition. There is a ~2-fold difference in the level of sulfation between each group, CDS30-FDS30 and CDS10-FDS10.

Table 03: Elemental Analysis of sulfated fractions of DHP

	C (%)	H (%)	O (%)	S (%)	S/unit
30CDS	44.9 (51.1)[a]	3.1 (3.7)	37.1 (39.1)	5.8 (5.7)	0.38
30FDS	52.7 (56.1)	4.4 (4.4)	34.7 (36.3)	3.2 (3.2)	0.20
10CDS	46.1 (52.3)	3.5 (3.7)	35.6 (38.7)	5.1 (5.2)	0.33
10FDS	48.4 (57.0)	4.4 (4.4)	36.4 (35.9)	3.0 (2.7)	0.16
05CDS	49.0 (54.1)	3.2 (3.9)	35.0 (38.0)	3.6 (4.0)	0.25

[a]Number in brackets show the predicted composition of a homogenous *β-O-4*-linked oligomer of appropriate sulfated DHP fraction. The peak average chain length was used in these calculations are represented in **Table 02**.
S/unit refers to average number of sulfates per monomeric unit, which was calculated from elemental sulfur composition and the size of an average unsulfated oligomer.

2.4.4 NMR

The ^{1}H NMR spectra of parent DHPs showed the presence of broad peaks (not shown), which on fractionation to lower molecular weight did not resolve enough for structural assignments **(figure 18A)** indicative of a polydisperse nature. The quantitative ^{13}C NMR like the ^{1}H was only indicative of the functional group type present in the DHP mixture **(figure 18B)**.

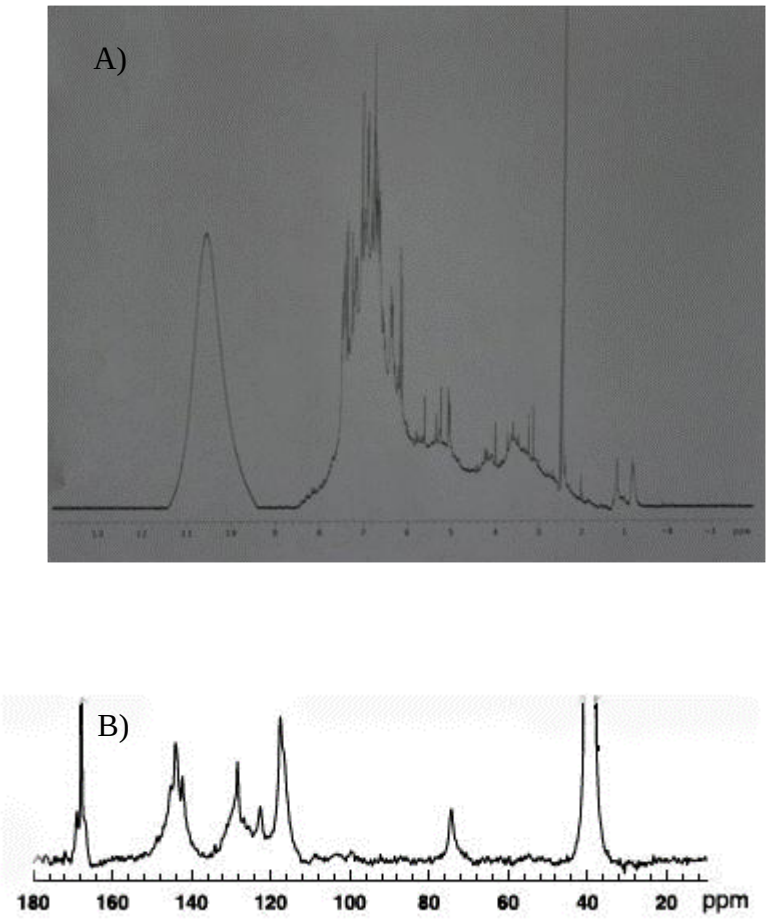

Figure 18. A) ^{1}H NMR spectra of FD and B) quantitative ^{13}C NMR spectra of CD both in DMSO-d6.
Four regions are apparent in both the spectra, the carboxylic acid region between 10-11ppm in ^{1}H or 160-170 ppm in ^{13}C, the aromatic and vinylic peaks between 6-8ppm in ^{1}H or 100-160 ppm in ^{13}C, the α and β-carbons of alkoxy groups between 5-5.2 ppm in ^{1}H or 70-80 ppm in ^{13}C, and the methoxyl groups at 3.8ppm in ^{1}H or 56 ppm in ^{13}C. Solvent signal is observed at 2.5 ppm in ^{1}H or 40 ppm in ^{13}C.

2.4.5 Plasma clotting assays

Prothrombin and activated partial thromboplastin time (PT and APTT) are reflective of the activity of the extrinsic and intrinsic pathways of coagulation. Both are commonly used to assess the coagulation status of human plasma. APTT and PT were measured in duplicate or triplicate over a range 10-12 different concentrations of sulfated and unsulfated DHP fractions. Water was used as blank and enoxaparin was used as a reference indicator. All fractions exhibited a significant concentration-dependent prolongation of PT and APTT. The anticoagulant activity is a measure of the amount of anticoagulant required to double the clotting time (2 x APTT or 2 x PT). The amount of sulfated and unsulfated CD fractions required to achieve the doubling of plasma clotting time ranged from 18 (6.3 µM) to 200 µg/mL (222.2 µM) and 51 (17.7 µM) to 682 µg/mL (757.8 µM) for APTT and PT respectively **(figure 19a & b)**. Likewise, concentrations ranging from 30 to 203 µg/mL (3.0 to 270.7 µM) and 74 to 248 µg/mL (7.6 to 597.3 µM) of sulfated and unsulfated FD fractions were required in the APTT and PT assays respectively **(figure 19c & d)**, refer **Table 04**. This indicated that our samples were more potent anticoagulant (1.8-3.4-fold) in acting through the intrinsic pathway. In contrast, enoxaparin brought about 2 x APTT at 5.4 µg/mL (1.2 µM) and 2 x PT at 338.9 µg/mL (75.3 µM). This imply that our samples were at least 2.5-fold weaker in the APTT assay and at most 9.9-fold more potent in the PT assay. Also, there is a clear trend with the longer chains in both CD and FD being more potent than the smaller ones. When sulfate and unsulfated CD and FD fractions are compared side by side there is no significant difference except for 30CDS and 30CD being 3.6 and 2.1-fold more active, which is still not enormous.

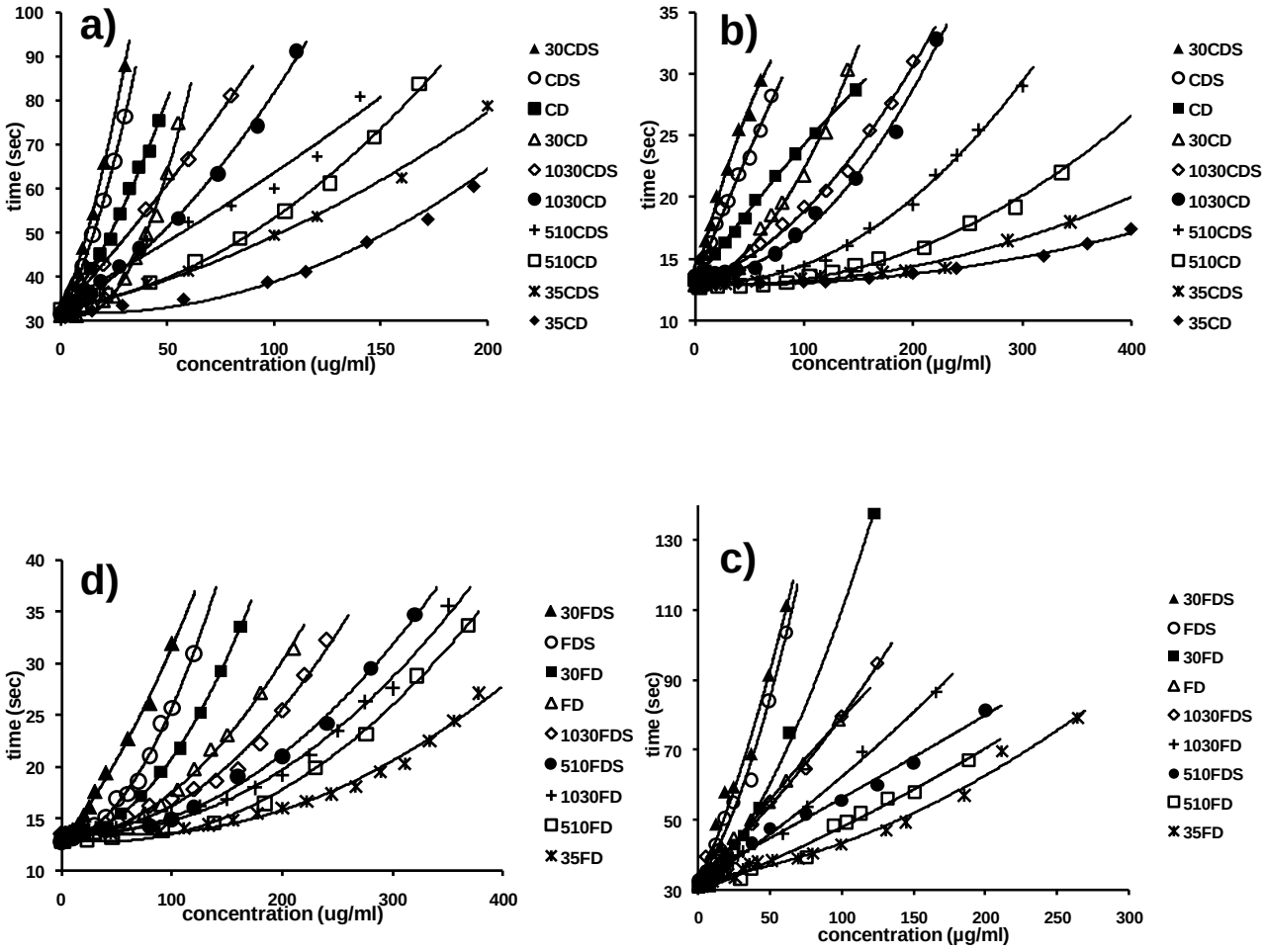

Figure 19: Plasma clotting assay for both unsulfated and sulfated CD and FD fractions
a) & b) figures represent APTT and PT results for CD and CDS fractions
c) & d) figures represent APTT and PT results for FD and FDS fractions

Table 04: Anticoagulation effect of DHP fractions on plasma

	APTT		PT	
	(µg/ml)	*(µM)*	*(µg/ml)*	*(µM)*
CDS	23 ± 1.8	8 ± 0.6	63 ± 5.0	21.8 ± 1.7
CD	36 ± 1.8	16.3 ± 0.8	125 ± 6.3	56.6 ± 2.8
30CDS	18 ± 1.3	6.3 ± 0.4	51 ± 3.6	17.7 ± 1.2
30CD	49 ± 1.5	24.8 ± 0.7	119 ± 3.6	60.1 ± 1.8
10CDS	57 ± 1.1	25.9 ± 0.5	166 ± 3.3	75.5 ± 1.5
10CD	72 ± 3.6	49 ± 2.5	191 ± 9.6	129.9 ± 6.5
05CDS	109 ± 3.3	64.5 ± 1.9	272 ± 8.2	161 ± 4.8
05CD	130 ± 7.8	118.2 ± 7.1	385 ± 23.1	350 ± 21
03CDS	160 ± 16	168.4 ± 16.8	542 ± 54.2	570.5 ± 57.0
03CD	200 ± 16	222.2 ± 17.8	682 ± 54.6	757.8 ± 60.6
FDS	36 ± 1.1	5.7 ± 0.2	98 ± 2.9	15.4 ± 0.5
FD	66 ± 1.3	12.1 ± 0.2	182 ± 3.6	33.5 ± 0.7
30FDS	29.5 ± 1.2	3.0 ± 0.1	74 ± 3.0	7.6 ± 0.3
30FD	53 ± 3.2	6.9 ± 0.4	132 ± 7.9	17.1 ± 1.0
10FDS	72 ± 3.6	22.7 ± 1.1	198 ± 9.9	62.5 ± 3.1
10FD	99 ± 4.0	37.4 ± 1.5	287 ± 11.5	108.3 ± 4.3
05FDS	144 ± 10.1	92.9 ± 6.5	265 ± 18.6	171 ± 12.0
05FD	165 ± 13.2	126.9 ± 10.2	290 ± 23.2	223.1 ± 17.9
03FDS	*nd*	*nd*	*nd*	*nd*
03FD	203 ± 22.3	270.7 ± 29.7	448 ± 49.3	597.3 ± 65.7

PT and APTT values were deduced in *in vitro* human plasma experiments where the clot initiator is either thromboplastin or ellagic acid,respectively. Experiments were performed in duplicate or triplicate. Errors represent ±1 SE.
nd – Not determined

2.4.6 Direct Inhibition of Coagulation Proteinases

It is evident by the APTT and PT assays that all DHP fractions are able to double the plasma clotting time. This signifies that most likely it is acting through the common pathway in the coagulation cascade. The two key proteinases in the common pathway being thrombin and fXa we chose to investigate if our DHP fractions indeed affect their proteolytic activities. Enzyme inhibition studies were performed where the substrate

hydrolysis was measured in presence of a range of inhibitor concentrations. The substrate hydrolysis decreased in sigmoidal fashion with the increase in concentration of the inhibitors. A standard dose-dependent equation was used to fit the curve and derive IC_{50} values.

The unsulfated and sulfated DHP fraction showed dual inhibition by inhibiting both thrombin and fXa. The IC_{50} values of unsulfated FD and CD fractions were found to be from 855 to 8610 ng/mL (0.111-11.5 µM) and 231 to 3360 ng/mL (0.117-3.7 µM) in case of thrombin **(figure 20 a-b)**, whereas for fXa it ranged from 1730 to 11143 ng/mL (0.225-14.9 µM) and 263 to 8240 ng/mL (0.133-9.2 µM) respectively **(figure 20 c-d)**. Likewise, IC_{50} values of sulfated FD and CD fractions vary 508 to 2320 ng/mL (0.052-1.5 µM) and 91.6 to 2840 ng/mL (0.032-2.9 µM) for thrombin **(figure 20 a-b)**; similarly for fXa inhibition the values were 1090 to 4990 ng/mL (0.112-3.2 µM) and 132 to 3750 ng/mL (0.046-3.9 µM) **(figure 20 c-d)**. See **Table 05 and 06** for inhibition related data of all fractions. This suggests few notable features of our fractionated DHPs. First, the inhibition pattern for both the proteases clearly shows chain length dependence; where longer chains are more active most probably due to better interactions with the large binding sites on thrombin and fXa. Secondly, in concurrence with the parent DHP mixture the fraction as expected inhibit thrombin better than fXa (up to 2.9-fold weaker). Lastly, the most striking observation is the difference in inhibition between the sulfated and unsulfated species. The sulfated DHP fractions are better inhibitors of both the proteases as compared to its unsulfated counterpart (up to 3.7-fold). This is not a huge difference considering the fact that these samples are being used for development of

better drugs through structure-based drug design. Lastly, the unsulfated possess less anionic character making it better suitable for further development as it reduces the possibility of untoward interactions with the blood coagulation proteases.

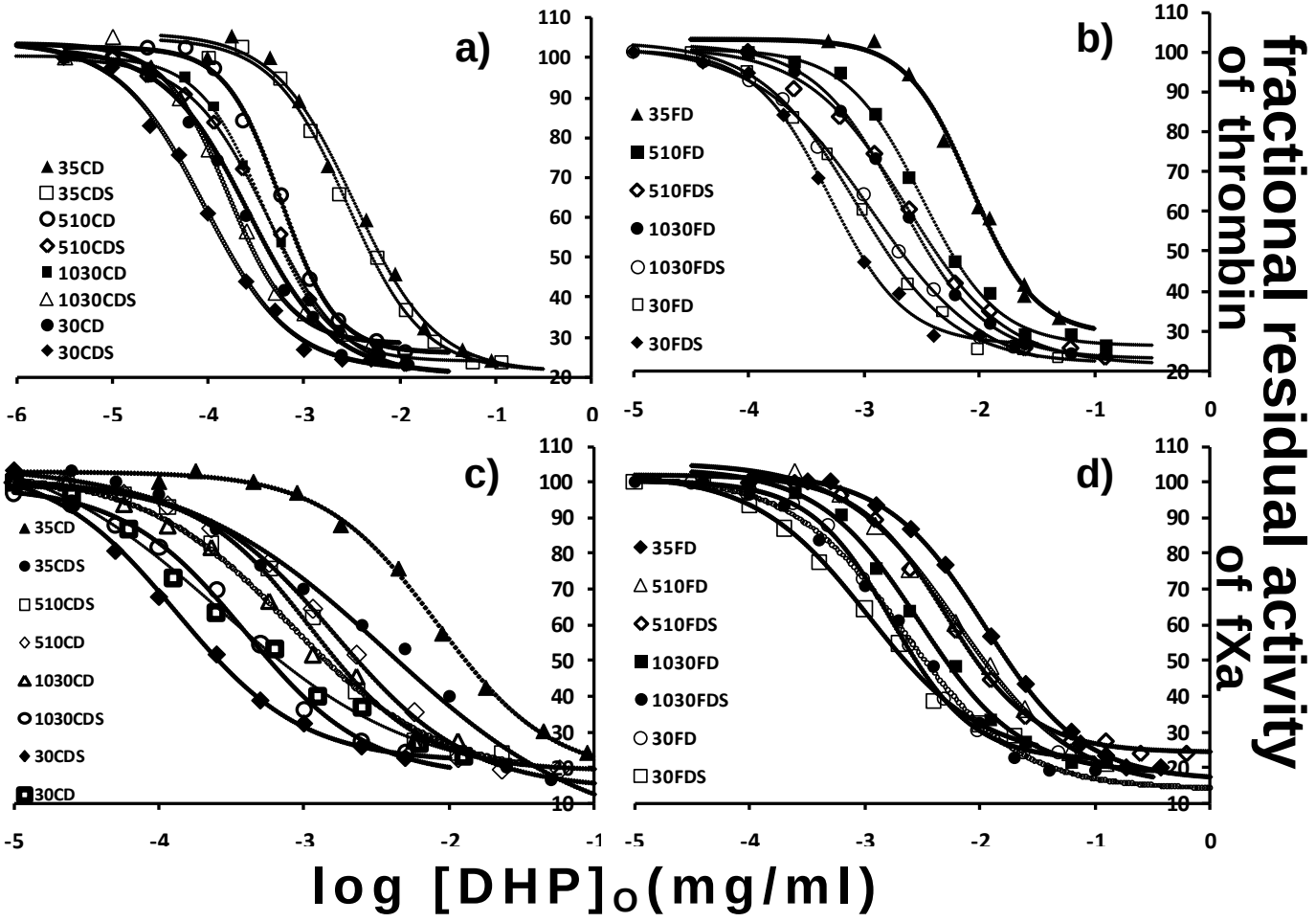

Figure 20. Inhibition of blood coagulation proteases, thrombin (a&b) and fXa (c&d) by sulfated and unsulfated DHP fractions

a) & b) represent the sigmoidal inhibition profile of thrombin by sulfated and unsulfated CD and FD fractions

c) & d) represent the sigmoidal inhibition profile of fXa by sulfated and unsulfated CD and FD fractions

Table 05: Inihibition of thrombin by sulfated and unsulfated DHP fractions

	log IC_{50} (mg/ml)	Y_O	Y_M	HS	IC_{50} (µg/ml)	IC_{50} (nM)
CDS	-3.97 ± 0.04	21.4 ± 1.7	103 ± 2.0	1.0 ± 0.1	0.108 ± 0.01	37.4 ± 3.5
CD	-3.59 ± 0.03	20.8 ± 1.4	102 ± 1.8	1.0 ± 0.1	0.258 ± 0.02	116.7 ± 9.1
30CDS	-4.04 ± 0.05	21.6 ± 2.0	104 ± 2.6	1.0 ± 0.1	0.092 ± 0.01	31.8 ± 3.5
30CD	-3.64 ± 0.03	22.1 ± 1.3	101 ± 1.5	1.1 ± 0.1	0.231 ± 0.02	116.7 ± 5.1
10CDS	-3.79 ± 0.04	28.3 ± 1.8	103 ± 1.7	1.3 ± 0.1	0.163 ± 0.01	74.1 ± 5.0
10CD	-3.41 ± 0.02	24.0 ± 0.8	100 ± 0.7	1.3 ± 0.1	0.391 ± 0.01	266.0 ± 7.0
05CDS	-3.38 ± 0.03	20.3 ± 1.7	100 ± 1.5	1.1 ± 0.1	0.420 ± 0.03	248.5 ± 18.0
05CD	-3.25 ± 0.03	25.9 ± 1.8	103 ± 1.4	1.5 ± 0.1	0.568 ± 0.04	516.4 ± 36.0
03CDS	-2.55 ± 0.04	21.8 ± 2.1	105 ± 2.5	1.1 ± 0.1	2.840 ± 0.28	2989 ± 295
03CD	-2.47 ± 0.07	21.4 ± 3.9	106 ± 3.5	1.0 ± 0.2	3.360 ± 0.50	3733 ± 555
FDS	-2.98 ± 0.05	17.6 ± 2.3	102 ± 1.1	0.7 ± 0.1	1.050 ± 0.11	92.6 ± 9.0
FD	-2.69 ± 0.01	22.4 ± 0.5	101 ± 0.8	1.6 ± 0.1	2.060 ± 0.06	264.7 ± 20.2
30FDS	-3.29 ± 0.03	26.5 ± 1.3	101 ± 1.4	1.3 ± 0.1	0.508 ± 0.03	51.9 ± 3.1
30FD	-3.07 ± 0.03	21.8 ± 1.4	103 ± 1.9	1.0 ± 0.1	0.855 ± 0.06	111.0 ± 7.8
10FDS	-2.94 ± 0.04	19.2 ± 2.4	102 ± 1.4	0.9 ± 0.1	1.150 ± 0.10	362.8 ± 31.5
10FD	-2.70 ± 0.01	23.2 ± 0.5	102 ± 0.8	1.2 ± 0.1	2.020 ± 0.06	762.3 ± 22.6
05FDS	-2.64 ± 0.05	21.5 ± 1.9	101 ± 2.7	1.0 ± 0.1	2.320 ± 0.02	1497 ± 12.9
05FD	-2.50 ± 0.03	26.4 ± 1.3	101 ± 1.5	1.3 ± 0.1	3.160 ± 0.20	2431 ± 154
03FDS	*nd*	*nd*	*nd*	*nd*	*nd*	*nd*
03FD	-2.07 ± 0.05	28.8 ± 4.3	103 ± 1.9	1.5 ± 0.2	8.610 ± 0.90	11480 ± 1200

Inhibition studies were performed in 20 mM Tris-HCl buffer, pH 7.4, containing 100 mM NaCl, 2.5 mM $CaCl_2$ and 0.1 % PEG 8000 in PEG 20,000-coated polystyrene cuvettes. Spectrozyme TH was used as substrate and the residual enzyme activity in the presence of inhibitor was assessed by measuring the initial rate of substrate hydrolysis at 405 nm. Logistic equation 4 was used to fit the dose dependence of the residual enzyme activity to obtain log IC_{50}, Y_0, Y_M and HS values. See Methods for details.
Errors represent ±1 SE

Table 06: Inihibition of fXa by sulfated and unsulfated DHP fractions

	log IC_{50} (mg/ml)	Y_O	Y_M	HS	IC_{50} (µg/ml)	IC_{50} (nM)
CDS	-3.77 ± 0.06	1.66 ± 4.4	110 ± 3.6	0.6 ± 0.1	0.171 ± 0.02	59.2 ± 6.9
CD	-3.43 ± 0.03	12.2 ± 1.9	105 ± 1.8	0.8 ± 0.1	0.368 ± 0.03	166.5 ± 9.1
30CDS	-3.88 ± 0.05	21.5 ± 2.6	105 ± 2.7	1.0 ± 0.1	0.132 ± 0.02	45.8± 3.5
30CD	-3.58 ± 0.09	16.5 ± 4.9	112 ± 6.3	0.7 ± 0.1	0.263 ± 0.05	132.8 ± 5.1
10CDS	-3.41 ± 0.06	17.4 ± 3.8	99 ± 1.9	1.0 ± 0.1	0.390 ± 0.05	177.3 ± 5.0
10CD	-3.10 ± 0.08	17.7 ± 5.3	102 ± 2.7	0.9 ± 0.1	0.804 ± 0.14	546.9 ± 7.0
05CDS	-2.95 ± 0.06	19.2 ± 3.5	99 ± 2.1	1.1 ± 0.2	1.110 ± 0.14	650.9 ± 18.0
05CD	-2.78 ± 0.04	14.0 ± 2.1	100 ± 1.3	1.0 ± 0.1	1.650 ± 0.14	1500 ± 36.0
03CDS	-2.43± 0.20	15.4 ± 1.3	105 ± 3.4	0.6 ± 0.1	3.750 ± 1.69	3947 ± 1800
03CD	-2.08 ± 0.02	18.0 ± 0.9	103 ± 1.0	1.1 ± 0.1	8.240 ± 0.39	9156 ± 433
FDS	-3.23 ± 0.02	30.9 ± 0.8	101 ± 0.8	1.7 ± 0.1	0.588 ± 0.06	164.9 ± 9.0
FD	-2.84 ± 0.03	22.9 ± 1.4	102 ± 1.7	1.1 ± 0.1	1.440 ± 0.11	377.9 ± 20.2
30FDS	-2.96 ± 0.06	22.4 ± 3.6	102 ± 2.2	0.9 ± 0.1	1.090 ± 0.15	111.5 ± 3.1
30FD	-2.76 ± 0.02	22.0 ± 1.1	100 ± 1.0	1.2 ± 0.1	1.730 ± 0.09	224.7 ± 7.8
10FDS	-2.62 ± 0.03	11.6 ± 1.9	102 ± 1.3	0.8 ± 0.1	2.380 ± 0.18	750.8 ± 31.5
10FD	-2.53 ± 0.04	18.2 ± 2.1	104 ± 2.5	1.0 ± 0.1	2.960 ± 0.28	1117 ± 22.6
05FDS	-2.30 ± 0.02	24.1 ± 0.8	102 ± 1.0	1.1 ± 0.1	4.990 ± 0.24	3219 ± 12.9
05FD	-2.19 ± 0.05	14.6 ± 3.8	105 ± 2.5	0.9 ± 0.1	6.530 ± 0.82	5023 ± 154
03FDS	*nd*	*nd*	*nd*	*nd*	*nd*	*nd*
03FD	-1.95 ± 0.02	16.5 ± 0.9	103 ± 0.9	1.0 ± 0.1	11.10 ± 0.44	14857 ± 1200

Inhibition studies were performed in 20 mM Tris-HCl buffer, pH 7.4, containing 100 mM NaCl, 2.5 mM $CaCl_2$ and 0.1 % PEG 8000 in PEG 20,000-coated polystyrene cuvettes. Spectrozyme fXa was used as substrate and the residual enzyme activity in the presence of inhibitor was assessed by measuring the initial rate of substrate hydrolysis at 405 nm. Logistic equation 4 was used to fit the dose dependence of the residual enzyme activity to obtain log IC_{50}, Y_0, Y_M and HS values. See Methods for details.
Errors represent ±1 SE

2.4.7 Identifying the binding site of CD10 and FD10

Based on the known mechanism of FDS and CDS mixtures we expected the fraction to behave the same way by acting through the exosite-2 on thrombin. We chose to work with an intermediate active fraction as the yields of the larger fractions were much higher after fractionation. This implies that the mixture possesses its activity mainly because of the larger fractions as evident by protease inhibition studies. To ascertain that indeed this was true we performed a quick study with one of the fractions from each and not surprisingly found the mechanism to be the same. Michaelis Menten kinetic studies with CD10 and FD10 were performed **(figure 21a & b)** to probe if the inhibitors were acting through binding at the active site. The K_M was found to be steady between 1.2 – 1.8 µM and the V_{MAX} steadily decreased from 24 – 11 mAbsU/min in presence of increasing concentration of the inhibitor (20 – 5000 ng/mL). The catalytic efficiency of the reaction steadily decreased from ~45 to ~18 s^{-1}, refer **Table 07**. These signify that there is no effect on substrate binding to the active site to form the thrombin–Spectrozyme TH Michaelis complex but the conversion of the complex to the final product is definitely retarded. To further ascertain that the fractions like the parent DHPs bind in the exosite-2 of thrombin, competitive binding studies in presence [5F]-Hir[54-65](SO3-), an exosite-1 binding ligand **(figure 22a & b)** and heparin, an exosite-2 binding ligand **(figure 23a & b)** was performed. Based on previous studies we chose to screen exosite-1 ligand at a concentration of 86nM (3 x K_D) and heparin at 20 µM (1 x K_D) and 100 µM (5 x K_D). These studies revealed that our fractions indeed bind in the exosite-2 of thrombin as $IC_{50,app}$ changed significantly from 210 nM to 946 nM and 600 nM to 7.3 µM for CD10

and FD10, respectively in presence of increasing concentration of exosite-2 competitor, whereas it remained unchanged in presence of exosite-1 competitor **(Table 08)**.

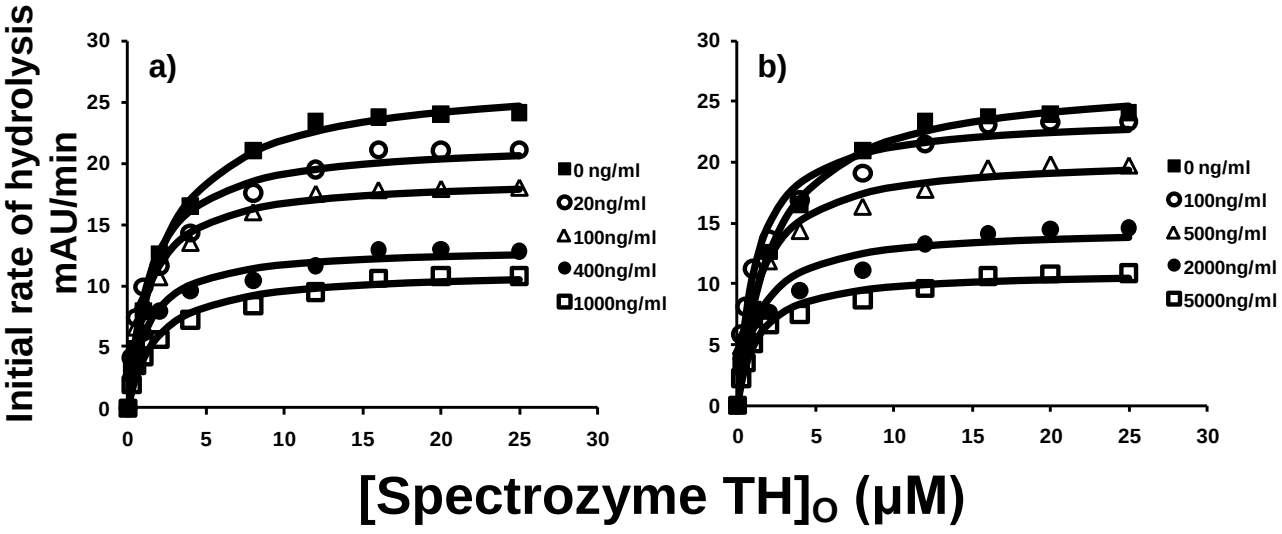

Figure 21a & b: Michaelis-Menten Kinetics of Spectrozyme TH Hydrolysis by Thrombin in the presence of DHP fractions.
Michaelis-Menten kinetics of Spectrozyme TH hydrolysis by thrombin in the presence of 10CD **(figure 20a)** and 10FD **(figure 20b).**
The initial rate of hydrolysis at various substrate concentrations was measured in pH 7.4 buffer as described in 'Experimental Procedures'. Solid lines represent non-linear regressional fits to the data using the Michaelis-Menten equation.

Table 07: Michaelis-Menten Kinetics of Spectrozyme TH Hydrolysis by Thrombin in the presence of inhibitors

$[10CD]_o$	Km	Vmax	kcat
(ng/mL)	*(µM)*	*(mAbsU/min)*	*(s^{-1})*
0	2.3 ± 0.1	27.0 ± 0.4	45.4 ± 0.7
20	1.4 ± 0.2	21.8 ± 0.7	36.6 ± 1.2
100	1.2 ± 0.1	18.8 ± 0.4	31.6 ± 0.7
400	1.2 ± 0.2	13.2 ± 0.3	22.2 ± 0.5
1000	1.8 ± 0.3	11.2 ± 0.4	18.8 ± 0.7
$[10FD]_o$			
0	2.3 ± 0.1	27.0 ± 0.4	45.4 ± 0.7
100	1.2 ± 0.2	23.8 ± 0.7	40.0 ± 1.2
500	1.4 ± 0.2	20.5 ± 0.5	34.4 ± 0.8
2000	1.3 ± 0.3	14.6 ± 0.7	24.5 ± 1.2
5000	1.3 ± 0.2	11.0 ± 0.3	18.5 ± 0.5

[a] K_M and V_{MAX} were measured as described in 'Experimental Procedures'.
[b] Error represents ±1 S.E.

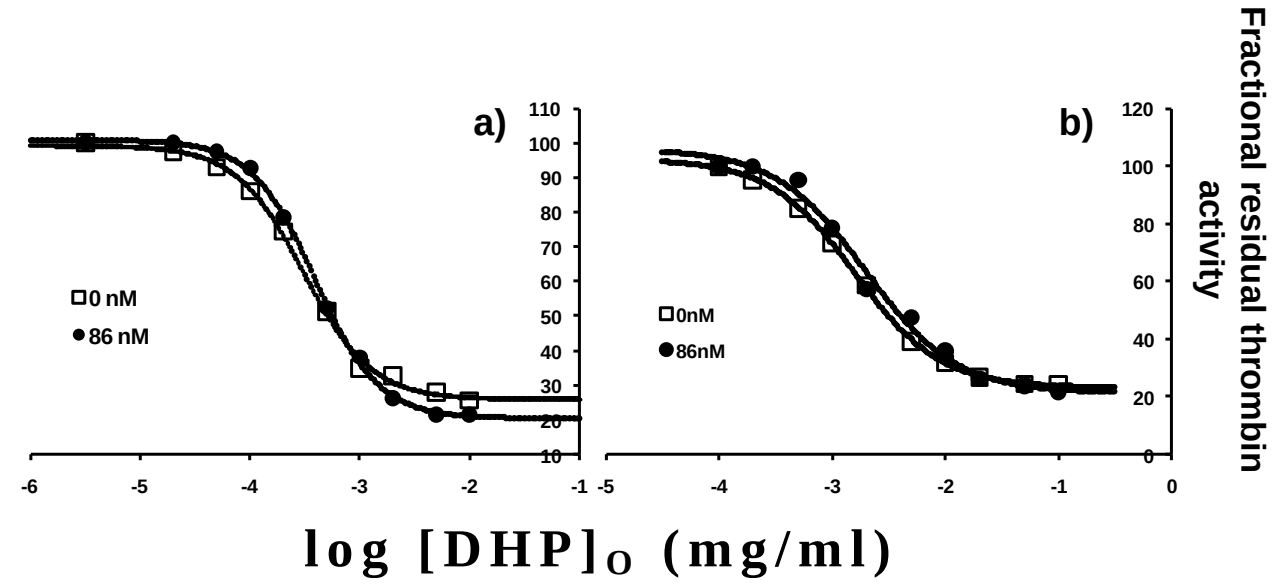

Figure 22. Inhibition of thrombin by DHP in presence of exosite-1 ligand
Competitive effect of [5F]-Hir[54-65](SO_3^-) on the inhibition of thrombin by 10CD **(figure 21a)** and 10FD **(figure 21b)**. Residual thrombin activity was measured through Spectrozyme TH hydrolysis in 20 mM Tris-HCl buffer, pH 7.4, containing 100 mM NaCl, 2.5 mM $CaCl_2$ and 0.1 % polyethylene glycol (PEG) 8000 at 37 ^{O}C in the presence of 0 and 86 nM [5F]-Hir[54-65](SO_3^-). Solid lines represent fits using the logistic equation 4 to obtain the apparent IC_{50}, as described in 'Experimental Procedures'.

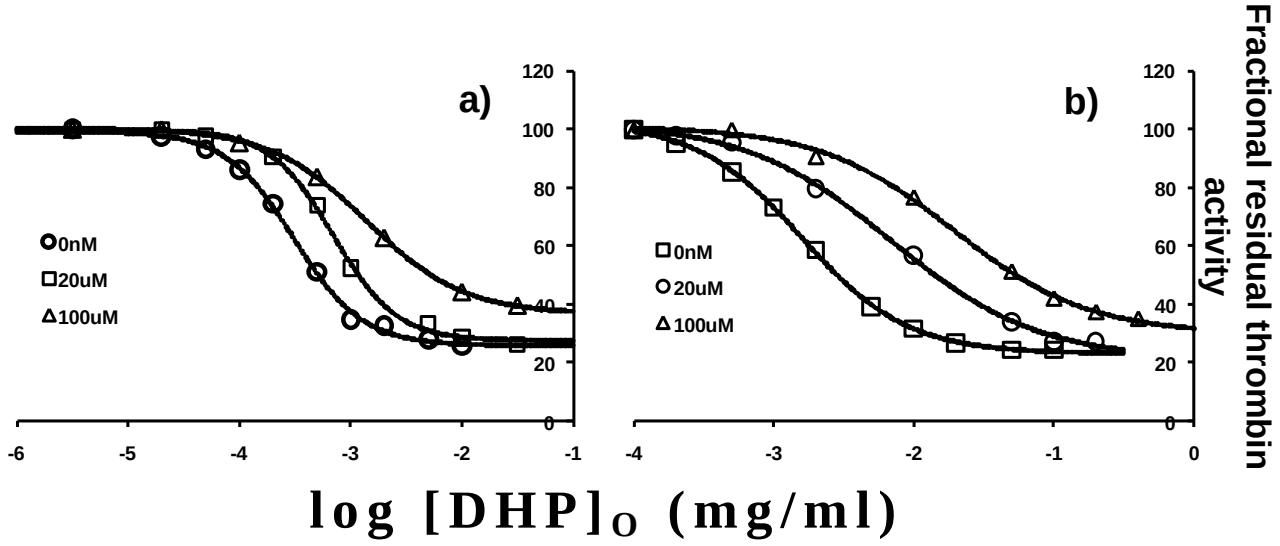

Figure 23. Inhibition of thrombin by DHP in presence of exosite-2 ligand
Competitive effect of porcine heparin on the inhibition of thrombin by 10CD **(figure 22a)** and 10FD **(figure 22b)**. Residual thrombin activity was measured through Spectrozyme TH hydrolysis in 20 mM Tris-HCl buffer, pH 7.4, containing 100 mM NaCl, 2.5 mM $CaCl_2$ and 0.1 % polyethylene glycol (PEG) 8000 at 37 ^{O}C in the presence of 0, 20 and 100 μM porcine heparin. Solid lines represent fits using the logistic equation 4 to obtain the apparent IC_{50}, as described in 'Experimental Procedures'.

Table 08: Inhibition of thrombin by 10CD and 10FD in the presence of hirugen analog [5F]-Hir[54-65](SO3-) and porcine heparin [a]

	[Competitor]	log IC_{50} (mg/ml)	Y_0	Y_M	HS	IC_{50} (µg/ml)	IC_{50} (nM)
	Hirugen Analog						
[10CD]	0nM	-3.51 ± 0.3	25.8 ± 1.2	99.2 ± 1.2	1.4 ± 0.1	0.31 ± 0.02	211 ± 13.6
	86nM	-3.41 ± 0.02	20.4 ± 0.9	101 ± 0.8	1.5 ± 0.1	0.39 ± 0.01	265 ± 6.80
[10FD]	0nM	-2.80 ±0.02	23.1 ± 0.6	102 ± 0.9	1.2 ± 0.1	1.59 ± 0.05	600 ± 18.9
	86nM	-2.70 ± 0.08	21.2 ± 3.5	106 ± 4.8	1.1 ± 0.2	1.98 ± 0.30	747 ± 113
	Porcine Heparin						
[10CD]	20µM	-3.16 ± 0.02	27.5 ± 1.2	99.8 ± 1.0	1.5 ± 0.1	0.70 ± 0.04	476 ± 27.2
	100µM	-2.86 ± 0.02	36.7 ± 0.9	100 ± 0.4	1.0 ± 0.1	1.39 ± 0.06	945 ± 40.8
[10FD]	20µM	-2.16 ± 0.06	21.0 ± 3.0	102 ± 2.1	0.8 ± 0.1	6.95 ± 0.90	2600 ± 340
	100µM	-1.72 ± 0.06	29.9 ± 2.7	101 ± 1.5	0.9 ± 0.1	19.3 ± 2.60	7300 ± 981

[a] Inhibition studies were performed in 20 mM Tris-HCl buffer, pH 7.4, containing 100 mM NaCl, 2.5 mM $CaCl_2$ and 0.1 % PEG 8000 in PEG 20,000-coated polystyrene cuvette. Spectrozyme TH was used as substrates and the residual enzyme activity in the presence of FDSO3 was assessed by measuring the initial rate of substrate hydrolysis at 405 nm. Logistic equation I was used to fit the dose dependence of the residual enzyme activity to obtain log IC_{50}, Y_0, Y_M and HS values. See Methods for details.
[b] represents 1 ±S.E.

2.4.8 Cellular toxicity studies

The alamar blue assay functions on the ability of viable cells to reduce alamar blue (resazurin) to resofurin (highly red fluorescent), which can be quantified using fluorimeteric methods. All fractions screened for cytoxicity were found to be non-toxic with more than 80% cell viability at concentration as high as 500 µg/mL **(figure 24)**.

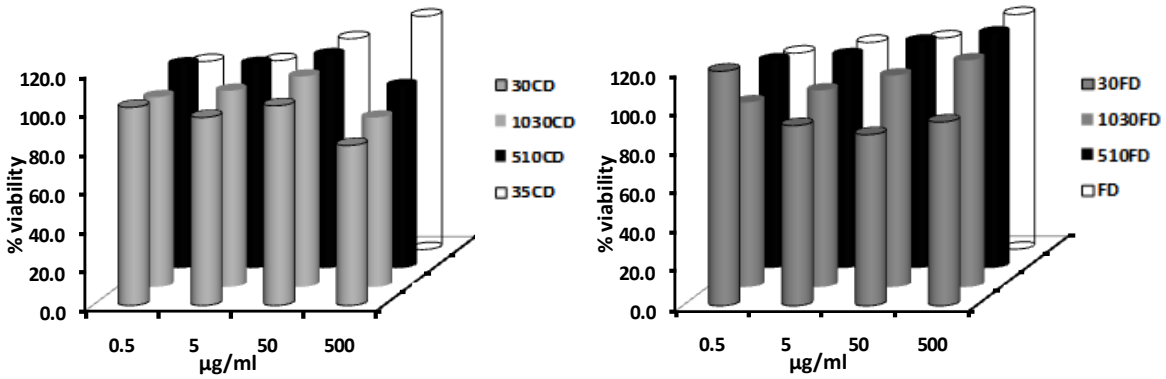

Figure 24. Toxicity studies on the unsulfated CD and FD fractions
The alamar blue assay was performed with a fluorimetric method using HepG cells. All fractions of both CD and FD were able to sustain cell viability at concentrations as high as 500 µg/ml.

2.5 Discussion

In an attempt to mimic structural features of heparin by replacing the carbohydrate backbone with an aromatic scaffold and also contain structural intricacy similar to that of heparin we chose to work with lignins containing the carboxylate functionality. However, natural lignins do not contain carboxylic acid groups. So, what does lignin have to offer? It is a complex and heterogenous polymer just like heparin. It has a rigid aromatic backbone with flexibility introduced at the point of attachment of each monomer, a property lacked by heparin. The aromatic skeleton might impart structural specificity due to its hydrophobic nature and restrained conformation. Lignins contain diverse type of linkages and the molecular weight is close to 5000 a property shared with LMWH. Lignins have free –OH groups, which could potentially make H-bonding or could be derivatized to yield its sulfated form. In terms of synthesis these are easy to synthesize even on bulk scale, which is not the case with heparins. Finally, lignins offer an avenue to

potentially discover sequence(s) similar to that of the potent pentasaccharide sequence in heparin.

We utilized HRP-catalyzed oxidative coupling conditions, such as high reactant concentrations and controlled gradual addition of the oxidant, which reduce chain termination, to obtain oligomers with peak average molecular weight between 750-7700. This corresponds to a very diverse chain length numbers ranging from a trimer up to 24-mer. The GPC profiles obtained were broad and reasonably symmetrical implying that each fraction contained nearly all types of chains. For example, although the average chain length of FD3 and CD3 is 3.4 and 3.3, both fractions contain chains as long as 24 and 8 units, respectively. This indicates that each type of the chain length is present in all fractions but in different proportions giving rise to polydispersity. This is possible because some of the longer chains are conformationally more flexible facilitating their passage through the sieves of the filter. The apparent molecular weight of the sulfated fractions of DHPs was measured using SEC with PSS as standards.

We have employed the use of chain lengths and difference in the number obtained between the sulfated and unsulfated fractions to get an insight into the apparent number sulfates present. The calculation for number of sulfate groups turns out to be 1-1.8 per monomer of CD and 0.5-0.8 sulfates per monomer of FD. Further, we attempted to obtain a correlation between sulfates group obtained by chromatography and elemental analysis. The number of sulfates for CDS30, CDS10, FDS30 and FDS10 using elemental analysis were found to be 0.38, 0.33, 0.2 and 0.16 per monomer. The level of sulfation determined

using both the techniques differ by 3-4-fold but the ratio between the sulfates remain the same. This can be attributed to two things; first, the highly heterogeneous nature of the samples and second the methods used to determine them. SEC measures the hydro-dynamic volume of the sample, hence for similar size molecules the molecular weights, might be different if the conformations are different. One sample might carry more solvent molecules with it than the other increasing its overall size and hence the apparent molecular weight.

Detailed structural characterization involving the exact type of inter-monomeric linkages is very challenging. The ^{13}C-NMR just like the IR revert only functional group information on these complex samples. Due to lack of powerful mass spectroscopy techniques and expertise in polymer chemistry assigning linkages based on daughter ions for this intricate mixture is not very reliable. All the functionality of the starting monomer; hydroxyl, -carboxylic acid, aliphatic side chains, aromatic backbone and methoxy (in case of FA) are retained in oligomers as evident by NMR.

Working with such a complex mixture would limit the discrete assignment of structures despite the availability of modern and powerful techniques like NMR, MS and XRD (X-ray diffraction). This drawback is outweighed by the fact that the mixture presents an opportunity for high throughput screening of a large library, which would yield an effective structure(s) rather than a discrete one. In the case of carboxylated lignins it is combinatorial because of the nearly random coupling of radicals.

The anticoagulation properties of DHP fractions were tested using an in vitro assay to assess APTT and PT. The results reveal that all the fractions are able to prolong the plasma clotting time for both APTT and PT assays. In addition, all samples show greater potency prolonging the clotting time in the PT assay compared to enoxaparin, a marketed LMWH used in clinical settings. The sulfated and unsulfated CD and FD fractions were 2.5 to 225- fold weaker in the APTT assay compared to enoxaprain, whereas in PT assay the change observed ranged from 0.1 to 10-fold based on the size of the oligomers **(figure 25a & b)**. The fraction implies that some of the samples were more potent in prolonging the clotting time compared to enoxaparin. Overall, it is evident from this study that the activity is a size dependent phenomenon, where larger samples are more active than the smaller ones. In addition, the larger samples are better in executing the coagulation through the intrinsic pathway. It is possible that the significant hydrophobic character of DHPs induces binding to cells resulting in significant sequestering of active agent. It is likely that this non-specific binding will be reduced with homogeneous, synthetic small molecules. Interestingly, the difference between sulfated and unsulfated samples in prolonging the clotting time was not huge. Sulfated CD fractions were better than unsulfated CD fractions by 1.3-3.9-fold and in case of FD fractions the difference was not more than 2.3-fold **(figure 26)**. This suggest that sulfation in not very critical as is the case with heparins, where it is the root cause of numerous side effects. Finally, since the samples work through both the coagulation cascade it lead us to predict that either the samples are inhibiting numerous coagulation factors in the cascade or it worked through the common pathway by either inhibiting thrombin and/or fXa, just like the parent sulfated DHPs reported by our lab.

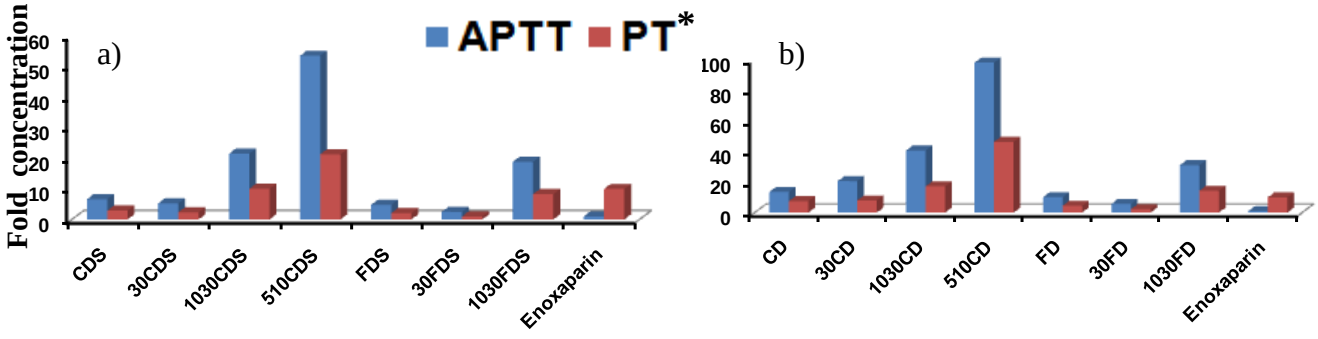

Figure 25. Comparison of sulfated and unsulfated DHP fractions against enoxaparin
When compared with DHP fractions, enoxaparin is more potent in APTT assay, while in case of PT assay only the higher fractions are more potent than enoxaparin.
*For comparison purposes of DHP fractions in PT assay, the fold concentrations have been further enhanced by 10-fold. Hence, the actual value of enoxaparin, which is 1, shows up as 10.

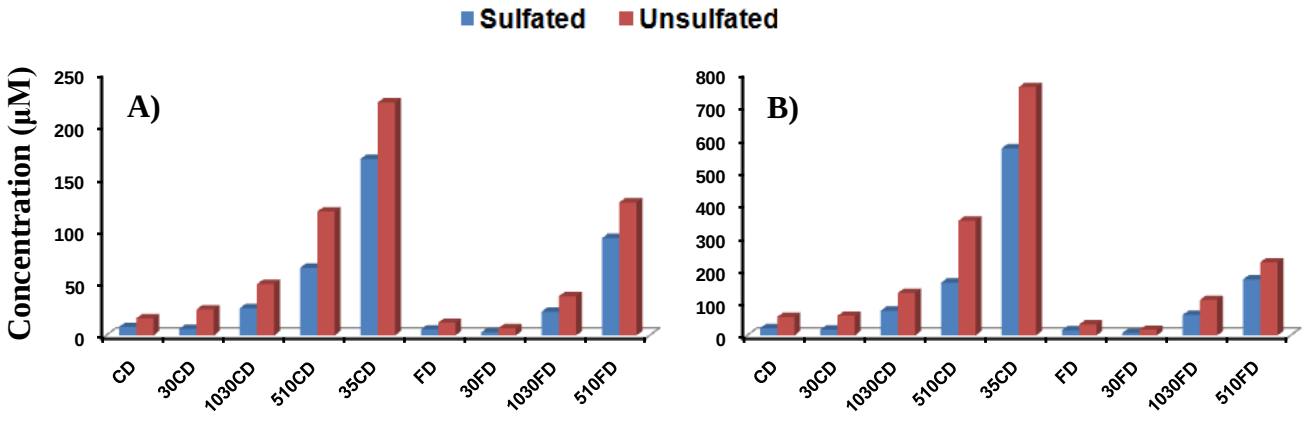

Figure 26. Comparison between sulfated and unsulfated DHP fractions in the APTT and PT assays.
A) Comparison for APPT results and B) PT results

In the light of our prediction we carried out direct enzyme inhibition studies on thrombin and fXa, which also revealed the mechanistic difference between our DHP samples and

enoxaparin. All our samples directly inhibited the hydrolysis of appropriate chromogenic substrate by thrombin and fXa, whereas enoxaparin is not a direct inhibitor of these proteases. The IC_{50} values for sulfated and unsulfated samples ranged from ten's of nanomolar to micromolar; the difference between the most and least active being ~3800-fold. As observed in the clotting assays the sulfated samples were more active than the unsulfated ones ranged from 1.2-3.7-fold based on the size of the sample **(figure 27)**. And the difference within the unsulfated and sulfated group of samples ranged from 20 to 80-fold with the larger samples being more active the smaller ones **(figure 28)**. Overall, this study suggests that the unsulfated DHPs possess size-dependent direct inhibition of thrombin and fXa, which are mechanistically different from heparins that work through the indirect AT mediated inhibition.

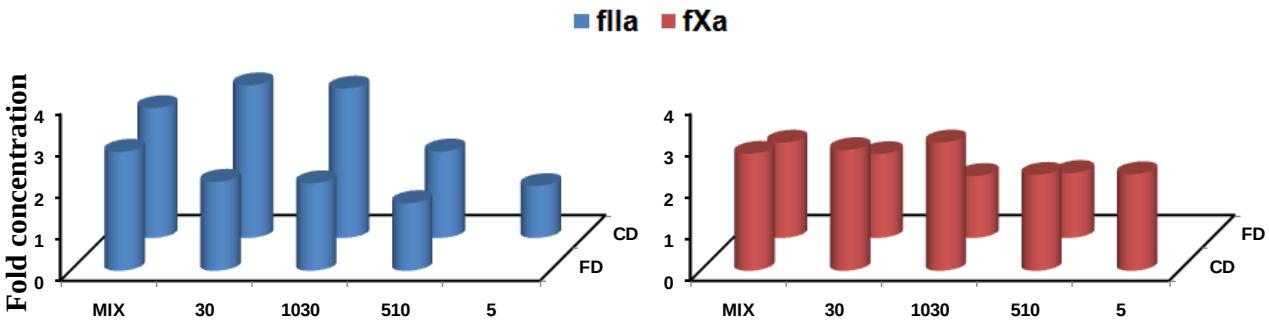

Figure 27. Comparison between sulfated and unsulfated DHP fractions for their potency in inhibiting thrombin and fXa.
Fold concentration was calculated by taking ratio of IC_{50} of unsulfated:sulfated fractions, indicative of greater potency of sulfated fractions.

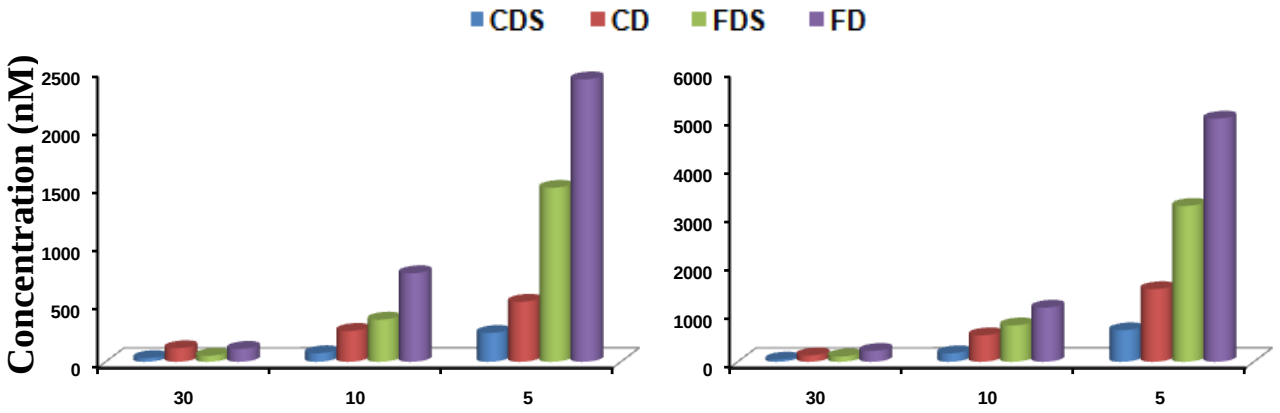

Figure 28. Size Dependent comparison of DHP fractions for their potency in inhibiting thrombin (A) and fXa (B).

Note: Sulfated DHP mixtures have been screened for other factors in the coagulation cascade and were found not to inhibit any enzyme up to 3 mM concentration. Also, these have been tested in presence of AT and the activity is not affected by more than 2-fold suggesting that our samples are indeed inhibitors of thrombin and fXa.

In-vitro toxicity studies show that our DHP samples are not toxic up to a concentration of 500 µg/mL. All fractions show excellent cell viability at the highest concentration used with the worst one 30FD showing more than 80% cell viability.

2.6 Conclusion

Although the heterogeneous and polydisperse nature of these DHP oligomers are structurally difficult to characterize it presents us with a wealth of information that could be used for rational design of advanced molecules. The molecules present in the mixture have a common scaffold of lignin carboxylate. Unsulfated DHPs have a reduced overall

negativity, which would arise only from the carboxylates on each monomer. This reduction in the overall anionic character of DHPs could potentially overcome the numerous unwanted interactions the sulfated DHPs might make while interacting with the serine proteases, thrombin and fXa. In order to find a sequence like the heparin pentasaccharide our chain length dependence studies revealed that an octamer size might be just right to work with, which can be finely tuned to generate more potent molecules. The other plausible strategy might be to further reduce the size to that of a tetramer or a hexamer and have strategically located functional groups that interact with the residues in the proteinase binding site and bring about inhibition. The samples represented in here, in an attempt to mimic heparin have a complete different mechanism of action. Heparins are indirect inhibitors, whereas our samples are direct inhibitors of thrombin and fXa.

On the whole, this entire exercise entails that it may be possible to design un-sulfated, synthetic molecules with an optimum size that would possess unique mechanism of action. A specific advantage expected of these un-sulfated homogeneous DHP-based structures is that absence of sulfate group would make the molecules orally bioavailable. This does not imply that our novel molecules will be clinically effective. Though *in-vitro* studies suggest that our samples are not toxic up to a concentration of 0.5 g/L, i*n-vivo* toxicity studies will have to be performed to ascertain that these novel structures do not induce abnormal effects. An important point to note in this regard is that *in-vivo* enoxaparin does not prolong PT and APPT at concentrations sufficient to anticoagulate suggesting that *in-vitro* potency does not translate directly into *in-vivo* effectiveness. Yet, the results described here suggest that the novel structures of DHPs with optimum size

and strategically placed functional groups may lead to a new class of potent anticoagulants.

CHAPTER 03

Novel and Specific Direct Thrombin Inhibitor

3.1 Background

Our earlier studies on DHPs had shown that it might be possible to design a potent anticoagulant that would possess an optimal size with some anionic character and hydrophobicity. In the same study we had postulated that our DHPs contain mainly two types of linkages *β-O-4* and *β-5*. The chain length and the linkage types were the main reason for the tremendous heterogeneity and polydispersity introduced in the DHP samples. Also, our DHP samples were found to be dual inhibitors of thrombin and fXa. As described earlier, multienzyme targeting is the main drawback that leads to numerous side effects that heparin carries. Our goal was to reduce the non-specific interaction as much as possible. Heparin targets several enzymes in the coagulation cascade, which we were able to overcome with our DHPs restricting it to act only as a dual inhibitor. After studying the size dependency on enzyme inhibition the next logical step was to study the structural decency. To study the inhibition arising from structural specificity we synthesized DHPs with only *β-O-4* type linkages, which will be referred as TK. The other notable modification in TK was the absence of carboxylate groups. As we believed that some anionic character was essential for the protease inhibition we derivatized the hydroxyl groups on TK to the sulfates, and this derivative is labeled as TKS. This chapter refers to the study of TKS as a specific inhibitor of thrombin and as a potential anticoagulant.

3.2 Experimental Methods

3.2.1 Proteins, biological fluids and chemicals

Human plasma proteinases, fVIIa, fIXa, fXa, fXIa and α-thrombin, were purchased from Haematologic Technologies (Essex Junction, VT). Stock solutions of proteins were prepared as follows: For fVIIa 25 mM HEPES buffer, pH 7.4, containing 100 mM NaCl and 5 mM $CaCl_2$. For fIXa 100 mM HEPES buffer, pH 8, containing 100 mM NaCl and 10 mM $CaCl_2$. For fXa 20 mM Sodium phosphate buffer, pH 7.4, 0.1mM EDTA, 0.1% PEG 8000. For fXIa and thrombin 20 mM Tris-HCl buffer, pH 7.4, containing 100 mM NaCl and 2.5 mM $CaCl_2$, 0.1% PEG 8000. Chromogenic substrates used - Spectrozyme FVIIa (methanesulphonyl-*D*-cyclohexylalanyl-butyl-Arg*p*-nitroanilide), Spectrozyme FIXa (*D*-Leu-Phe-Gly-Arg-*p*nitroanilide), Spectrozyme FXa (Methoxycarbonyl-*D*cyclohexylglycyl-Gyl-Arg-*p*-nitroanilide), Spectrozyme TH (H-*D*hexahydrotyrosol-Ala-Arg-*p*-nitroanilide). All substrates were purchased from American Diagnostica (Greenwich, CT). Competitive ligands used - Exosite 1 ligand Tyr63-sulfated hirudin-(54-65) labeled with 5-(carboxy)fluorescein ([5F]-Hir[54-65](SO3-)). Exosite 2 ligand unfractionated porcine heparin (Sigma-Aldrich St. Louis, MO). Plasma and blood work – Pooled citrated human plasma for coagulation time assays (Valley Biomedical Winchester, VA). Activated partial thromboplastin time reagent containing ellagic acid (APTT-LS), thromboplastin-D and 25 mM $CaCl_2$ (Fisher Diagnostics Middletown, VA) Fresh human whole blood (self donor not on any medication for 4 weeks before sample collection) was collected in tubes containing sodium citrate 3.2% (0.109M). LMWH (MR 5,060 Da), TEAST complex (Sigma St. Louis, MO). Enoxaparin (MR 4,500 Da) (Aventis

Pharmaceuticals). All other chemicals were analytical reagent grade from either Sigma Chemicals (St. Louis, MO) or Fisher (Pittsburgh, PA) and used as obtained.

3.2.2 Synthesis of TKS

TK, a β-O-4 polymer was obtained from Takao Kishimoto and sulfated as described below. **Figure 29** shows the ^{13}C-NMR spectra of TK. Sulfation of TK was carried out using TEAST as described earlier. Briefly, TK was sulfated with TEAST complex. Briefly, dry TK powder (50 mg) was dissolved in dry DMF (15 mL) containing TEAST (200 mg) and stirred for 24 h at 60 °C. After the removal of most of the DMF in vacuo, the remaining product was taken up in 30% aqueous sodium acetate, the sodium salt precipitated using ~10 volume of cold ethanol. The precipitated product was further purified using dialysis membrane (MWCO 5K).

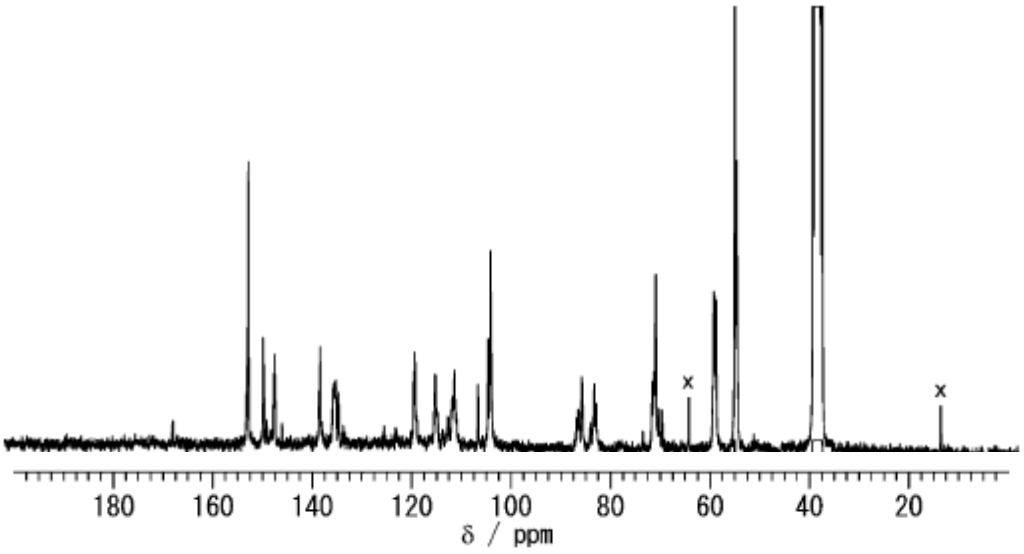

Figure 29. ^{13}C-NMR spectra of β-O-4 type artificial lignin polymer.[126]

3.2.3 Molecular weight determination of TKS using size exclusion chromatography (SEC).

The apparent number and weight average molecular weight of TKS was determined using SEC on a Shimadzu chromatography system composed of LC10Ai pumps and a SPD-10A VP UV-Vis detector controlled by a SCL-10A VP system controller connected to a computer. TKS was eluted on an Asahipak GS320 HQ column with an isocratic flow rate of 0.7 mL/min of 0.1 N NaOH at pH 11.0. The wavelength of detection for fractions was set to 280 nm. Polystyrene sulfonate standards (PSS) were used for calibration purposes. The relationship between logarithm of the molecular weight and the elution volume (V) of the standards was found to be linear with a correlation co-efficient of 0.99. Each chromatogram was sliced into 1000 time periods providing 1000 M_R with the corresponding absorbance (A) values. These values were used to calculate M_N, M_W and P parameters from **equations 1, 2 and 3**, respectively, for TKS.

$$M_N = \frac{\sum A_i \times M_i}{\sum A_i} \quad \ldots\ldots (1) \qquad M_W = \frac{\sum A_i \times M_i^2}{\sum A_i \times M_i} \quad \ldots\ldots (2)$$

$$P = \frac{M_W}{M_N} \quad \ldots\ldots (3)$$

3.2.4 Direct TKS inhibition of coagulation proteinases.

Direct inhibition of fVII, fIX, fXa, fXIa and thrombin by TKS was determined using chromogenic substrate hydrolysis assays at physiological temperature. For these assays, TKS having final concentrations ranging from 0.23 ng/mL to 230 μg/mL was used with

appropriate buffer system in PEG 20,000-coated polystyrene cuvettes. The proteinase solution was then added each time to yield final concentrations ranging from 1 to 10 nM of each enzyme. The experiment was carried out at physiological temperature with an incubation time of 10 minutes. Following incubation, appropriate amount of chromogenic substrate was rapidly added to yield a final concentration of 20 to 50µM. The residual thrombin activity was quantified by measuring the initial rate of hydrolysis from the linear increase in absorbance at 405 nm as a function of time under conditions wherein less than 10% substrate is consumed. Relative residual proteinase activity at each activity measured under otherwise identical conditions, except for the absence of TKS. Logistic **equation 4** was used to fit the dose dependence of residual proteinase activity to obtain IC_{50}.

$$Y = Y_O + \frac{Y_M - Y_O}{1 + 10^{(\log[L]_O - \log IC_{50}) \times HC}} \quad \ldots\ldots (4)$$

In this equation Y is the ratio of residual thrombin activity in the presence of TKS to that in its absence; Y_M and Y_0 are the maximum and minimum possible values of the fractional residual thrombin activity, respectively; IC_{50} is the concentration of TKS that results in 50% inhibition of enzyme activity, and HS is the Hill slope. HS does not represent co-operativity because TKS is a polydisperse species that may possess multiple binding modes and geometries. Sigmaplot 10.0 (SPSS, Inc. Chicago, IL) was used to perform non-linear curve fitting in which Y_M, Y_O, IC_{50} and HS were allowed to float.

3.2.5 Michaelis-Menten kinetics of substrate hydrolysis by thrombin in the presence of TKS.

Several concentrations of Spectrozyme TH (0.5 to 40 μM) were treated with by 4 nM thrombin in presence of fixed concentration of TKS (0 - 2.3 μg/mL). The initial rate of substrate hydrolysis was monitored from the linear increase in A_{405} in 20 mM Tris-HCl buffer, pH 7.4, containing 100 mM NaCl, 2.5 mM $CaCl_2$ and 0.1 % PEG 8000 at 25 °C. The data obtained was fitted by the standard Michaelis-Menten equation to calculate that apparent K_M and V_{MAX}.

3.2.6 Competitive binding studies with exosite ligands

TKS-dependent thrombin inhibition studies in the presence of [5F]-Hir[54-65](SO_3-) or porcine heparin were performed in a manner similar to that described above using the chromogenic substrate hydrolysis assay. Briefly, a solution of TKS (0 - 23 μg/mL) and thrombin (4nM) was incubated for 10 minutes at 37°C with either [5F]-Hir[54-65](SO_3-) (0 – 86 nM) or porcine heparin (0 – 100 μM) in 20 mM Tris-HCl buffer, pH 7.4, containing 100 mM NaCl, 2.5 mM $CaCl_2$ and 0.1 % PEG 8000. Following incubation, Spectrozyme TH was added to yield a final concentration of 20μM and its hydrolysis was measured as the initial change in absorbance at 405 measured. The molecular weight of bovine heparin was assumed to be 15000 Da, as reported in the literature. The dose-dependence of the fractional residual proteinase activity at each concentration of the competitor was fitted by **equation 4** to obtain the apparent concentration of TKS required to reduce thrombin activity to 50% of its initial value ($IC_{50,app}$).

3.2.7 Prothrombin time and Activated Partial Thromboplastin Time for plasma clotting assays in presence of TKS

Clotting time was determined in a standard 1-stage recalcification assay with a BBL Fibrosystem fibrometer (Becton-Dickinson, Sparles, MD). For PT and APTT assays, the reagents were pre-warmed to 37 °C. For PT assays, 10 μL the anticoagulant (or the reference molecule) was mixed with 90 μL of citrated human plasma, incubated for 30 s at 37 °C quickly followed by addition of 200 μL pre-warmed thromboplastin. For APTT assays, 10 μL of the anticoagulant was mixed with 90 μL citrated human plasma and 100 μL 0.2% ellagic acid. After incubation for 240 s, clotting was initiated by quickly adding 100 μL of 25 mM $CaCl_2$. Each experiment was performed in duplicate. The averaged data was fitted by a quadratic equation to calculate the concentration of the anticoagulant necessary to double the clotting time (2 × PT or 2 × APTT).

3.2.8 Thromboelastograph (TEG®) Analysis of Clot Formation in the Presence of TKS

The assays were performed using Thromboelastograph® Coagulation Analyzer 5000 (TEG®) (Haemoscope Corporation Niles, IL). Typically, these assays are performed to analyze the rate and structure of a clotting sample and its breakdown. Briefly, in the assays 20 μL of 200 mM $CaCl_2$ was transferred into the Haemoscope™ disposable cup, oscillating through 4°45’ angle at 0.1 Hz. This was followed by the addition of a mixture of 340 μL of sodium citrated whole blood containing 10 μL the anticoagulant or saline (control) at 37 °C. This recalcification initiates clot formation in the TEG® coagulation

analyzer, which operates until all necessary data collection (R, K, α and MA) is completed in an automated manner.

3.2.9 Hemostasis Analysis System (HAS^{TM}) Analysis of Clot Formation in the presence of TKS

Analysis of platelet function, clot formation and structure was performed using the HAS^{TM} (Hemodyne, Inc., Richmond, VA). A mixture of 700 µl of citrated whole blood and 10 µl of the anticoagulant or saline (control) was co-incubated at room temperature for 5 minutes and then 700 µl was placed in a disposable cup. Clotting was initiated with addition of 50 µl of 150 mM $CaCl_2$ to the blood – anticoagulant mixture to give a final $CaCl_2$ concentration of 10 mM, while the cone was simultaneously lowered into the recalcified blood sample. As the clotting proceeds, platelets attach to both surfaces generating tension within the fibrin meshwork. This tension is measured with a displacement transducer in terms of platelet contractile force (PCF). The onset of PCF is a measure of thrombin generation time (TGT), while clot elastic modulus (CEM) is the ratio of the applied force (stress) by the transducer to the measured displacement (strain). The HAS^{TM} system operates in an automated manner until all data is collected.

3.3 RESULTS

3.3.1 Structure of TKS

TK was prepared by Kishimoto et al. in a multi-step synthesis **(figure 30)**. Synthesis of TK results in generation of mixture of oligomeric species of *β–O-4* type linked lignin that ranged up to 20 monomer units in size. TK is thus structurally homogeneous but highly polydispered mixture of molecules a property shared with heparins. However, the aromatic scaffold makes TK more hydrophobic in nature as opposed to heparins. TK completely lacks the anionic character that might be critical to make fruitful interactions with the electropositive site on thrombin. This void was filled with introduction sulfate moieties imparting an overall anionic feature to TK.

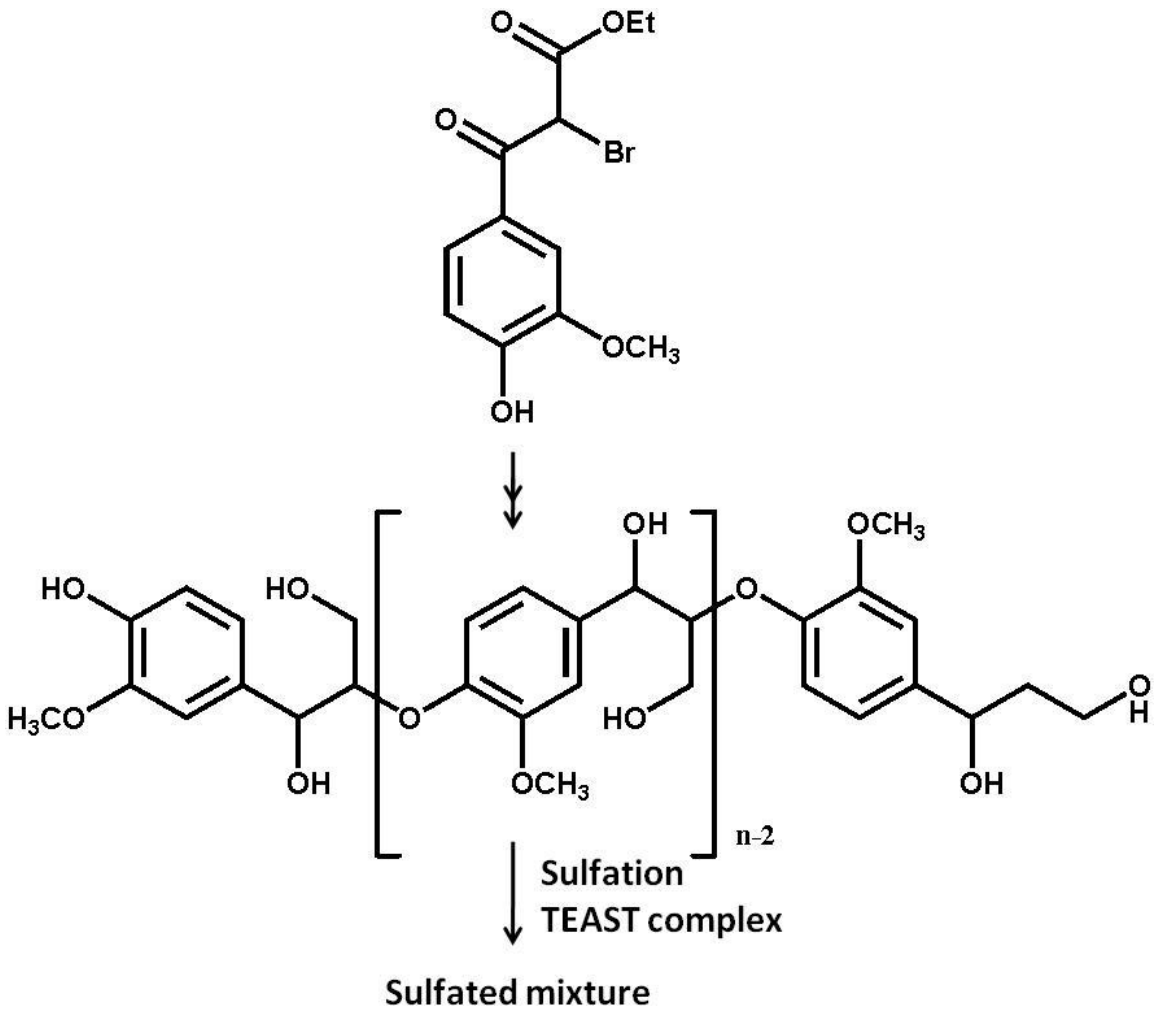

Figure 30. Schematic representation for synthesis of TKS[126]
TK was synthesized in a multistep process, which was ultimately sulfated using TEAST-complex to yield TKS.

3.3.2 Size Determination of TKS

Apparent molecular weight of TKS was determined with SEC using 0.1N NaOH at pH 11.0 as an eluent. M_W, M_N, M_P and P for TKS were calculated using PSS as a reference standard and were found to be 12,305 Da, 9,208 Da, 9,090 Da and 1.34 respectively. The chromatograms were broad and had a good symmetry, indicating the polydisperse nature of TKS **(figure 31)**. Sulfated TK (TKS) retained the polydispersity as its parent TK.

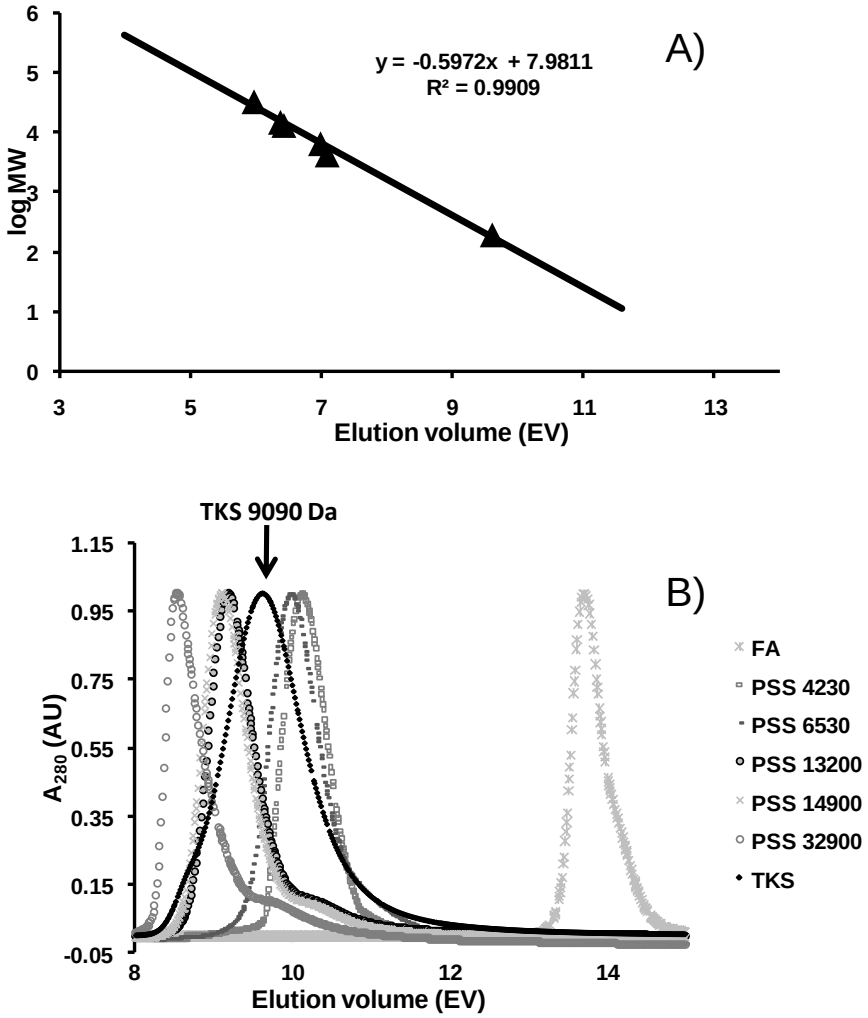

Figure 31. a) Standard curve generated using PSS for SEC b) SEC profiles of PSS and TKS.
Chromatogram of TKS is fairly symmetrical eluting between PSS 6530 and PSS 13200

3.3.3 Direct Inhibition Assay on Coagulation Proteinases.

TKS showed high potency in direct inhibition of thrombin as compared to some other enzymes in the coagulation cascade. TKS direct inhibition of thrombin in absence of AT was at least 91-5,000-fold better as compared to fVIIa, fIXa, fXa and fXIa under similar pseudo first order experimental conditions **(figure 32)**. In these experiments substrate hydrolysis of spectrozyme TH was monitored using spectrophotometer. The residual proteinase activity decreased with increase in the concentration of TKS. Whereas, the known AT activator enoxaparin had no direct inhibitory effect on thrombin and fXa in absence of AT. The decrease in the proteinase activity was fitted to a logistic dose response **equation 4** to obtain the IC_{50} value. TKS directly inhibits thrombin, fVIIa, fXa and fXIa with IC_{50} values of 18.7 nM, 1.70 µM, 56 µM and 90 µM respectively **(Table 09)**. TKS did not inhibit fIXa at all up to a concentration of 25 µM.

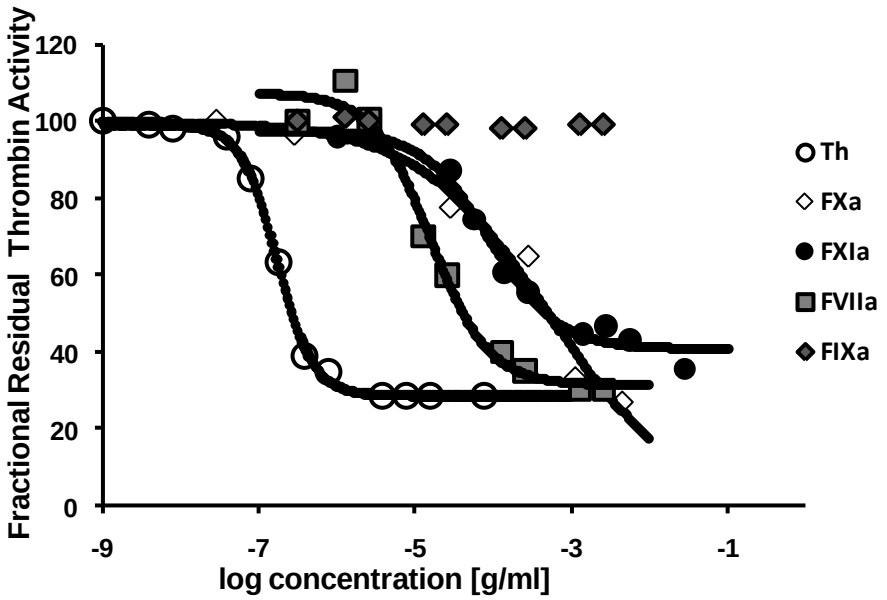

Figure 32. Inhibition of blood coagulation proteases, thrombin, fXa, fXIa, fVIIa and fIXa by TKS.
TKS inhibits thrombin at an IC_{50} value of 18.7 nM which is at least 91-fold more potent in inhibiting thrombin compared to other coagulation proteases.

Table 09: Inhibition of coagulation enzymes by TKS

Proteinase	log IC_{50} (g/ml)	Y_O	Y_M	HS	IC_{50} (µM)
Thrombin	-6.77 ± 0.02	29 ± 1	99 ± 1	1.9 ± 0.1	0.019 ± .001
fVIIa	-4.80 ± 0.10	31.3 ± 3	107 ± 5	1.2 ± 0.4	1.70 ± 0.10
fIXa	NI	100	100	NA	NA
fXa	-3.30 ± 0.60	0 ± 0	100 ± 4	0.5 ± 0.2	55.7 ± 2.0
fXIa	-4.05 ± 0.10	40 ± 2	98 ± 3	1.0 ± 0.2	9.9 ± 0.40

Inhibition studies were performed in 20 mM Tris-HCl buffer, pH 7.4, containing 100 mM NaCl, 2.5 mM $CaCl_2$ and 0.1 % PEG 8000 in PEG 20,000-coated polystyrene cuvettes. Spectrozyme TH was used as substrate and the residual enzyme activity in the presence of inhibitor was assessed by measuring the initial rate of substrate hydrolysis at 405 nm. Logistic equation 4 was used to fit the dose dependence of the residual enzyme activity to obtain log IC_{50}, Y_0, Y_M and HS values. See Methods for details.
Errors represent ±1 SE

3.3.4 TKS Disturbs the Catalytic Machinery of Thrombin

To understand the molecular basis for TKS inhibition of thrombin, we studied the Michaelis-Menten constants derived by non-linear regression analysis of the initial rate *versus* Spectrozyme TH concentration profiles at pH 7.4 and 37 °C in the presence of TKS **(figure 33)**. Plots of the initial rates *versus* Spectrozyme TH concentration were hyperbolic, as expected, from which the apparent Michaelis constant ($K_{M,app}$) and maximal velocity of the reaction (V_{MAX}) were derived. The results show that although the concentration of TKS increased from 0 µg/mL to 2.3 µg/mL (0 – 253nM), the $K_{M,app}$ value fluctuated around 1.5 µM, or alternatively remained essentially invariant in the range of 2.8 to 1.3 µM **(Table 10)**. This suggests that the presence of TKS does not much affect the binding of the chromogenic substrate to the active site of the enzyme. In contrast, the V_{MAX} value decreased steadily from a high of 25.5 mAbsU/min in the absence of TKS to a low of 7.4 mAbsU/min at 2.3 µg/mL TKS corresponding to a decrease in k_{CAT} value from 42.8 to 12.4 s^{-1}, respectively. Thus, the presence of TKS does not directly affect the binding of substrate in the active site but indirectly brings about structural changes in the active site of thrombin, which do not alter the formation of the thrombin–Spectrozyme TH Michaelis complex, but significantly reduce the rate of conversion of the complex into products.

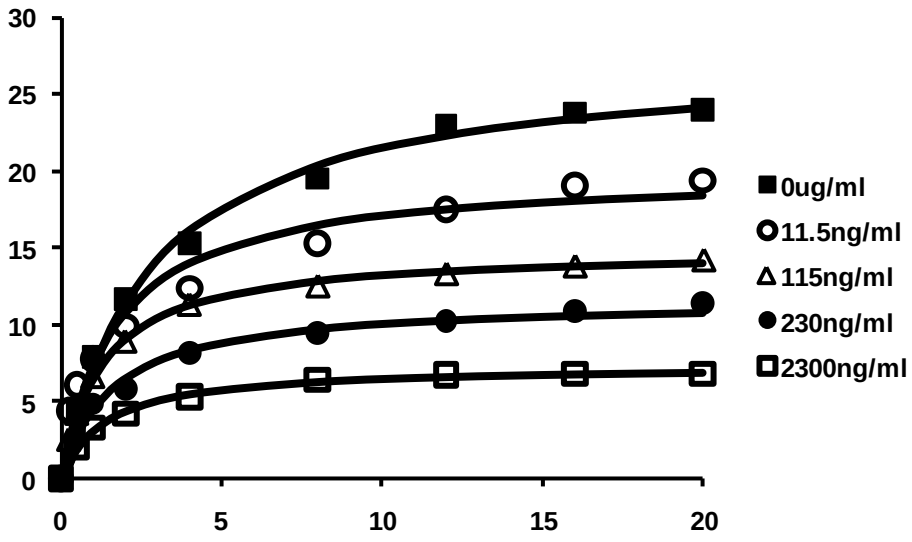

Figure 33: Michaelis-Menten Kinetics of Spectrozyme TH Hydrolysis by Thrombin in the presence of TKS.
The initial rate of hydrolysis at various substrate concentrations was measured in pH 7.4 buffer as described in 'Experimental Procedures'. Solid lines represent non-linear regressional fits to the data using the Michaelis-Menten equation.

Table 10: Michaelis-Menten Kinetics of Spectrozyme TH Hydrolysis by Thrombin in the presence of TKS

$[TKS]_o$ *(ng/ml)*	K_M *(μM)*	V_{MAX} *(mAU/min)*	kcat *(s^{-1})*
0	2.8 ± 0.2	25.5 ± 0.7	42.8 ± 0.3
11.5	1.7 ± 0.3	20.0 ± 1.0	33.6 ± 0.3
115	1.3 ± 0.1	14.8 ± 0.1	24.9 ± 1.2
230	1.6 ± 0.3	11.5 ± 0.5	19.3 ± 0.2
2300	1.4 ± 0.1	7.4 ± 0.1	12.4 ± 0.1

K_M and V_{MAX} were measured as described in 'Experimental Procedures'.
Error represents ±1 S.E.

3.3.5 TKS Binds at the Heparin Binding Site of Thrombin

To test whether TKS binds in one of the two anion-binding sites, we sought to measure the effect of a hirudin-based peptide, [5F]-Hir[54-65](SO_3-), an exosite-1 binding ligand on the IC_{50} values of TKS-inhibition of thrombin. Earlier studies have shown that [5F]-Hir[54-65](SO_3-) binds thrombin with 28 nM affinity in exosite-1 with 1:1 stoichiometry and enhances the forward rate constant (k_{CAT}) of Spectrozyme TH hydrolysis. Utilizing this knowledge we studied the competition between these two ligands by measuring the $IC_{50,app}$ values of thrombin inhibition by TKS in the presence of the dodecapeptide over a concentration range up to 3.2-fold higher than the K_D of the thrombin-[5F]-Hir[54-65](SO_3-) complex. The $IC_{50,app}$ values were measured in the standard dose-response assay, which we had used to determine thrombin inhibition. As the concentration of the dodecapeptide was increased from 0 to 86nM, $IC_{50,app}$ essentially remained unchanged varying between 16 nM to 20 nM **(figure 34a)**. This suggest that the interaction of [5F]-Hir[54-65](SO_3-) with thrombin does not affect TKS inhibition of thrombin. Thus, it appears that TKS does not preferentially bind thrombin in anion-binding exosite I. A similar enzyme inhibition study was carried out in presence of an exosite-2 binding ligand **(figure 34b)**. Exosite-2 ligand like bovine heparin does not affect the proteolytic activity of thrombin, while TKS is a potent inhibitor. Thus, if TKS binds in or near the heparin binding site, its inhibition potency is expected to decrease as a function of the concentration of the competitor **(Table 11)**. As the concentration of heparin was increased from 0 μM to 100 μM, the $IC_{50,app}$ values of thrombin inhibition increases from 18 nM to 138 nM. This clearly implies that heparin is competing with TKS to bind in or near the anionic-binding exosite-2 of thrombin.

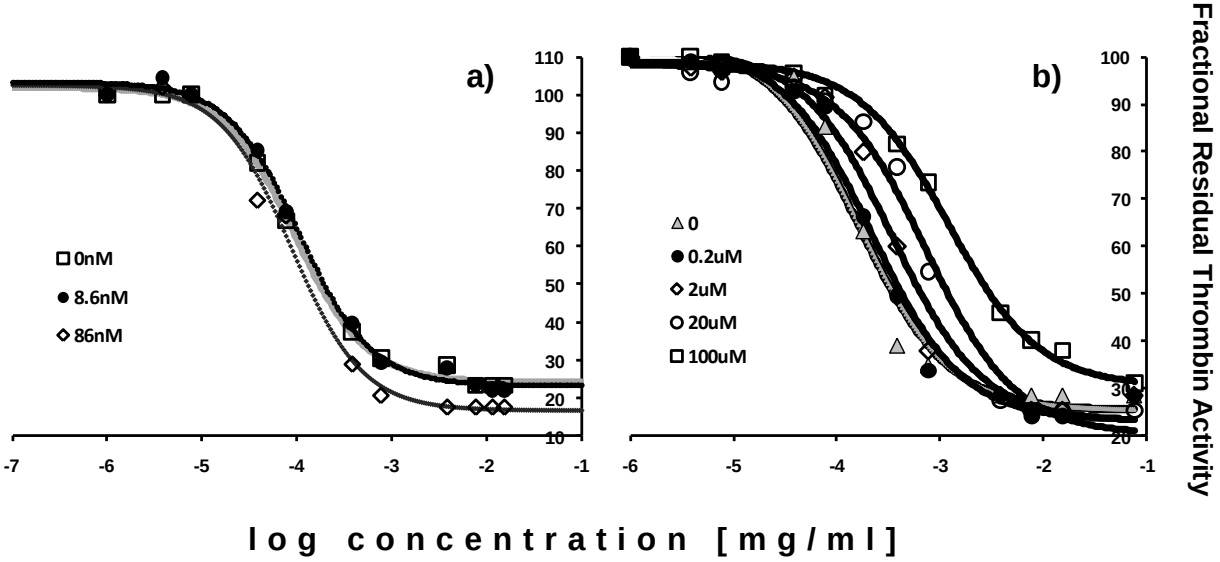

Figure 34. Inhibition of thrombin by TKS in presence of exosite-1 & 2 ligands
Competitive effect of [5F]-Hir[54-65](SO_3^-) **(figure 29a)** and porcine heparin **(figure 29b)** on the inhibition of thrombin by TKS. Residual thrombin activity was measured through Spectrozyme TH hydrolysis in 20 mM Tris-HCl buffer, pH 7.4, containing 100 mM NaCl, 2.5 mM $CaCl_2$ and 0.1 % polyethylene glycol (PEG) 8000 at 37 ^{O}C in the presence of 0 and 86 nM [5F]-Hir[54-65](SO_3^-) and 0 -100 μM of porcine heparin. Solid lines represent fits using the logistic equation 4 to obtain the apparent IC_{50}, as described in 'Experimental Procedures'.

Table 11: Inhibition of thrombin by TKS in the presence of hirugen analog [5F]-Hir[54-65](SO3-) and porcine heparin

[Competitor]	log IC_{50} (mg/ml)	Y_0	Y_M	HS	IC_{50} (ng/ml)	IC_{50} (nM)
0nM	-3.77 ± 0.02	28.6 ± 0.70	99.1 ± 0.8	1.9 ± 0.1	170 ± 6.5	18.0 ± 0.7
Hirugen						
8.6nM	-3.72 ± 0.04	22.8 ± 0.12	106 ± 2.2	1.1 ± 0.1	187 ± 17.0	20.6 ± 1.9
86nM	-3.81 ± 0.07	16.3 ± 2.0	105 ± 4.0	1.1 ± 0.2	153 ± 24.0	16.8 ± 2.6
Porcine Heparin						
0.2 μM	-3.65 ± 0.03	25.9 ± 1.1	98.7 ± 1.2	1.6 ± 0.1	222 ± 14.0	24.4 ± 1.5
2.0 μM	-3.47 ± 0.02	26.3 ± 0.9	97.8 ± 0.9	1.8 ± 0.1	340 ± 16.0	37.4 ± 1.8
20 μM	-3.18 ± 0.03	24.3 ± 1.4	95.9 ± 1.1	1.6 ± 0.2	655 ± 49.0	72.1 ± 5.4
100 μM	-2.90 ± 0.05	28.2 ± 1.8	99.7 ± 1.0	0.9 ± 0.1	1250 ± 142.0	137.5 ± 15.6

Logistic equation 4 was used to fit the dose dependence of the residual enzyme activity to obtain log IC_{50}, Y_0, Y_M and HS values. See Methods for details.
Error represents 1 ±S.E.

3.3.6 Effect on Clotting Times

PT and APTT are commonly used to assess the coagulation status of human plasma. TKS exhibited a significant concentration-dependent prolongation of PT and APTT. A typical parameter for describing anticoagulant activity in these assays is the concentration of the anticoagulant needed for doubling the normal plasma clotting time (2 × PT or 2 × APTT). The 2 × PT and 2 × APTT value for TKS was found to be 68.6 µg/mL (7.6µM) and 23.6 µg/mL (2.6µM), whereas that for enoxaparin was 75.3 µM and 1.2 µM respectively, suggesting that TKS is 9.9-fold more potent in the PT assay and approximately 2.2-fold weaker anticoagulant in the APTT assay as compared with enoxaparin **(figure 35a & b)**.

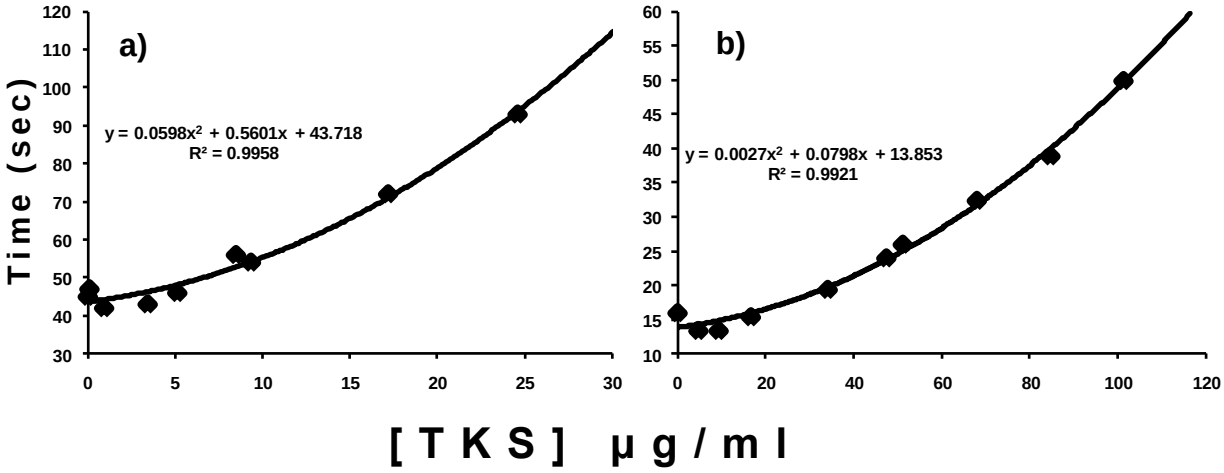

Figure 35: Plasma clotting assay performed using APTT and PT for TKS
a) & b) figures represent APTT and PT results TKS.

3.3.7 Effect of TKS on whole blood clotting

Whole blood clotting is a dynamic process that involves many components, including cells, which may alter anticoagulant potency. To compare TKS and enoxaparin in a whole blood system, we employed TEG, a technique used in clinical settings for following anticoagulation with LMWHs. TEG measures various responses of a formed clot to shearing force. In this technique, a pin is inserted into an oscillating cup containing whole blood. As fibrin polymerizes, the pin starts to move with the oscillating cup, and the movement of the pin is recorded as amplitude, which in time reaches maximum amplitude. The stronger the clot, the more the pin moves with the cup and the higher the maximum amplitude. Shear elastic modulus strength (*G*), a measure of clot stiffness, is calculated from maximum amplitude. Additionally, *R* and angle α are also obtained in a TEG experiment. *R* is the time required for the initial fibrin formation, whereas α is the acute angle in degrees between an extension of the *R* tracing and the tangent of the maximum slope produced by the TEG tracing during clot stiffening. Angle α is a measure of the rate of formation of three-dimensional fibrin network. Parameters that affect maximum amplitude include fibrin concentration and structure, concentration and functional state of platelets, deficiency of coagulation factors and the presence of clotting inhibitors. TKS affects all the parameters *R*, α, maximum amplitude and *G* parameters in a dose-dependent manner. Briefly, as the concentration of TKS increases from 0 to 414 μg/mL, *R* increases from 7.7 to 25.9 min. Likewise, TKS lowers the value of angle α from 56° for normal blood to 22° at the highest concentrations studied. This indicates that the kinetics of fibrin polymerization and networking is significantly retarded by the presence of TKS **(figure 36)**. Enoxaparin exhibits similar characteristics,

except that it is 7.9-fold more potent than TKS when comparisons are made at doubling the *R* value from its value in the absence of any anticoagulants. Likewise, enoxaparin is 12.2-fold and 12.9-fold more potent when comparisons are made for a 50% reduction in the angle α and shear elastic modulus *G*, respectively **(Table 12)**.

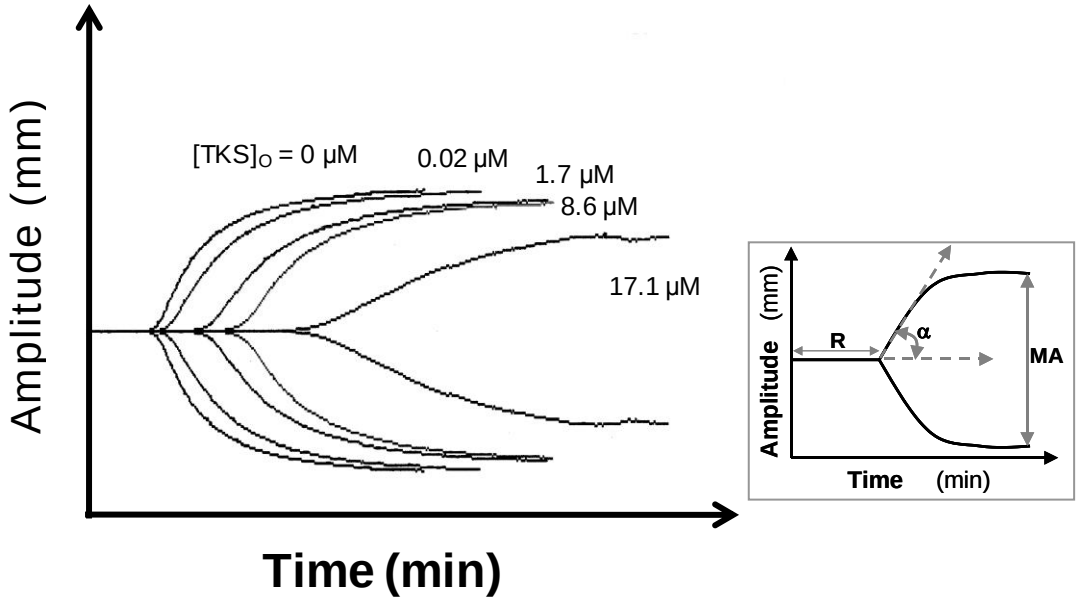

Figure 36. Effect of TKS on clot formation in whole blood using TEG®.
Inset in shows a typical thromboelastogram expected of any anticoagulant. MA, R, α and G are parameters obtained from TEG® analysis. See Methods for details. Figure shows change in thromboelastograph as a function of increasing concentration of TKS.

Table 12: Parameters obtained from thromboelastograph (TEG®) study of TKS and enoxaparin in human whole blood.[a]

		TEG® Parameters[a]			
	conc	***R[b]***	***α[c]***	***MA[d]***	***G[e]***
	(μM)	*(min)*	*(degrees)*	*(mm)*	*(Dynes/cm²)*
TKS	0	7.7	56.0	61.0	7821
	0.0171	8.9	50.5	50.5	7658
	1.71	13.2	42.5	57.0	6628
	8.6	16.9	43.0	55.5	6236
	17.1	25.9	22.0	41.5	3547
Enoxaparin	0	7.0	59.0	56.5	6456.5
	0.3	8.0	49.0	51	5204.0
	0.44	9.5	39.5	51	5204.0
	0.6	11.5	43.0	47.0	4434.0
	0.75	14.0	41.0	46	4259.5
	0.89	17.0	36.5	47.0	4434.0
	1.0	17.0	31.5	42.0	3620.5

[a]TEG parameters were obtained in an automated manner from the TEG® coagulation analyzer. See Experimental Procedures for a description of the setup. [b]Reaction time R is the time interval between the initiation of coagulation and the appearance of first detectable signal of no less than 2 mm in amplitude. [c]Angle α is the acute angle in degrees between an extension of the R value tracing and the tangent of the maximum slope produced by the TEG® tracing. [d]Maximum amplitude (MA) is the maximum distance the pin of TEG® moves at the end. [e]The shear elastic modulus strength (G) is a calculated parameter ($G = 5000 \times MA / (100 - MA)$) and is a measure of clot strength.

To further compare the whole blood anticoagulant potential of TKS with enoxaparin, we performed an ex-vivo study using HAS, which measures the forces generated by platelets within a clot. In this technique, the clot is allowed to form between a temperature controlled lower surface (cup) and a parallel upper surface (cone). As the clot grows, it attaches to both the surfaces, pulling the fibrin strands inward. This pull is measured by a displacement transducer, which produces an electrical signal on the cone proportional to the amount of force generated by the platelets. HAS also provides detailed information on clot structure through the measurement of CEM, which is the ratio of stress induced by platelets to strain arising from the change in clot thickness. PCF is observed to increase as soon as thrombin is formed, suggesting that the appearance of PCF can be used as surrogate marker for TGT, the minimal time required for production of thrombin following initiation of clotting. In addition to its dependence on thrombin, PCF is sensitive to platelet number, platelet metabolic status, presence of thrombin inhibitors and the degree of glycoprotein IIb/IIIa exposure. Likewise, CEM is a complex parameter that is sensitive to changes in clot structure, fibrinogen concentration, the rate of thrombin generation and red blood cell flexibility, whereas TGT is sensitive to clotting factor deficiencies, antithrombin concentration and the presence of anticoagulants. Low PCF and CEM coupled with a prolonged TGT are associated with increased bleeding risk, whereas elevated PCF and CEM paired with a decreased TGT are associated with thrombotic disease states. TKS affects TGT, PCF and CEM parameters in a dose-dependent manner with 6.7 μM TKS required to double the TGT value using HAS. This effect parallels the results obtained in TEG. More importantly, the presence of TKS in blood decreases PCF from 8 to 0.66 kdynes at 8.3 μM **(figure 37a)**, whereas enoxaparin

induces a PCF of 0.66 kdynes at 0.47 μM, a difference of 17.7-fold. Likewise, TKS decreases CEM from 18.25 kdynes/cm^2 for normal blood to 0.62 kdynes/cm2 at 8.3 μM **(figure 37b)**. Comparison of TKS for a 50% reduction in CEM values indicates that enoxaparin is 23.5-fold more potent than TKS **(Table 13)**. These results confirm that TKS behaves in a manner similar to enoxaparin, except for the concentration at which it is effective. When compared with FDS, TKS has slightly better potency in whole blood, 1.4 – 2.9-fold based on the parameter evaluated. This slight reduction in potency can be attributed to the more heterogeneous nature of FDS, which is structurally more diverse than TKS.

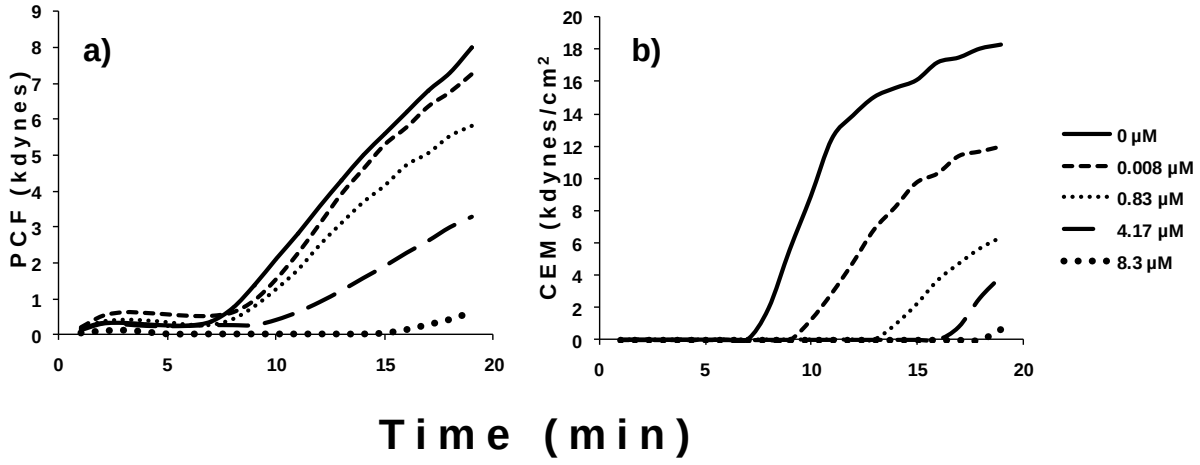

Figure 37. Effect of TKS on platelet function in whole blood using HAS™.
HAS™ profiles obtained with show the variation in a) PCF and b) CEM, as a function of concentration of TKS.

Table 13: Parameters obtained from the Hemostasis Analysis System (HAS™) study of TKS and enoxaparin in human whole blood.[a]

		HAS™ Parameters[a]		
	Conc	***TGT*[b]**	***PCF*[c]**	***CEM*[d]**
	(μM)	*(min)*	*(Kdynes)*	*(Kdynes/cm²)*
TKS	0.0	6.25	8.00	18.25
	0.008	5.05	7.27	12.00
	0.83	6.55	5.82	6.31
	4.17	11.25	3.30	3.94
	8.3	13.55	0.66	0.62
Enoxaparin	0.0	3.55	7.60	21.60
	0.146	5.15	5.30	15.10
	0.218	9.05	3.60	12.70
	0.346	11.00	2.80	8.50
	0.437	12.45	0.90	2.90

[a]HAS™ parameters were obtained in an automated manner from the Hemostasis Analysis System. See Experimental Procedures for a description of the setup. [b]Thrombin generation time is the time interval between the initiation of coagulation and the onset of detectable platelet contractile force. [c]Platelet contractile force describes the forces generated by platelets during clot retraction. [d]Clot elastic modulus is the ratio of the applied force (stress) to the measured displacement of the clot.

3.4 Discussion

In an effort to mimic heparin's structural features we have reported at least 3 different types of carboxylated lignins. All three were a fairly complex mixture of molecules arising from different sizes and linkage types. Further, we studied the size based potency of one of the better DHPs, FD while still retaining the structural heterogeneity. In our continuing efforts to achieve relevant and meaningful information out of this complex mixture we have synthesized structurally homogenous lignin-like mixture. The main difference from the earlier DHPs is the lack of carboxylic acid functionality, which has been replaced by sulfates to achieve an overall anionic nature.

While conducting the literature search for synthesis of a β-O-4 type lignin polymers we stumbled across Kishimoto and co-workers who have already synthesized this structurally homogenous mixture.[126] Before going through an arduous task of multi-step synthesis we obtained 100 mg sample from Dr. Kishimoto's group as a generous gift. *Note:* A fellow graduate student, Akul Mehta is currently working on synthesis of TK to generate larger amounts to be studied in animal models.

TK polymer received as a gift was subjected to sulfation using TEAST complex to yield TKS. The molecular weight characteristics of TKS were evaluated using SEC. The M_N and M_P were found to be 9,208 and 9,090 respectively suggesting that there is equal distribution of samples on either side of the bell shaped curve indicative of a symmetric chromatogram. The polydispersity derived from the relationship between M_W (12,305) and Mn (9,208) indicated that TKS like DHPs are polydisperse in nature with a P value

of 1.34. When compared with DHPs (P = 2.0 - 4.0) TKS is fairly less polydisperse implying the advantage of controlled polymerization over random polymerization. When DHPs are formed the enzyme horse radish peroxidase (HRP) randomly couples the monomers to generate *β-O-4* and *β-5* linked structures as opposed to synthetically made TKS, where the linkages are formed as directed to yield just the *β-O-4* type polymer. Using the per sulfated form of the starting monomer the apparent chain length was calculated to be 25.

Since TKS was a result of the complex DHP mixture of FA, we opted first to evaluate TKS for direct inhibition of the coagulation factors in the common pathway rather than conduct the APPT and PT assays. TKS potently inhibited thrombin with an IC_{50} of 18.7 nM, which is a 2.7-fold improvement over the most potent sulfated FD. Interestingly, TKS could inhibit fXa only at a very high concentration of 56μM. This is a 3000-fold increase, which indicates the excellent specificity of TKS for thrombin over fXa. To probe into the specificity of TKS, which lacks the carboxylic acid group we chose to screen several other important factors in the coagulation cascade. The IC_{50} values obtained for inhibition of fVIIa, and fXIa were 1.7 μM and 90 μM and TKS completely failed to inhibit fIXa at concentrations as high as 25 μM. TKS inhibition for fVIIa and fIXa being 94.4-fold and 5000-fold weaker than thrombin strengthens the conclusion that indeed TKS is a specific inhibitor of thrombin. Probably, this also implies that thrombin specificity arises due to the structural uniqueness of TKS, which possess only the *β-O-4* type linkages and not due to the absence of carboxylic acids. Presence of sulfates instead of carboxylic acid imparting such a huge specificity in inhibition seems highly unlikely,

though it remains to be determined if it was true. Also, from our previous work on sulfated and unsulfated DHP fractions it is evident that there is none to insignificant change (1.07 to 1.4-fold) in the specificity with the introduction of sulfates.

To understand the mechanism of inhibition of TKS by which it brings about the change in binding of the substrate at the active site we chose to study all three potential binding sites on thrombin. We performed Michaelis-Menten type kinetics to investigate the active site binding phenomenon and competitive ligand binding studies to probe the allostericity for exosite-1 and 2. TKS did not compete with the substrate during binding but it brought about the change in the hydrolysis of the substrate through allosteric modulation. This was apparent by the decrease in the V_{MAX} and K_{CAT} values, whereas the Michaelis-Menten constant remained unchanged. The competitive ligand binding studies with site specific ligands [5F]-Hir[54-65](SO_3-) (exosite-1) and heparin (exosite-2) revealed that TKS competes with heparin to bind at the exosite-2 of thrombin. This was concluded based on worsening of the $IC_{50,app}$ values for TKS inhibition of thrombin with increasing concentration of exosite-2 competitor. And in case of exosite-1 ligand a very insignificant change in the $IC_{50,app}$ values was observed. At this point it is important to recall that both the exosites are electropositive with exosite-2 being less compensated and less hydrophobic than exosite-1.

We further evaluated TKS for their effect as an anticoagulant in human plasma and whole blood. This is an important study that had to be undertaken considering the fact that heparins and LMWH non-specifically bind to plasma proteins resulting in the numerous

side effects they carry. The plasma anticoagulation effect of TKS was tested using APTT and PT assays, which would assess its ability to work via the intrinsic and the extrinsic pathway of the coagulation system. Comparative studies with enoxaprain, a LMWH revealed that TKS was 2.2-fold weaker in the APTT assay, while it was 9.9-fold more potent in acting through the extrinsic pathway. Based on these comparisons it is hard to conclude if TKS evades non-specific interactions with the plasma proteins as both enoxaparin and TKS work through a complete different mechanism. A similar study using an FDA approved DTI would yield a more relevant comparison. Nevertheless, the plasma study indicates that TKS still retains its anticoagulant potency when subjected to a higher system like plasma. Also, when compared with the most potent sulfated FD fraction, TKS has essentially same effect on APTT and PT implying a cumulative effect in case of DHPs, which works through thrombin and fXa. Hence, we can conclude that though TKS is more potent in inhibiting thrombin as compared to DHPs they bring about the same effect in higher systems like plasma through a complete different mechanism.

Based on the results achieved from plasma studies TKS was subjected to a more complex system to prove its anticoagulant potency. Whole human blood assays performed using TEG® and HAS™ indicated that TKS was 7.9-12.9-fold and 17.7-23.5-fold less active in comparison with enoxaparin. It is possible that the significant hydrophobic character of TKS induces binding to cells resulting in significant sequestering of active agent. It is likely that this non-specific binding will be reduced with less polydisperse, synthetic small molecules.

Overall, TKS demonstrates a major improvement over DHPs in terms structural homogeneity, which has led to a greater specificity in targeting thrombin. It also possesses a better plasma and whole blood anticoagulation activity suggesting the reduction in the non-specific binding of the plasma proteins. Toxicity studies have to be performed to ascertain that TKS do not induce abnormal effects.

3.5 Conclusion

The entire study points towards specificity of TKS, which arises due to the *β-O-4* type of linkage. Our DHPs are structural heterogeneous leading us to believe that structural features like the linkages are dictating the specificity in targeting enzymes. We cannot hold back to hypothesize that *β-5* type linkages, which is the second most abundant in lignin and our enzymatically synthesized DHPs might be fXa specific. This hypothesis if proven would revolutionize the entire process of anticoagulant drug design. Also, studies from the previous chapter indicate that an octamer might be the optimum working range. Utilizing the information from these studies a tetramer of *β-O-4* type synthesized would be an appropriate chain length to start with, which can be easily converted to an octamer by combining the two tetramers. Further, slight functional group modification might be essential to achieve greater potencies. By and large, this study puts forward a new class of molecule as a potential anticoagulant.

CHAPTRT 04

Non-sulfated Cinnamic Acid-Based Lignins As Potent Antagonists of HSV-1 Entry Into Cells

4.1 Background

4.1.1 Introduction

Herpes viruses are a leading cause of human viral disease, second only to influenza and cold viruses. They are capable of causing overt disease or remaining silent for many years only to be reactivated. The herpes family contains more than hundred viruses that infect organisms of which eight are known to infect human beings. In general herpes viruses cannot survive at room temperature, especially outside of the body where they can dry out. Direct contact between susceptible cells and secretions of infected cells is usually required for transmission. The herpes virus has an excellent ability to remain dormant for years and the sporadic reappearance of herpetic lesions is a perturbing aspect of the infection.[127-128] For reasons that are poorly understood the latent, inactive, infection can become active and cause illness. Reactivation of dormant viruses occurs when they start to reproduce inside cells, eventually causing them to burst and spread the virus particles to propagate infection.[129] The virus particles can also attack neurons causing neurotropic disorders. Breakage of latency can occur in these cells and the virus can travel back down the nerve axon, where lesions are seen.[130] This means that recurrence of infection (and therefore symptoms) can occur at the same site as the initial infection. There are several agents that seem to trigger recurrence, most of which are stress-related. It also appears that exposure to strong sunlight and perhaps fever can lead to recurrence.

These factors may cause some degree of immune suppression that leads to renewal of virus proliferation in the nerve cell.

Herpes infections are highly prevalent affecting at least 1 in 3 individuals in the US. Of the eight strains known to infect humans, herpes simplex virus, HSV-1 and HSV-2 are the most common ones. Refer **Table 14** for the list of 8 strains of herpes virus and their site of latency. The primary difference between the two is their "site of preference" when establishing latency in the body.[131] HSV-1 usually establishes latency in the trigeminal ganglion, a collection of nerve cells found in close proximity to the ears and recurring herpes outbreaks will commonly occur around the mouth or facial region. HSV-2 usually establishes latency in the sacral ganglion, a collection of nerves found at the lower base of the spine and recurring outbreaks will commonly occur in the genital region. Though this is the most commonly noted difference, it is not absolute. Both HSV-1 and HSV-2 can reside in either or both parts of the body and infect orally and/or genitally.

HSV-1 is often transmitted in childhood through kissing, but can be transmitted at any age through direct skin-to-skin contact. In the US about 50% of adults are carrier of HSV-1 antibodies by the time they are young adults and by the time they are 50 years 80-90% of Americans carry HSV-1 antibodies.[132] For both types, at least two-thirds of infected people have no symptoms, or symptoms too mild to notice such as cold sores. However, both types can recur and spread even when no symptoms are present. Occasionally, the virus spreads to the central nervous system causing meningitis or encephalitis. So far, vaccines, ILs, IFNs, therapeutic proteins, antibodies,

immunomodulators and small-molecule drugs with specific or non-specific modes of action lacked either efficacy or the required safety profile to replace the nucleosidic drugs acyclovir, valacyclovir, penciclovir and famciclovir as the first choice of treatment.[133-135] All of these drugs are classified, as "Nucleoside Antimetabolites" and they are inhibitors of viral DNA polymerase. These drugs are phosphorylated by viral thymidylate kinase to the monophosphate, which is further bioactivated to the triphosphate. The triphosphate is selective inhibitor of viral DNA polymerase.

4.1.2 Diseases caused by the Herpes virus

Oral herpes, Herpes keratitis, Herpes whitlow, Herpes gladiatorum, Eczema herpeticum, Genital herpes, HSV proctitis, HSV Encephalitis, HSV Meningitis, HSV infection of neonates (This results from HSV-2 and is often fatal, although such infections are rare. Infection is especially possible if the mother is shedding virus at the time of delivery).

Table 14: Types of herpes viruses infecting humans and the site of latency

Acronym	*Name*	*Site of Latency*
HSV-1	Herpes Simplex Virus 1	Sensory Neurons
HSV-2	Herpes Simplex Virus 2	Sensory Neurons
VZV	Varicella-Zoster Virus	Sensory Neurons
CMV	Cytomegalo Virus	Monocytes, Endothelial cells
EBV	Epstein Barr Virus	B Lymphocytes
HHV-6	Human Herpes Virus 6	T cells, Monocytes
HHV-7	Human Herpes Virus 7	T cells, Monocytes
HHV-8	Kaposi Sarcoma Associated Virus	Monocytes ?

4.1.3 Structure of Herpes Virus

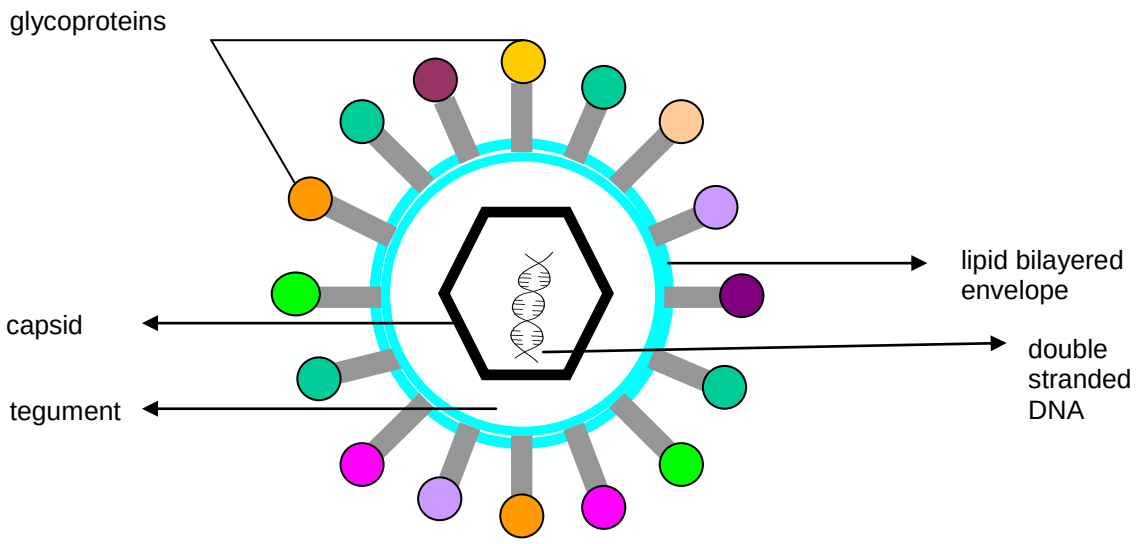

Figure 38. General structure of the herpes virus

The general structure of the herpes virus consists of the following: (refer **figure 38)**

Envelope

Herpes viruses are enveloped viruses with close to a dozen glycoproteins attached to the cell surface. They bud from the inner nuclear membrane, which has been modified by the insertion of herpes glycoproteins. These glycoproteins determine the cell to be infected.

The viral membrane is quite fragile and a virus with a damaged envelope is not infectious. Besides drying, the virus is also sensitive to acids, detergents and organic solvents as might be expected for a virus with a lipid envelope.

Tegument

The space between the envelope and the capsid is the amorphous tegument. This contains virally-encoded proteins, such as VP16 and *vhs* (virus host shut off), and enzymes that are involved in the initiation of replication.

Capsid

These viruses have a doughnut shaped capsomere of about 100-200 nm in diameter with an icosahedral proteinaceous nucleocapsid. The latter contains 162 capsomeres or morphological elements.

Genome

Inner core of the herpes viruses have a linear double stranded DNA viral genome encoding about 100-200 genes. Many of these proteins (about half) are not directly involved in the virus structure or controlling its replication, but function in the interaction with the host cell or the immune response of the host. HSV-1 and HSV-2 have characteristic resemblances in their genome. The genome of HSV encodes a number of enzymes: DNA-dependent DNA polymerase, thymidine kinase (phosphorylates thymidine and other nucleosides), ribonucleotide reductase (converts ribonucleotides to deoxyribonucleotide) and serineprotease (converts a scaffolding protein to its final form). The genome also encodes 11 surface glycoproteins. These are involved in attachment (gB, gC, gD and gH), fusion of the viral membrane with that of the host cell (gB, gH and gL), immune escape and other functions (gC, gE and gI), production of virus in cell culture (gK), and unknown function (gG, gJ and gM).[136-145]

4.1.4 HSV-1 Infection

HSV-1 infection of cells can be divided into two phases, the binding phase and the penetration phase **(figure 39)**. The first phase involves the binding of the viral glycoprotein gC and/or gB to the glycosaminoglycans (GAGs) chains on cell surface proteoglycans.[146-148] The major type of GAG chain found on the cell surface is heparan sulfate (HS). This initial binding is not sufficient for viral penetration, which further involves fusion of the viral envelope with the cell membrane. This step involves interaction of viral glycoprotein gD with one or several receptors for gD on the cell surface, before the viral particle can fuse with the cell plasma membrane and the viral capsid is released into the cytoplasm. The fusion process is a complex set of events involving multiple interactions between various gD receptors on the cell surface and the viral glycoprotein gD, gB and hetero-oligomers of gH and gL. Depending on the nature of interaction and size of HS chain, a single chain may bind multiple viral ligands on a virion.[149-151] The entry receptors discovered to date fall into three categories. They include HVEM (herpes virus entry mediator), a member of TNF receptor family, nectin-1 and nectin-2, members of the immunoglobin superfamily and specific site in HS generated by certain 3-O-sulfotransferases (3-OST).[152-160]

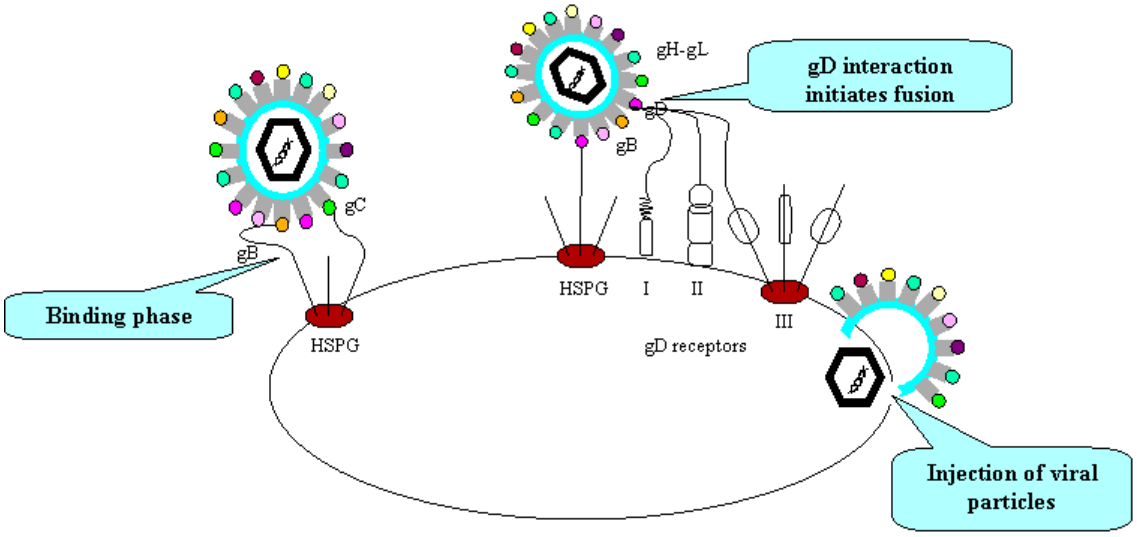

Figure 39. Pictorial representation of the mechanism of herpes virus entering into human cell.

4.1.5 Evidence Showing Role of HS

There is convincing evidence indicating that HS is critical for HSV-1 adsorption on the cell surface and its subsequent entry into cells.[161-162] First, cells that are devoid of HS (but not other GAGs) because of enzymatic treatment or genetic mutation are markedly less susceptible to HSV-1. These cells have greatly reduced number of receptors for viral binding. It has been shown that HSV-1 attaches weakly to HS-deficient Chinese hamster ovary (CHO) cells.[163-164] Second, soluble heparin, which is structurally similar to HS, inhibits binding of viruses to cells, whereas the structurally less similar GAG chondroitin sulfate fails to inhibit binding or infection. Third, gC and gB bind selectively and independently to heparin-sepharose columns under physiological conditions. Also, degree of sulfation of GAGs is an important determinant for recognition by viral glycoprotein gB2.[165] Heparin, which has higher degree of sulfation as compared to HS, is a better

competitive inhibitor of gB2 binding.[166] In 2002, Liu *et.al* have characterized a HS-based octasaccharide that binds to HSV-I gD.[167] The distinguishing feature in the composition of the octasaccharide is the presence of 3-O-sulfate glucosamine residue, which is an uncommon structural modification in heparin sulfate. Its presence in the HSV-I gD binding sequence must probably confer specificity of interaction by generating a unique protein binding site, hence assisting HSV-I entry into the cell.[168] Thus, HS is required for both viral binding and penetration –the two early events in infection. HS also plays important role in attachment of other viruses such as the human immunodeficiency virus (HIV) (E gp120 and gp41), dengue virus (gC, gE and gM), foot and mouth disease virus (E VP1-4), vaccinia virus (E A27L), Sindbis virus (E2 glycoprotein), respiratory syncytial virus, and Echovirus.[169-174] In each of these viruses, cell surface HS is used for gaining entry into the cell.

4.1.6 Heparan Sulfate

HS is the most complex polysaccharide on the surface of the mammalian cells. GAG polysaccharides are long, polyanionic chains consisting of repeating disaccharide units.[175] HS is a GAG covalently attached to the protein core (in the cell membrane - syndecan-1, N-syndecan, fibroglycan, amphiglycan and glypican) of proteoglycans, which are expressed on nearly all cell surfaces, in the extracellular matrices and are even segregated into intracellular granules.[176-177] Structurally, HS is a heterogeneous linear co-polymer of glucosamine (GlcN*p*) and glucuronic acid (GlcA*p*) residues linked in a 1-4 manner, of which the GlcN*p* residues are typically acetylated at 2- position **(figure 40)**.[178] Despite this apparently simple monomeric disaccharide structure, HS perhaps represents the most

structurally complex molecule nature biosynthesizes because of two critical, essentially incomplete,

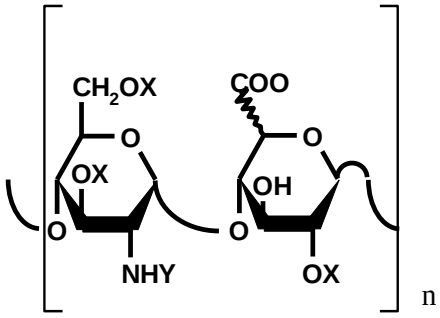

X = H or SO_3^-
Y = H or Ac or SO_3^-

Figure 40. General structure of heparan sulfate showing the disaccharide unit, glucosamine and uronic acid residues linked in a 1-4 manner

structure modification steps. One, some GlcA*p* residues are epimerized to iduronic acid (IdoA*p*) and two, incomplete sulfation occurs at the 3-O-, 6-O-, and 2-N positions of GlcN*p* in addition to sulfation at 2-O-position of few IdoA*p* residues.[178] This primary structural diversity is further complicated by another level of complexity wherein sulfate groups may cluster in small regions and form differentially charged domains. The number of structural sequences possible with these variations, especially taking into account the size recognized by proteins and receptors run into millions. The final structure of HS depends upon the incompleteness of the reactions that occur during the biosynthetic process. The modification process is more complete in heparin where the final disaccharide IdoA*p*(2-*OSO*$_3$)-Glc*NpSO*$_3$(6-*OSO*$_3$) represents up to 70% of the chain, leading to a heavily *O*-sulfated polysaccharide with a high IdoA*p*/GlcA*p* ratio. In contrast, the modifications that occur during the biosynthesis of HS are less extensive;

leading to HS molecules characterized by lower IdoA*p* content and a lower overall degree of *O*-sulfation and resulting in high heterogeneity of distribution of the sulfate groups along the chain.[179-182] This diversity arguably plays a key role in numerous biological processes like maintaining cell surface architecture; modulating critical biological events and also interacting with a variety of ligands. Typical concentrations of HS proteoglycans on the cell surface are in the range of 10^5-10^6 molecules/cells as measured in various cell culture systems. The interactions are largely electrostatic in nature and depend on the distribution of hexuronic acid residues and sulfate groups along the polysaccharide chain. The prolific expression of HS and their strong interactive ability are two features that have made them attractive adhesion molecules providing initial docking sites for all sorts of viruses and other microorganisms during their evolution. In addition, the negative charge arising from sulfates/carboxylates on HS makes it well suited to interact with positively charged basic amino acid domains on viral proteins.

4.1.7 HS Mimics

HS plays a vital role in the entry of the HSV-1 into cells. Thus, structural or functional mimics of HS are likely to competitively inhibit the entry of the virus into cells. In this context, numerous sulfated molecules have been explored as mimics of HS in the inhibition of HSV-1 entry into cells **(figure 41)**.[183] These include heparin and its chemically modified derivatives, non-anticoagulant heparin, pentosan polysulfate, dextran sulfate, sulfated maltoheptaose, fucan sulfate, fucoidans, spirulan, sulfated galactans, and miscellaneous sulfated polysaccharides.[184-186] These compounds compete

with cell surface HS for binding to the virus particles and therefore are most active when present during the attachment phase of the viral entry. Not unexpectedly, each HS mimic found to-date as an inhibitor of viral entry has a linear polysaccharide backbone with varying degrees of sulfation.

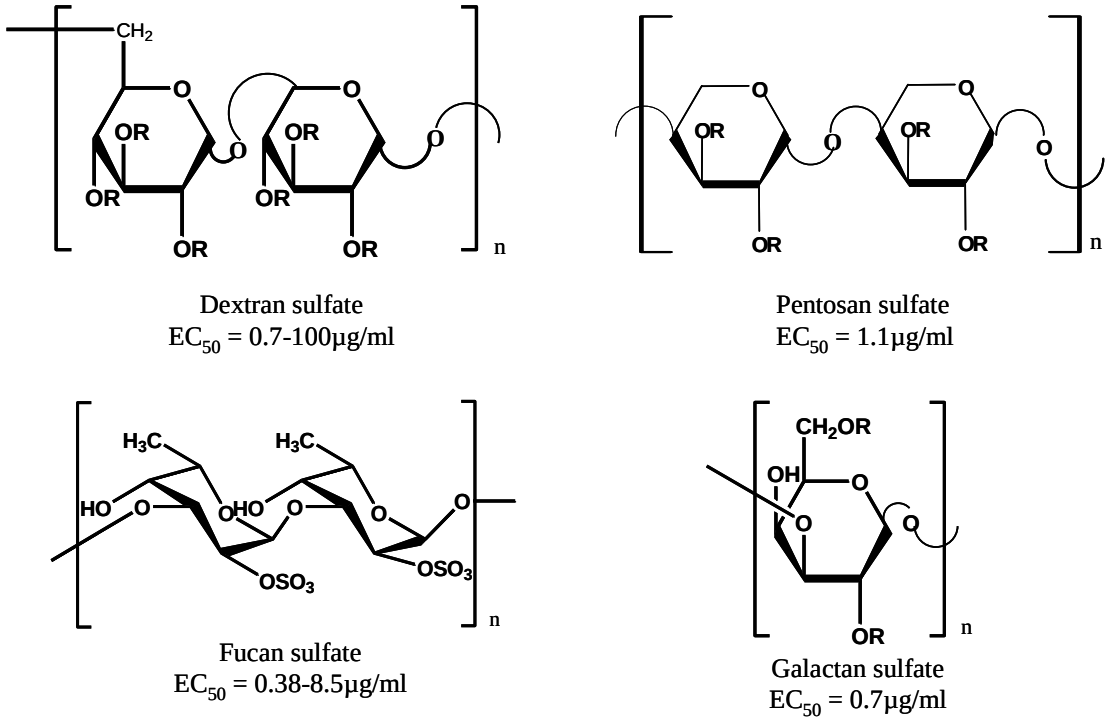

Figure 41. Some of the sulfated polysaccharides that have been tried as heparan sulfate mimics for HSV-1 inhibition activity.

A study of molecular weight dependence of infection inhibition activity shows that the antiviral potency increases with increasing sulfation levels and length of chain. Yet, detailed aspects of interactions at molecular level, their nature and contributions, the order of interactions, and the step-wise molecular mechanism remains unclear.

4.2 Rationale

From the literature study, it is clear that HS on the cell surface plays an imperative role in assisting the entry of the HSV-1 into cells. Therefore, designing a drug that would inhibit the entry of the virus at the very first stage and thus preventing any further proliferation seems crucial. A simple rational drug approach that comes to mind is designing HS mimics that would competitively inhibit the entry of the virus into cells. Literature survey shows that HS mimics have been developed to competitively inhibit viral entry. However, most HS mimics reported so far have been polysaccharide-based sulfated molecules. In an effort to discover non-polysaccharide-based macromolecular mimics of HS, we previously designed sulfated lignins, which are sulfated derivatives of the natural biopolymer lignin.[123-124,187-188] Lignin is a complex, heterogeneous polymer made up of repeating phenylpropanoid units containing multiple hydroxyl groups **(figure 42)**.[189-190] Our sulfated lignins were found to be excellent antagonists of HSV and HIV infections of cells.[187-188] Although the biochemical chemical basis for the anti-HSV and anti-HIV activity of sulfated lignins is not known, a plausible hypothesis relies on the similarity of sulfated lignin's electrostatic surface with that of HS.[123] In contrast to sulfated polysaccharide, the sulfated lignin scaffold that we proposed is an attractive alternative because its phenylpropanoid units afford numerous opportunities for structural variations to fine-tune biological activity. In addition, lignin can be rather easily synthesized in high yields in the laboratory using enzymatic oxidative coupling. We reasoned that it should be possible to devise a lignin scaffold that is completely devoid of sulfate moieties and yet possess an electrostatic surface equivalent to that of HS so as to retain potent antagonism of viral entry into cells. The average negative charge density of HS is nearly

1.0-1.4.[189-193] Thus, a lignin monomer containing one negative charge, which is not a sulfate, for example, caffeic or ferulic acid is likely to afford a nonsulfated lignin polymer with HS mimicking properties **(figure 43)**.

We found that the two carboxylated lignins are not only potent inhibitors of HSV-1 entry into mammalian cells, but are much more effective than sulfated lignins. In addition, the

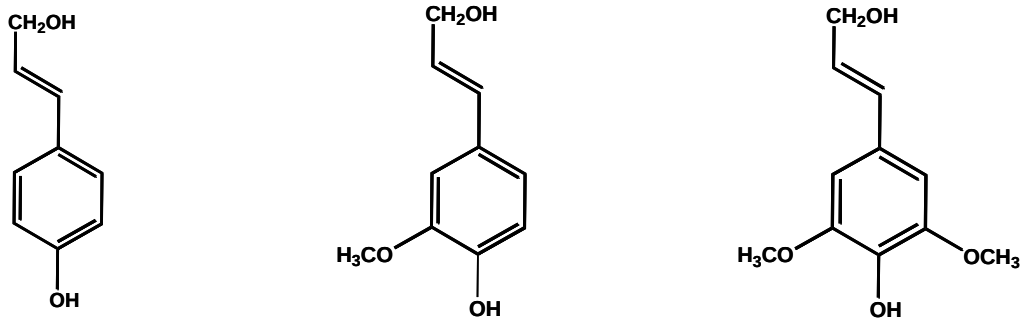

Figure 42. Monomers which serve as the precursor for lignin biosynthesis

results show that the shorter carboxylated lignins are very potent in preventing HSV-1 infection suggesting the possibility that structural features, in addition to carboxylate groups, may be important. The results present major opportunities for developing orally available small molecular weight lignin-based antiviral strategies.

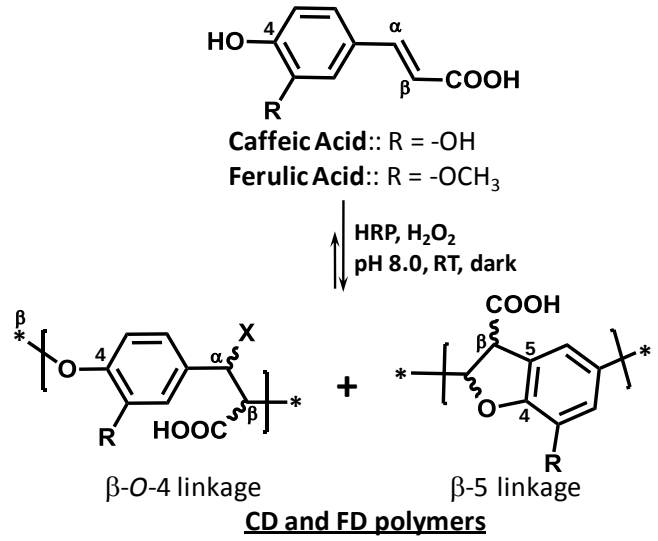

Figure 43. Structure of carboxylated lignins CD and FD obtained from horseradish peroxidase-catalyzed oxidative coupling of caffeic and ferulic acid, respectively.
Carbon designations (α, β, 4, 5, and others), unique to the lignin field, are as shown. X can be either -H or -OH. Oxidative coupling through radical intermediates give rises to oligomers with different types of intermonomeric linkages. The most common linkages formed include β-*O*-4 and *β*-5. Other less common linkages include *β*-*β*, 5-5, and 5-*O*-4, for which oligomerization tends to arrest chain growth.(ref) The length of the chain greatly depends on the conditions of oligomerization.

4.3 Experimental Methods

4.3.1 Chemicals, Cells, and Viruses

Horseradish peroxidase (HRP) with activity of 250-330 units/mg was from Sigma (St. Louis, MO). *β*-Galactosidase substrate *o*-nitrophenyl *β*-D-galactopyranoside (ONPG) was performed from Pierce (Rockford, IL). High purity water, obtained from NERL Diagnostics (RI, U.S.A.), was used in all experiments. Dr. Patricia Spear (Northwestern University, Chicago) provided HeLa cells and the HSV reporter viruses listed here. HSV-1 virus strain carrying the *lacZ* gene of *E. coli* and capable of expressing *β*-galactosidase as a reporter of entry included HSV-1(KOS) gL86.[193-194] Polystyrene sulfonate standards

(PSS) (4-33 kDa) were from Sigma (St. Louis, MO). Other chemicals and solvents used in the work were purchased from either Sigma-Aldrich (St. Louis, MO) or Fisher (Agawam, MA).

4.3.2 Synthesis of Carboxylated Lignin Polymers

The lignin polymers from caffeic acid and ferulic acid monomers, CD and FD, respectively, were prepared in a manner following earlier work.[123-124] Briefly, caffeic acid or ferulic acid (25 mM, 200 mL) and H2O2 (75 mM, 100 mL) were added dropwise to a 50 mL solution of 10 mg HRP in 10 mM sodium phosphate buffer, pH 8.0, over a period of 5 h at room temperature in dark. Three additional aliquots H2O2 (75 mM, 100 mL) were added over the next 72 h. At the end of polymerization the solution was freeze-dried to obtain approximately 2 g of CD and FD polymers.

4.3.3 Fractionation of CD and FD Using Centrifugal Filtration.

The polymerization reaction mixture (~2 g) was dissolved in deionized water (8 mL) and filtered through Millipore filter (NMWC 30 kDa) at 4000 g. Filtration was continued until the retentate volume was approximately 200 μL. This process was repeated three more times and the final retentate was labeled as **F30** fraction. The filtrates from the above process were pooled, lyophilized, redissolved in deionized water and then further fractionated in the manner described above using a 10 kDa filter. The retentate so obtained was labeled as **F10** fraction. This process was repeated to obtain **F5** and **F3** fractions using 5 and 3 kDa membranes. The retentates were collected and lyophilized to obtain four fractions in yields of 15-20, 5-8, 3-5, and 1-2%, respectively.

4.3.4 Determination of Molecular Weight of Carboxylated Lignin Fractions

The number and weight average molecular weight of CD and FD fractions was measured using gel permeation chromatography (GPC) on a Shimadzu chromatography system composed of LC10Ai pumps and a SPD-10A VP UV-vis detector controlled by a SCL-10A VP system controller connected to a computer. Each fraction was analyzed using Phenogel 5 μ (Phenomenex, Torrance, CA, 7.6 mm i.d. x 300 mm). The mobile phase consisted of 100% tetrahydrofuran at a constant flow rate of 0.7 mL/min. Polystyrene standards, caffeic acid, and ferulic acid were used for calibration purposes. The relationship between logarithm of the molecular weight and the elution volume (V) of the standards was found to be linear with a correlation coefficient of 0.99. The wavelength of detection for CD and FD fractions was set at 280 nm. Each chromatogram was sliced into 1000 time periods providing 1000 *M*R with the corresponding absorbance (*A*) values. These values were used to calculate number average molecular weight (*M*N), weight average molecular weight (*M*W) and polydispersity (*P*) parameters from equations 1, 2, and 3, respectively, for each CD and FD fraction.

$$M_N = \frac{\sum A_i \times M_i}{\sum A_i} \quad \ldots\ldots (1) \qquad M_W = \frac{\sum A_i \times M_i^2}{\sum A_i \times M_i} \quad \ldots\ldots (2)$$

$$P = \frac{M_W}{M_N} \quad \ldots\ldots (3)$$

4.3.5 Assay for HSV-1 Entry into Cells

Assays for infection of cells were based on the quantification of β-galactosidase expressed by the mutant HSV viral genome containing the lac*Z* gene, as described earlier.[195-196] HeLa cells were grown in 96-well tissue culture dishes (2-4 x 10^4 cells/well), washed after 16 h of growth, and exposed to 10 plaque forming units (PFU) per cell of the HSV virus in 50 μL of phosphate-buffered saline (PBS) containing glucose and 1% calf serum for 6 h at 37 °C. To test for inhibitory activity, the sulfated compounds were simultaneously added to this 50 μL medium in varying amounts ranging from 0 to 2 μg. Following incubation, the cells were solubilized in 100 μL of PBS containing 0.5% NP-40 and 10 mM ONPG. The initial rate of hydrolysis of the substrate was monitored spectrophotometrically at 410 nm, which corresponds to the expressed level of β-galactosidase within HeLa cell. The initial rate of hydrolysis of the substrate in the absence of any added antagonist was used as the control and assigned a value of 100% HSV infection. Assays were performed in duplicate. Logistic equation 4 was used to fit the dose-dependence of HSV infection to obtain the IC_{50}.

$$Y = Y_O + \frac{Y_M - Y_O}{1 + 10^{(\log[L]_O - \log IC_{50}) \times HC}} \quad \ldots\ldots (4)$$

In this equation, Y is the observed β-galactosidase activity (in %) in the presence of carboxylated lignin (L) to that in its absence, Y_M and Y_0 are the maximum and minimum

possible values of the β-galactosidase activity, IC_{50} is the concentration of L that results in 50% antagonism of HSV-1, and HC is the Hill Cooperativity Index.

4.4 Results and Discussion

4.4.1 Caffeic and Ferulic Acids Polymerize with Ease To Generate Long Chains

Enzymatic polymerization of phenylpropenoid monomers to produce synthetic lignins has been explored for a long time.[197-201] Yet, previous reports on the oxidative coupling of 4-hydroxycinnamic acids resulted only in oligomers with an average chain length of less than three monomers.[202-203] HRP-catalyzed polymerization of caffeic and ferulic acid monomers at pH 8.0 with gradual addition of H_2O_2 over a period of more than 3 days resulted in CD and FD polymers, respectively, in nearly quantitative yields **(See figure 43)**. The M_N and M_W values of these polymeric mixtures, measured using GPC, were found to be 4264 and 13272 Da for CD and 5322 and 11525 Da for FD **(Table 15)**. These values indicate that CD is more polydisperse and probably more heterogeneous than FD. The average chain length of the two polymers was found to be 12 (CD) and 29 (FD). This is the first report of such long polymers obtained through enzymatic polymerization of 4-hydroxycinnamic acids. A probable reason for the higher level of polymerization is the higher concentration of enzyme used in the reaction as well as the prolonged addition of the oxidant.

Table 15. Physical Properties of Size Fractionated Carboxylated Lignins

	M_N[a] (Da)	M_W[a] (Da)	M_P[a] (Da)	P[b]	L_R[c]
FD_3	1300	5300	700	4.17	3.6 (2−27)[c]
FD_5	2800	9700	1300	3.52	6.5 (2−50)
FD_{10}	5000	13200	2700	2.64	13.7 (2−68)
FD_{30}	7600	16500	7700	2.18	39.9 (2−85)
FD_{MIX}	5300	11500	5600	2.16	29.1 (2−59)
CD_3	1100	2100	860	1.98	4.7 (2−12)
CD_5	1600	6900	1100	4.25	5.8 (2−38)
CD_{10}	2500	8600	1400	3.45	5.8 (2−48)
CD_{30}	3900	12800	1900	3.24	10.8 (2−71)
CD_{MIX}	4300	13200	2200	3.11	12.1 (2−74)

[a]Number, weight, and peak average molecular weights were obtained by GPC analysis. [b]Polydispersity. [c]The peak average chain length was calculated from the ratio of *M*P and molecular weight of the two monomers. Numbers in brackets refer to the range of chain lengths (see Experimental Methods).

4.4.2 CD and FD Are Less Globular than Natural Lignins

To assess the size dependence of putative antiviral activity of CD and FD, the two polymeric mixtures were separated into four fractions of varying sizes using 3K, 5K, 10K, and 30K membrane-based centrifugal filtration. The GPC profiles of fractions were found to be broad and reasonably symmetrical **(figure 44)**. This implied that each fraction contained nearly all types of chains. For example, although the average chain length of FD3 and CD3 is 3.6 and 4.7, both fractions contain chains as long as 27 and 12 units, respectively **(Table 15)**. Thus, the difference between the membrane-separated fractions arises primarily due to chains being present in different proportions. A probable explanation for why high molecular weight chains are present in CD3 and FD3 fractions is that carboxylated lignins are more linear polymers than natural lignins. The random oxidative coupling mechanism of enzymatic polymerization affords chain elongation along nonlinear centers resulting in multidimensional polymerization[189-190] which can generate globular structures. Globular structures typically cannot pass through molecular membranes or sieves. In contrast, linear structures can pass through sieves through

reptile-like motion. Thus, carboxylated lignins appear to be less globular than natural lignins. This is important because greater the linearity of the lignin polymer greater is its probability of mimicking HS, which has a 100% linear structure.

The M_N, M_W, and polydispersity (P) values calculated from the GPC profiles confirm the above conclusions. The M_N values ranged from 1052 to 7558, while M_W was found to be in the range of 2084 and 16464 **(Table 15)**. The molecular weight at the peak maximum (M_P) was found to more closely resemble M_N than M_W suggesting a larger proportion of smaller chains. The average chain length varied from 3.6 to 39.9 for FD fractions, while it was between 4.7 and 12.1 oligomeric units for CD fractions **(Table 15)**. This implies that the chain length range was found to be much greater for FD (~11-fold) than for CD (2.5-fold).

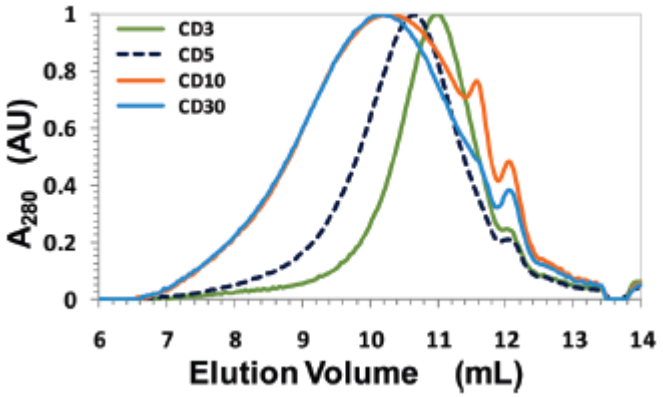

Figure 44. Normalized GPC profiles of fractions CD3 through CD30 obtained from membrane-based centrifugal filtration of CD mixture.
A_{280} refers to the absorbance at 280 nm. The profiles for FD fractions were similar (not shown). See Experimental Methods for details.

4.4.3 CD and FD are Potent Antagonists of HSV-1 Entry into Cells.

The ability of CD and FD to prevent the entry of HSV-1 particles into mammalian cells was studied using a standard cellular assay.[204-205] In this assay, HeLa cells were exposed to a reporter HSV-1 containing the lac*Z* gene in the presence and absence of CD, FD, and their size fractionated preparations. The large size and significant anionic character of the lignins prevents them from entering the mammalian cell, while the viral particle is internalized through the concerted action of multiple cellular receptors, including HS.[202,203] Assuming CD and FD mimic cell-membrane-bound HS, the lignins would competitively reduce the levels of the virus internalized by HeLa cells. Thus, the *β*-galactosidase activity of the internalized HSV-1 serves as a measure of the activity of lignins in preventing viral entry.

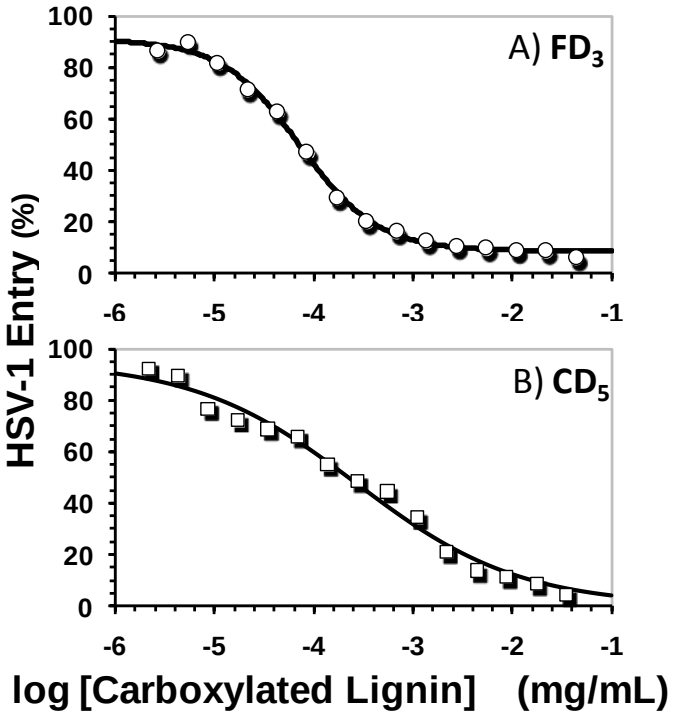

Figure 45. Profile of HSV-1 entry into cells in the presence of FD3 (A) and CD5 (B) using a *β*-galactosidase activity-based viral entry assay.
Profiles of other fractions were similar and not shown. IC_{50} values calculated from these profiles are listed in **Table 16**. See Experimental Methods for details.

Figure 45 shows the viral entry profile for two representative lignin fractions, FD3 and CD5. The profiles for other fractions were similar (not shown). A concentration-dependent antagonism of entry of HSV-1 into HeLa was noted for all preparations, which was fitted using the standard dose-response equation to calculate the concentration of carboxylated lignin required for 50% antagonism **(*IC*$_{50}$; Table 16)**. For size-fractioned carboxylated lignins FD and CD, the *IC*$_{50}$ values were found to be in the range of 72 and 284 ng/mL, which correspond to nanomolar potencies (13-56 nM). This indicates that our new carboxylated lignin scaffold is highly effective in preventing the entry of HSV-1.

Table 16. Inhibition of HSV-1 Entry into Mammalian Cells by Size-Fractionated Carboxylated Lignins CD and FD[a]

fractions	IC_{50} (ng/mL)	IC_{50}[b] (nM)	HC
FD_3	72 ± 1[c]	13.6 ± 0.2	1.1 ± 0.1
FD_5	127 ± 4	13.1 ± 0.4	1.0 ± 0.1
FD_{10}	111 ± 2	8.4 ± 0.2	1.0 ± 0.1
FD_{30}	284 ± 12	17.3 ± 0.4	1.2 ± 0.1
CD_3	153 ± 7	28.9 ± 1.4	0.5 ± 0.1
CD_5	269 ± 21	50.8 ± 4.0	0.5 ± 0.1
CD_{10}	295 ± 14	55.7 ± 2.7	0.6 ± 0.1
CD_{30}	220 ± 8	17.2 ± 0.6	0.8 ± 0.2

[a]The *IC*$_{50}$ values are concentrations of carboxylated lignins that result in 50% reduction in level of HSV-1 entry. *IC*$_{50}$ and HC values were obtained through nonlinear regression analysis of viral entry data in the presence and absence of carboxylated lignins (see Experimental Methods). [b]Calculated using *M*W values from **Table 15**. [c]Errors represent ±2 S.E.

A closer look reveals that FD fractions are typically more potent than corresponding CD fractions **(Table 16)**. For example, FD3 is approximately 2-fold more potent than CD3. Another difference between the two polymers appears in the Hill Cooperativity indices. Whereas FD fractions display a HC of ~1, CD fractions show a value of ~0.5. In a traditional multisite interaction of a macromolecule with its receptor, HC corresponds to

cooperativity of interaction. A value of 1.0 implies no cooperativity, while values less than 1.0 imply negative cooperativity. It is difficult to ascribe the phenomenon of cooperativity in the antagonism of HSV-1 by CD and FD because both are heterogeneous and polydisperse. Rather, HC values may reflect the degree of structural complexity of the mixture, which can generate many different types of ligand – receptor complexes. This possibility is greater for CD due to the presence of an additional -OH group that is known to be more reactive than the corresponding -OMe in FD.

The potency of inhibition is minimally affected for FD fractions despite the change in their molecular weights. For example, FD3 exhibits an IC_{50} of 13 nM, which is not different from the value of 17 nM for FD30, although the average chain length increases nearly 11-fold. The results for CD fractions are similar. Although the IC_{50} increases from 29 nM for the CD3 to 56 nM for CD10 and then decreases to 17 nM for CD30 **(Table 16)**, the apparently nonlinear change is most likely due to its greater heterogeneity.

The viral inhibition profile of nonsulfated carboxylated lignins is dramatically different from that of the sulfated lignins. For sulfated lignins, as the average chain length increased so did their ability to antagonize viral entry.[123,206] The reason for this size dependence is the well-known statistical advantage offered by multiple binding sites likely to be present in longer polymers. Yet, size-dependence is nearly completely eliminated for carboxylated lignins. This implies that even the smallest FD and CD chains are able to effectively prevent HSV-1 entry into cells, an observation that carries major pharmaceutical value.

4.5 Conclusions

Although a large number of polymers have been designed to inhibit viral entry into mammalian cells, nearly each is a sulfated polysaccharide. Our success with sulfated lignins led to the current work on carboxylated lignins, which do not contain any sulfate group. The two enzymatically synthesized carboxylated lignins are polymers of phenylpropanoid residues connected primarily through *β*-*O*-4 and *β*-5 linkages **(figure 43)**. [123-124,188-189] Other linkages including *β*-*β* and 5-5 are also likely. These varying inter-residue linkages and chain lengths introduce considerable structural heterogeneity in the polymeric mixture. Structural heterogeneity is a major impediment in the drug discovery process. Yet, it affords a high probability of discovering an initial lead, which may be fine-tuned to result in a new pharmaceutical agent. The potent antagonism of HSV-1 entry into mammalian cells by all FD and CD fractions highlights the importance of investigating scaffolds outside of the traditional saccharide scaffolds to discover novel pharmaceuticals.

The IC_{50} value of HSV-1 inhibition by FD and CD fractions range from 8 to 56 nM **(Table 16)**. In comparison, our previous study with sulfated lignins demonstrated values in the range of 1.7 to 1450 nM. This indicates that most carboxylated lignins are better antagonists of HSV-1 infection of cells. More specifically, FD3 (M_P = 698 Da) and CD3 (M_P = 854 Da) displayed IC_{50} of 13 and 29 nM, respectively, which are 50-106-fold lower than that found for the smallest sulfated lignin (M_P = 1900 Da) earlier. This implies that either carboxylated lignins are better at mimicking HS in comparison to sulfated

lignins or that these new molecules possess a completely different mechanism of antagonism of HSV-1.

A key discovery of this work is the high potency of FD (and CD) irrespective of chain length. For example, FD3 is almost as antiviral as FD30 **(Table 16)**. A plausible explanation for this observation is that FD possesses discrete structure(s) that induce anti-HSV-1 activity. The average chain length of FD3 is 3.6. This implies that small, carboxylate group containing, FD-based molecules, for example, trimers with molecular weight of 582 (194 x 3) are likely to exhibit significant anti-HSV-1 activity. In addition to the small size, the presence of carboxylic acid groups in these polymers affords an excellent route to design orally bioavailable anti-HSV-1 agents. Orally bioavailable designs would contain ester protecting groups, which will undergo nonspecific hydrolysis in vivo to release the small, carboxylated lignin-based inhibitor.

The carboxylated lignins studied here have additional advantages over sulfated lignins as well as other polysaccharide-based agents. These polymers can be easily synthesized in high yields in a fairly consistent manner. Chemical sulfation, on the other hand, is a difficult reaction and is typically considerably variable.[207-208] A large number of structural variants of ferulic and caffeic acid monomers are available, which implies that new agents can be studied for fine-tuning anti-HSV activity.

Overall, this study puts forward a carboxylated lignin polymer as a potent antagonist of HSV-1 entry into mammalian cells. It can be expected that carboxylated lignins also

antagonize the entry of other enveloped viruses, for example, HIV-1, dengue, Kaposi's sarcoma-associated herpes virus, and hepatitis C virus. In fact, a review of literature suggests that effort to develop carboxylated lignins as anti-HIV agents has been made in the past.[209-211] Interestingly, the carboxylated lignins discussed here are about 1000-fold more potent at inhibiting HSV-1 than those studied earlier as anti-HIV agents. The reason for this massive selectivity in targeting HSV is not clear at the present time, but in combination, the results present the possibility of preparing topical formulations of these polymers for preventing infections arising from multiple pathogens.

References:

1. Paoli, G.; Merlini, P. A.; Ardissino, D. Curr. Pharm. Design **2005**, *11*, 3919-29.
2. Yang, E.H.; Brilakis, E.S.; Reeder, G.S.; Gersh, B.J. Curr. Probl. Cardiol. **2006**, *31*, 769-817.
3. American Heart Association. Heart disease and stroke statistics–2003 update. Dallas, TX: American Heart Association, **2002**
4. Sans, S.; Kesteloot, H., Kromhout, D. Eur. Heart J. **1997**, *18*, 1231–1248.
5. Fenton, J. W. 2nd; Ofosu, F. A.; Brezniak, D. V.; Hassouna, H. I. Hematol. Oncol. Clin. North Am. **1993**, *7*, 1107-19.
6. Jakubowski, H. V.; Owen, W. G. J. Biol. Chem. **1989**, *264*, 11117–21.
7. Hart, R. G.; Halperin, J. L. Ann. Intern. Med. **1999**, *131*, 688-695.
8. McRae, S. J.; Ginsberg, J. S. Health Risk Management **2005**, *1*, 41–53.
9. Sahoo, S.; Dash, K.; Sahu, A.; Sahu D.; Sahoo, S. Der Pharmacia Lettre **2010**, *2*, 437-451.
10. Schmaier, A. H.; Petruzzelli, L. M. Hematology for medical students. Philadelphia: Lippincott Williams & Wilkins **2003**, 71-125.
11. Walsh, P. N.; Ahmad, S. S. Essays Biochem. **2002**, *38* 95-111.
12. http://ahdc.vet.cornell.edu/clinpath/modules/coags/introf.htm
13. Nylander, S.; Mattsson, C. Blood Coagul. Fibrinol. **2003**, *14*, 159-67.
14. Mannucci, P. M.; Tuddenham, E. G. N. Engl. J. Med. **2001**, *344*, 1773-1779.
15. Broze, G. J. Jr.; Higuchi, D. A. Blood **1996**, *88*, 3815-3823.
16. Mosnier, L. O.; Lisman, T.; Van den Berg, H. M.; Nieuwenhuis, H. K.; Meijers,J. C. M.; Bouma, B. N. Thromb. Haemost. **2001**, *86*, 1035-1039.
17. Kalafatis, M.; Egan, J. O.; Cawthern, K. M.; Mann, K. G. Crit. Rev. Eukaryot. Gene Expr. **1997**, *7*, 241-280.
18. Brouns, R.; Heylen, E.; Willemse, J. L.; Sheorajpanday, R.; De Surgeloose, D.; Verkerk, R.; De Deyn, P. P.; Hendriks, D. F. J Thromb. Haemost. **2010**, *8*, 75-80.
19. Furie, B.; Furie, B. C. New Eng. J. Med. **2008**, *359*, 938–949.
20. Schreijer, J. M.; Cannegieter, S. C.; Doggen, C.; Rosendaal, F. Br. J. Haematol. **2008**, *144*, 425–429.
21. Mosnier, L. O.; Elisen, M. G.; Bouma, B. N.; Meijers, J. C. Thromb. Haemost. **2002**, *86*, 1057–64.
22. Boffa, M. B.; Reid, T. S.; Joo, E.; Nesheim, M. E.; Koschinsky, M. L. Biochem. **1999**, *38*, 6547–58.
23. Nemerson, Y. Blood, **1988**, *71*, 1-8.
24. Jesty, J.; Silverberg, S. A. J. Biol. Chem. **1979**, *254*, 12337-12345
25. Rand, M. D.; Lock, J. B.; van't Veer, C.; Gaffney, D. P.; Mann, K. G. Blood **1996**, *88*, 3432-3445.
26. Bouma, B. N.; Griffin, J. H. Blood Coagul. **1996**.
27. Kravtsov, D. V.; Matafonov, A.; Tucker, E. I.; Sun, M. F.; Walsh, P. N.; Gruber, A.; Gailani, D. Blood **2009**, *114*, 452-458.
28. Esmon, N. L.; DeBault, L. E.; Esmon, C. T. J. Biol. Chem. **1983**, *258*, 5548-5553.

29. Kalafatis, M., Rand, M. D., and Mann, K. G. J. Biol. Chem. **1994**, *269*, 31869-31880
30. Walker, J. B.; Nesheim, M. E. J. Biol. Chem. **2001**, *276*, 3138-3148.
31. Arthur J. C.; Curr. Vasc. Pharmacol. **2004**, *2*, 199-228.
32. Fareed, J.; Hoppensteadt, D. A.; Fareed, D.; Demir, M.; Wahi, R.; Clarke, M.; Adiguzel, M.; Bick, R. Seminars in thrombosis and hemostasis **2008**, *34*.
33. Fulcher, C. A.; Gardiner, J. E.; Griffin, J. H.; Zimmerman, T. S. Blood **1984**, *63*, 486-489.
34. Suzuki, K.; Stenflo, J.; Dahlback, B.; Teodorsson, B. J. Biol. Chem. **1983**, *258*, 1914-1920.
35. Spronk, H. M.; Govers-Riemslag, J. W.; ten Cate, H. Bioessays **2003**, *25*, 1220-8.
36. Boffa, M. B.; Maret, D.; Hamill, J. D.; Bastajian, N.; Crainich, P.; Jenny, N. S.; Tang, Z.; Macy, E. M.; Tracy, R. P.; Franco, R. F.; Nesheim, M. E.; Koschinsky, M. L. Blood **2008**, *111*, 183-189.
37. Ishii, H.; Kojima, Y.; Masuda, Y.; Takada, K.; Sugimoto, K.; Ikeda, T. Thromb. Haemost. **2009**, *102*, 1204-1211.
38. Bajzar, L.; Morser, J.; Nesheim, M. J. Biol. Chem. **1996**, *271*, 16603–16608.
39. Jandl, J. H. Blood: textbook of hematology. Boston/Toronto: Little, Brown & Co. **1987**.
40. Jenny, N. S.; Mann, K. G. Thrombin. In: Colman, R. W.; Hersh, J.; Marder, V.J.; Clowes, A. W.; George, J. N. Hemostasis and thrombosis: basic principles and clinical practice. 4th edition. Philadelphia Lippencott Williams & Wilkins; **2001**. 172–89.
41. Greenberg, C. S.; Orthner, C. L. Blood coagulation and fibrinolysis. In: Lee, G. R.; Foerster, J.; Lukens, J.; Paraskevas, F.; Greer, J.; Rogers, G. editors. Wintrobe's clinical hematology. 10th edition. Philadelphia Lippencott Williams & Wilkins; **1999**. p. 684– 764.
42. Cristofaro, R.; Candia, E. J. Thromb. Thrombolysis. **2003**, *15*, 151-63.
43. Cera, E.; Dang, Q. D.; Ayala, Y. M.; **1997**, *53*, 701-30.
44. Huntington, J. A.; Baglin, T. P. Trends Pharmacol. Sci. **2003**, *24*, 589-95.
45. Levi, M.; Keller, T. T.; van Gorp, E.; ten Cate, H. Cardiovasc. Res. **2003**, *60*, 26-39.
46. Fuentes-Prior, P.; Iwanaga, Y.; Huber, R.; Pagila, R.; Rumennik, G.; Seto, M.; Morser, J.; Light, D.R.; Bode, W.; Nature **2000**, *404*, 518-25.
47. Cosmi, B.; Cini, M.; Legnani, C.; Pancani, C.; Calanni, F.; Coccheri, S. Thromb. Res. **2003**, *109*, 333-339.
48. Frenkel, E.; Shen, Y.; Haley, B. Hematol. Oncol. Clin. N Am. **2005**, *19*, 119–145.
49. Tracy, R. P. Chest **2003**, *124*, 49S-57S.
50. Chung, A. W.; Jurasz, P.; Hollenberg, M. D.; Radomski, M. W. Br. J. Pharmacol. **2002**, *135*, 1123-32.
51. Sambrano, G. R.; Weiss, E. J.; Zheng, Y. W.; Huang, W.; Coughlin, S. R. Nature **2001**, *413*, 74-8.

52. Callahan, K. P.; Malinin, A. I.; Gurbel, P. A.; Alexander, J. H.; Granger, C. B.; Serebruany, V. L. Cardiol. **2001**, *95*, 55-60.
53. Covic, L.; Gresser, A. L.; Kuliopulos, A. Biochem. **2000**, *39*, 5458-67.
54. Borensztajn, S. K.; von der Thusen, J.; Spek, C. Curr. Pharma. Design **2011**, *17*, 9-16.
55. Marin, V.; Farnarier, C.; Kaplanski, S.; Su, M.; Dinarello, C.; Kaplanski, G. Blood. **2001**, *98*, 667-673.
56. Bae, J.; Kim, I.; Rezaie A. R. J. Cell. Phys. **2010**, *225*, 233–239.
57. Yepes, M.; Lawrence, D. Exp. Biol. Med. **2004**, *229*, 1097-1104.
58. Crawley, J.T.; Zanardelli, S.; Chion, C. K.; Lane, D. A. J. Thromb. Haemost. **2007**, *5*, 95-101.
59. Snyder, K. M.; Kessler, C. M. Semin. Thromb. Hemost. **2008**, *34*, 734-41.
60. Fareed, J.; Hoppensteadt, D. A.; Bick, R. L. Clin. Appl. Thromb. Hemost. **2003**, *9*, 101-8.
61. Bjork, I.; Lindahl, U. Mol. Cell Biochem. **1982**, *48*, 161-82.
62. Hirsh, J. Thromb. Res. **2003**, *109*, 1-8.
63. Blossom, D. B.; et al. N. Engl. J. Med. **2008**, *359*, 2674-84.
64. Golan, D. Principles of pharmacology: the pathophysiologic basis of drug therapy. 402-403.
65. Stromicha, J.; Webera, A.; Mirzaeia, Y.; Caldwellb, M.; Lewisa, D. Bioorg. Med. Chem. Lett. **2010**, *20*, 1928-1932.
66. Hirsh, J.; Bauer, K.; Donati, M.; Samama, M.; Weitz, J. Parenteral Anticoagulants* American College of Chest Physicians Evidence-Based Clinical Practice Guidelines (8th Edition). Chest **2008**, *133*, 141S-159S.
67. Umesh R. Desai. Med. Res. reviews, **2004**, *24*, 151-181.
68. Pan, J.; Qian, Y.; Zhou, X.; Zhang, L. Glycobiol. Insights **2010**, *2*, 1-12.
69. Chuang, Y. J.; Swanson, R.; Raja, S. M.; Olson, S. T. J. Biol. Chem. **2001**, *4*, 14961-71.
70. Markwardt, F. Semin. Thromb. Hemost. **2002**, *28*, 405-14.
71. Bates, S.M. and Weitz, J.I. Am. J. Cardiol, **1998**, *82*, 12P-18P.
72. Gustafsson, D. and Elg, M. Thromb. Res. **2003**, *10*, S9-15.
73. Choudhury, A., Goyal, D., and Lip, G.Y. Drugs Today **2006**, *42*, 3-19.
74. Murtagh, B.; Smalling, R. W. **2006**, *8*, 310-6.
75. http://www.encyclo.co.uk/define/ACS
76. http://www.in.gov/isdh/files/HeartDiseaseArticleRx.pdf
77. http://www.nlm.nih.gov/medlineplus/ency/article/000726.htm
78. Kissela, B.; Broderick, J.; Woo, D.; Kothari, R.; Miller, R.; Khoury, J.; Brott, T.; Pancioli, A.; Jauch, E.; Gebel, J.; Shukla, R.; Alwell, K.; Tomsick, T. Stroke **2001**, *32*, 1285-90.
79. Leary, M. C.; Saver, J. L.; Cerebrovasc. Dis. **2003**, *16*, 280-5.
80. Kelley, R. E.; Minagar, A. South Med. J. **2003**, *96*, 343-9.
81. Tullio, M. R.; Homma, S. Curr. Cardiol. Rep. **2002**, *4*, 141-8.
82. Ansell, J. J. Thromb. Haemostasis **2007**, *5*, 60–64.

83. Turpie, A. Curr. Opin. Drug Discovery Dev. **2009**, *12*, 497-508.
84. Phillips, K.; Ansell, J. Thromb. Haemost. **2010**, 103, 34–39.
85. Weitz, J. Thromb. Res. **2011**, *127*, 5–12.
86. Gosselin, R.; Dager, W.; King, J.; Janatpour, K.; Larkin, E.; Owings, J. Am. J. Clin. Pathol. **2004**, *121*, 593-599.
87. Rupprecht, H. J.; Blank, R. Drugs **2010**, *70*, 2153-2170.
88. Boneu, B.; Necciari, J.; Cariou, R.; et al. Thromb. Haemost. **1995**, *74*, 1468-73.
89. Paolucci, F.; Clavies, M.; Donat, F.; et al. Clin. Pharmacokinet. **2002**, *41*, 11-8.
90. Follet, V.; Vivier, N.; Trellu, M.; Sanderink. C. J. Thromb. Haemostasis **2009**, *7* 559–565.
91. Perzborn, E.; Strassburger, J.; Wilmen, A.; et al. J. Thromb. Haemostasis **2005**, *3*, 514-21.
92. Chu, V.; Brown, K.; Colussi, D.; et al. Thromb. Res. **2001**, *103*, 309-24.
93. Pinto, D. J.; Orwat, M. J.; Koch, S.; et al. J. Med. Chem. **2007**, *50*, 5339-56.
94. Gerotziafas, G.; Samama1, M. Curr. Pharma. Design **2005**, *11*, 3855-3876.
95. Borensztajn, K.; Stiekema, J.; Nijmeijer, S.; Reitsma, P.; Peppelenbosch, M. P.; Spek, C. A. Am. J. Pathol. **2008**, *172*, 309-20.
96. Weitz, I.; Hudoba, M.; Massel, D.; Maraganore, J.; Hirsh J. J. J. Clin. Invest. **1990**, *86*, 385-91.
97. Franchini, M.; Mannucci, P. M. Eur. J. Internal Med. **2009**, *20*, 562–568.
98. Elliott M. A. Circulation **1996**, *94*, 911-921.
99. Szaba, F.; Smiley, S. Blood **2002**, *99*, 1053-1059.
100. Panettieri, R. A. Jr.; Hall, I. P.; Maki, C. S.; Murray, R. K. Am. J. Respir. Cell. Mol. Biol. **1995,** *13*, 205-16.
101. Greinacher, A. Exp. Rev. Cardiovasc. Ther. **2004**, *2*, 339-357.
102. Prisco, D.; Grifoni, E.; Poli, D. RIMeL / IJLaM **2009**, *5*.
103. Fager, G.; Cullberg, M.; Eriksson-Lepkowska, M.; Frison, L.; Eriksson, U. G. Eur. J. Clin. Pharmacol. **2003**, *59*, 283-9.
104. Dobesh, P. P. Pharmacoth. **2004,** *24*, 169-178.
105. http://www.fda.gov/NewsEvents/Newsroom/PressAnnouncements/ucm230241.htm
106. Weitz, J. Thromb Haemostasis **2010**, *103*, 62–70.
107. Levi, M. M.; Eerenberg, E.; Löwenberg, E.; Kamphuisen, P. W. Neth. J. Med. Rev. **2010**, *68*, 2.
108. Bauer, K. J. Thromb. Thrombolysis **2006**, *21*, 67–72.
109. Kranjc, A.; Kikelj, D. Curr. Med Chem. **2004**, *11*, 2535-47.
110. Philipp, R.; Greach, E. Brit. Med. J. **2003**, *327*, 43-46.
111. Bode, W. Semin. Thromb. Hemostasis **2006**, 16-31 and references there in.
112. Davie, E.; Kulman, J. Semin. Thromb. Hemostasis **2006**, *32*, 3-15. and references there in.
113. Herny, B. L. Novel sulfated 4-hydroxycinnamic acid oligomers as potent anticoagulants. Dissertation **2007**.
114. Frenkel, E.; Shen, Y.; Haley, B. Hematol. Oncol. Clin. N Am. **2005**, *19*, 119–145.

115. Esmon, C. T.; Lollar, P. J. Biol. Chem. **1996**, *271*, 13882-7.
116. Sheehan, J. P.; Sadler, J. E. Proc. Natl. Acad. Sci. U S A. **1994**, *91*, 5518-22.
117. Fredenburgh, J. C.; Stafford, A. R.; Weitz, J. I. J. Biol. Chem. **1997**, *272*, 25493-9.
118. Brandstetter, H.; Kühne, A.; Bode, W.; Huber, R.; von der Saal, W.; Wirthensohn, K.; Engh, R. A. J. Biol. Chem. **1996**, *271*, 29988-92.
119. Gunnarsson, G. T.; Desai, U. R. J. Med. Chem. **2002**, *45*, 1233-1243.
120. Gunnarsson, G. T.; Desai, U. R. J. Med. Chem. **2002**, *45*, 4460-4470.
121. Gunnarsson, G. T.; Desai, U. R. Bioorg. Med. Chem. Lett. **2003**, *13*, 579-583.
122. Monien, B. H.; Desai, U. R. J Med Chem. **2005**, *48*, 1269-73.
123. Monien, B. H.; Cheang, K. I.; Desai, U. R. J. Med. Chem. **2005**, *48*, 5360-8.
124. Monien, B. H.; Henry, B. L.; Raghuraman, A.; Hindle, M.; Desai, U. R. Bioorg Med Chem **2006**, *14*, 7988-98.
125. Henry, B. L.; Monien, B, H.; Bock. P. E.; Desai, U. R. J. Biol. Chem. **2007**, *282*, 31891-31899.
126. Kishimoto, T.; Uraki, Y.; Ubukata, M. J. Wood Chem. Technol. **2008**, *28*, 97–105.
127. Corey, L. S., P. G. N. Engl. J. Med. **1986**, *314*, 749-757.
128. Corey, L. S., P. G. N. Engl. J. Med. **1986**, *314*, 686-691.
129. Mitchell, B. M.; Bloom, D. C.; Cohrs, R. J.; Gilden, D. H.; Kennedy, P. G. J. Neurovirol. **2003**, *9*, 194-204.
130. Immergluck, L. C.; Domowicz, M. S.; Schwarts, N. B.; Herold, B. C. J. Gen. Virol. **1998**, *79*, 549-559.
131. Herold, B. C.; Gerber, S. I.; Belval, B. J.; Siston, A. M.; Shulman, N. J Virol **1996**, *70*, 3461-3469.
132. Corey L and Handsfield H H. JAMA **2000,** 283, 791-794.
133. Cheshenko, N.; Keller, M. J.; MasCasullo, V.; Jarvis, G. A.; Cheng, H. et al. Antimicrob. Agents Chemother. **2004**, *48*, 2025-2036.
134. Kleymann, G. Herpes **2003**, *10*, 46-52.
135. Kleymann, G. Expert Opin. Investig. Drugs **2003**, *12*, 165-183.
136. Cai, W. H.; Gu, B.; Person, S. J. Virol. **1988**, *62*, 2596-2604.
137. Campadelli-Fiume, G.; Stirpe, D.; Boscaro, A.; Avitabile, E.; Foa-Tomasi, L. et al. Virology **1990**, *178*, 213-222.
138. Cheshenko, N.; Herold, B. C. J. Gen. Virol. **2002**, *83*, 2247-2255.
139. Gerber, S. I.; Belval, B. J.; Herold, B. C. Virology **1995**, *214*, 29-39.
140. Herold, B. C.; WuDunn, D.; Soltys, N.; Spear, P. G. J. Virol. **1991**, *65*, 1090-1098.
141. Hutchinson, L.; Browne, H.; Wargent, V.; Davis-Poynter, N.; Primorac, S. J. Virol. **1992**, *66*, 2240-2250.
142. Johnson, R. M.; Spear, P. G. J. Virol. **1989**, *63*, 819-827.
143. Pertel, P. E.; Fridberg, A.; Parish, M. L.; Spear, P. G. Virol. **2001**, *279*, 313-324.
144. Roop, C.; Hutchinson, L.; Johnson, D. C. J. Virol. **1993**, *67*, 2285-2297.

145. Tal-Singer, R.; Peng, C.; Ponce De Leon, M.; Abrams, W. R.; Banfield, B. W. et al. J. Virol. **1995**, *69*, 4471-4483.
146. Laquerre, S.; Argnani, R.; Anderson, D. B.; Zucchini, S.; Manservigi, R. et al. J. Virol. **1998**, *72*, 6119-6130.
147. Lycke, E.; Johansson, M.; Svennerholm, B.; Lindahl, U. J. Gen. Virol. **1991**, *72*, 1131-1137.
148. Shieh, M. T.; WuDunn, D.; Montgomery, R. I.; Esko, J. D.; Spear, P. G. J. Cell. Biol. **1992**, *116*, 1273-1281.
149. Spear, P. G. Cell. Microbiol. **2004**, *6*.
150. Spear, P. G.; Shieh, M. T.; Herold, B. C.; WuDunn, D.; Koshy, T. I. Adv. Exp. Med. Biol. **1992**, *313*, 341-353.
151. WuDunn, D.; Spear, P. G. J. Virol. **1989**, *63*, 52-58.
152. Geraghty, R. J.; Krummenacher, C.; Cohen, G. H.; Eisenberg, R. J.; Spear, P. G. Science **1998**, *280*, 1618-1620.
153. Montgomery, R. I. W., M. S.; Lum, B. J.; Spear, P. G. Cell **1996**, *87*, 427-436.
154. Shukla, D.; Liu, J.; Blaiklock, P.; Shworak, N. W.; Bai, X. et al. Cell **1999**, *99*, 13-22.
155. Spear, P. G.; Eisenberg, R. J.; Cohen, G. H. Virol. **2000**, *275*, 1-8.
156. Warner, M. S. G., R. J.; Martinez, W. M.; Montgomery, R. I.; Whitbeck, J. C.; Xu, R.; Eisenberg, R. J.; Cohen, G. H.; Spear, P. G. Virol. **1998**, *246*, 179-189.
157. Whitbeck, J. C.; Peng, C.; Lou, H.; Xu, R.; Willis, S. H. et al. J. Virol. **1997**, *71*, 6083-6093.
158. Williams, R. K.; Straus, S. E. J. Virol. **1997**, *71*, 1375-1380.
159. Xia, G.; Chen, J.; Tiwari, V.; Ju, W.; Li, J. P. et al. J. Biol. Chem. **2002**, *277*, 37912-37919.
160. Xu, D.; Tiwari, V.; Xia, G.; Clement, C.; Shukla, D. et al. Biochem. J. **2005**, *385*, 451-459.
161. Liu, J.; Thorp, S. C. Med. Res. Rev. **2002**, *22*, 1-25.
162. Shukla, D.; Spear, P.G. J. Clin. Invest. **2001**, *108*, 503-510.
163. Bame, K. J.; Esko, J. D. J. Biol. Chem. **1989**, *264*, 8059-8065.
164. Bame, K. J.; Lidholt, K.; Lindahl, U.; Esko, J. D. J. Biol. Chem. **1991**, *266*, 10287-10293.
165. Herold, B. C.; Visalli, R. J.; Susmarski, N.; Brandt, C. R.; Spear, P. G. J. Gen. Virol. **1994**, *75*, 1211-1222.
166. Herold, B. C.; Gerber, S. I.; Polonsky, T.; Belval, B. J.; Shaklee, P. N. et al. Virol. **1995**, *206*, 1108-1116.
167. Liu, J.; Shriver, Z.; Pope, R. M.; Thorp, S. C.; Duncan, M. B. et al. J. Biol. Chem. **2002**, *277*, 33456-33467.
168. Tiwari, V.; Clement, C.; Duncan, M. B.; Chen, J.; Liu, J. et al. J. Gen. Virol. **2004**, *85*, 805-809.
169. Patel, M.; Yanagishita, M.; Roderiquez, G.; Bou-Habib, D. C.; Oravecz, T. et al. **1993**, *9*, 167-174.

170. Chen, Y.; Maguire, T.; Hileman, R. E.; Fromm, J. R.; Esko, J. D. et al. Nat. Med. **1997**, *3*, 866-871.
171. Jackson, R. L.; Busch, S. J.; Cardin, A. D. Physiol. Rev. **1991**, *71*, 481-539.
172. Byrnes, A. P.; Griffin, D. E. J. Virol. **1998**, *72*, 7349-7356.
173. Feldman, S. A.; Audet, S.; Beeler, J. A. J. Virol. **2000**, *74*, 6442-6447.
174. Goodfellow, I. G.; Sioofy, A.; Powell, R. M.; Evans, D. J. J. Virol. **2001**, *75*, 4918-4921.
175. Shriver, Z.; Liu, D.; Sasisekharan, R. Trends Cardiovasc. Med. **2002**, *12*.
176. Bernfield, M.; Kokenyesi, R.; Kato, M.; Hinkes, M. T.; Spring, J. et al. Annu. Rev. Cell. Biol. **1992**, *8*, 365-393.
177. Bernfield, M. G., M.; Park, P. W.; Reizes, O.; Fitzgerald, M. L.; Lincecum, J.; Zako, M. Annu. Rev. Biochem. **1999**, *68*.
178. Esko, J. D.; Lindhal, U. J. Clin. Invest. **2001**, *108*, 169-173.
179. Kjellen, L.; Lindahl, U. Annu. Rev. Biochem. **1991**, *60*, 443-475.
180. Lindahl, U.; Kusche-Gullberg, M.; Kjellen, L. J. Biol. Chem. **1998**, *273*, 24979-24982.
181. Rabenstein, D. L. Nat. Prod. Rep. **2002**, *19*, 312-331.
182. Salmivirta, M.; Lidholt, K.; Lindahl, U. Faseb J. **1996**, *10*, 1270-1279.
183. Nyberg, K.; Ekblad, M.; Bergstrom, T.; Freeman, C.; Parish, C. R.; Ferro, V.; Trybala, E. Antiviral Res. **2004,** *63*, 15-24.
184. Carlucci, M. J.; Pujol, C. A.; Ciancia, M.; Noseda, M. D.; Matulewicz, M. C.; Damonte, E. B.; Cerezo, A. S. J. Biol. Macromol. **1997**, *20*, 97-105.
185. Dyer, A. P.; Banefield, B. W.; Martindale, D.; Spannier, D. M.; Tufaro, F. B. J. Virol. **1997**, *71*, 191-198.
186. Feyzi, E.; Trybala, E.; Bergstrom, T.; Lindahl, U.; Spillmann, D. J. Biol. Chem. **1997**, *272*, 24850-24857.
187. Raghuraman, A.; Tiwari, V.; Zhao, Q.; Shukla, D.; Debnath, A. K.; Desai, U. R. Biomacromolecules **2007**, *8*, 1759–1763.
188. Raghuraman, A.; Tiwari, V.; Thakkar, J. N.; Gunnarsson, G. T.; Shukla, D.; Hindle, M.; Desai, U. R. Biomacromolecules **2005**, *6*, 2822–2832.
189. Reale, S.; Di Tullio, A.; Spreti, N.; De Angelis, F. Mass Spectrom. Rev. **2004**, *23*, 87–126.
190. Boerjan, W.; Ralph, J.; Baucher, M. Annu. Rev. Plant Biol. **2003**, *54*, 519–546.
191. Warda, M.; Gouda, E. M.; Toida, T.; Chi, L.; Linhardt, R. J. Comp. Biochem. Physiol., Part B: Biochem. Mol. Biol. **2003**, *136*, 357–365.
192. Warda, M.; Linhardt, R. J. Comp. Biochem. Physiol., Part B: Biochem. Mol. Biol. **2006**, *143*, 37–43.
193. Tiwari, V.; Clement, C.; Duncan, M. B.; Chen, J.; Liu, J.; Shukla, D. J. Gen. Virol. **2004**, *85*, 805–809.
194. O'Donnell, C. D.; Kovacs, M.; Akhtar, J.; Valyi-Nagy, T.; Shukla, D. Virol. **2010**, *397*, 389–398.
195. Montgomery, R. I.; Warner, M. S.; Lum, B. J.; Spear, P. G. Cell **1996**, *87*, 427–436.

196. Warner, M. S.; Geraghty, R. J.; Martinez, W. M.; Montgomery, R. I.; Whitbeck, J. C.; Xu, R.; Eisenberg, R. J.; Cohen, G. H.; Spear, P. G. Virol. **1998**, *246*, 179–189.
197. Holmgren, A.; Henriksson, G.; Zhang, L. M. Biomacromolecules **2008**, *9*, 3378–3382.
198. Bunzel, M.; Heuermann, B.; Kim, H.; Ralph, J. J. Agric. Food Chem. **2008**, *56*, 10368–10375.
199. Touzel, J. P.; Chabbert, B.; Monties, B.; Debeire, P.; Cathala, B. J. Agric. Food Chem. **2003**, *51*, 981–986.
200. Kim, H.; Ralph, J.; Lu, F. C.; Ralph, S. A.; Boudet, A. M.; MacKay, J. J.; Sederoff, R. R.; Ito, T.; Kawai, S.; Ohashi, H.; Higuchi, T. Org. Biomol. Chem. **2003**, *1*, 268–281.
201. Holmgren, A.; Norgren, M.; Zhang, L.; Henriksson, G. Phytochem. **2009**, *70*, 147–155.
202. Ward, G.; Hadar, Y.; Bilkis, I.; Konstantinovsky, L.; Dosoretz, C. G. J. Biol. Chem. **2001**, *276*, 18734–18741.
203. Pan, G. X.; Spencer, L.; Leary, G. J. J. Agric. Food Chem. **1999**, *47*, 3325–3331.
204. Shukla, D.; Liu, J.; Blaiklock, P.; Shworak, N. W.; Bai, X.; Esko, J. D.; Cohen, G. H.; Eisenberg, R. J.; Rosenberg, R. D.; Spear, P. G. Cell **1999**, *99*, 13–22.
205. Tiwari, V.; Clement, C.; Duncan, M. B.; Chen, J.; Liu, J.; Shukla, D. J. Gen. Virol. **2004**, *85*, 805–809.
206. Suzuki, H.; Tochikura, T. S.; Iiyama, K.; Yamazaki, S.; Yamamoto, N.; Toda, S. Agric. Biol. Chem. **1989**, *53*, 3369–3372.
207. Raghuraman, A.; Riaz, M.; Hindle, M.; Desai, U. R. Tetrahedron Lett. **2007**, *48*, 6754–6758.
208. Al-Horani, R. A.; Desai, U. R. Tetrahedron **2010**, *66*, 2907–2918.
209. Nakashima, H.; Murakami, T.; Yamamoto, N.; Naoe, T.; Kawazoe, Y.; Konno, K.; Sakagami, H. Chem. Pharm. Bull. **1992**, *40*, 2102–2105.
210. Shimizu, N.; Naoe, T.; Kawazoe, Y.; Sakagami, H.; Nakashima, H.; Murakamim, T.; Yamamoto, N. Biol. Pharm. Bull. **1993**, *16*, 434–436.
211. Ichimura, T.; Otake, T.; Mori, H.; Maruyama, S. Biosci., Biotechnol., Biochem. **1999**, *63*, 2202–2204

VITA

Jay Thakkar was born on March 30, 1981 in Bombay (Mumbai), India. Jay graduate with a B. Pharmacy degree from University of Mumbai in 2003. After graduating Jay went on to pursue his Master's (2003) followed by Ph.D. (2007) in the department of Medicinal Chemistry from the Pharmaceutical Science's program at Virginia Commonwealth University, Richmond, Virginia.